POLITECNICO DI TORINO
Master Degree course in Biomedical Engineering

Master Degree Thesis

User-guided interface for motion tracking in controlled functional electrical stimulation

Supervisors
Prof. Jacopo Secco
Eng. Elisabetta Spinazzola

Candidate
Gabriele Azzena

Academic Year 2024-2025

Abstract

The need for rehabilitation arises from injuries and diseases that impair movement and independence. Traumas, accidents, and neurological or degenerative disorders- such as stroke, spinal cord, and brain injuries- are major causes of long-term disability, often resulting in partial or total loss of motor control. Stroke, in particular, is among the leading causes of disability worldwide, frequently affecting upper-limb functionality and limiting patients' autonomy. Rehabilitation thus plays a crucial role in restoring motor abilities and promoting recovery through targeted and personalized interventions. In recent decades, alongside the rapid development of technology and computer science, physical rehabilitation has increasingly benefited from advanced tools that support clinical practice. Among these, one of the most relevant is Functional Electrical Stimulation (FES), which uses low-energy electrical pulses to retrain- or, in same case, restore- functional mobility in patients with neuromuscular disorders. The effectiveness of FES can be enhanced by modulating the stimulation delivery according to the natural activation patterns of muscles. In this context, Average Threshold Crossing (ATC) represents an event-driven approach applied to Surface Electromyography (sEMG) signals to estimate muscle contraction force and optimizing FES therapy. A key limitation of this technique is its lack of objectivity. Currently, pulse width and frequency are adjusted manually, forcing clinicians to rely on personal experience to identify suitable parameters. Moreover, therapy effectiveness is often evaluated through subjective observation rather than quantitative metrics, affecting reproducibility and comparability of outcomes. To address these issues, this project aims to develop an innovative system designed to complement an ATC-based FES approach, the Lazarus FES device, providing an objective and patient-specific support tool. By analyzing real-time movements using YOLOv8-pose, the system can suggest to physicians the most appropriate set of stimulation parameters, thereby supporting clinical decision-making, enhancing the effectiveness of FES therapy, and increasing the objectivity of its application. The evaluation process is further refined through the extraction of quantitative features that allow a more accurate and reproducible assessment of patient's motor performance and therapy outcomes. Finally, the project includes the development of an experimental protocol aimed at testing the system first on healthy subjects and, at a later stage, on patients affected by chronic stroke. These steps represent a key phase toward transforming the proposed device into a telemedicine tool. This thesis is structured into seven chapters. The first introduces rehabilitation and provides an overview of stroke as a major cause of motor impairment. The second outlines upper limb assessment techniques and main rehabilitation approaches, both conventional and FES-based. The third describes the Lazarus FES device, the fourth presents the RehabCam software and the experimental protocol, the fifth discusses the results, the sixth outlines the forthcoming clinical trial, and the last chapter summarizes the key findings and conclusions.

Contents

1 Rehabilitation and Stroke 5
- 1.1 Stroke . . . 5
  - 1.1.1 Consequences of stroke . . . 6
- 1.2 Rehabilitation . . . 7
  - 1.2.1 Steps of Rehabilitation . . . 7

2 Functional Assessment and Rehabilitation Protocols for the Upper Limb 9
- 2.1 Assessment Scales and Clinical Tests . . . 9
  - 2.1.1 Scales and Clinical Tests for Assessing Upper Limb Motor Limitations . . . 10
- 2.2 Instrumental Tests for Upper Limb Assessment . . . 10
- 2.3 Traditional Rehabilitation of the Upper Limb . . . 13
- 2.4 Rehabilitation Treatment with Functional Electrical Stimulation . . . 14
  - 2.4.1 Open-loop and Closed-Loop FES systems . . . 16
  - 2.4.2 Clinical Application of Open-Loop FES for Upper Limb Rehabilitation After Stroke . . . 17
  - 2.4.3 Clinical Application of Closed-Loop BCI-FES for Upper Limb Rehabilitation After Stroke . . . 18
  - 2.4.4 Clinical Application of closed-Loop EMG-FES for Upper Limb Rehabilitation After Stroke . . . 20

3 The Lazarus FES device 23
- 3.1 Apollox Unit . . . 24
- 3.2 Steps of the Rehabilitation Process Using Lazarus and Patient Database Registration . . . 28
  - 3.2.1 Creation of Rehabilitation Pattern and Calibration Phase . . . 30
  - 3.2.2 Rehabilitation Session using the Lazarus device . . . 34
- 3.3 Limitations of the Lazarus Device . . . 36

4 RehabCam: an Assistive Software for the Lazarus Device and Preparatory Tests for the Trial 39
- 4.1 RehabCam Homepage and Patient Registration . . . 40
- 4.2 Key Movement Parameters Computed by the RehabCam software . . . 42
- 4.3 Rehabcam Rehabilitation Steps . . . 43
- 4.4 Experimental Testing of the Lazarus Device Integrated with RehabCam . . . 47
- 4.5 Data processing . . . 49

5 Results and discussion 53
- 5.1 Qualitative Analysis of Parameter Updates . . . 53
- 5.2 Quantitative Analysis of Motion . . . 56
  - 5.2.1 Elbow Flexion-Extension in Pronation and Supination . . . 56
  - 5.2.2 Eyeglasses Donning and Removal Task . . . 61
  - 5.2.3 Box Opening and Closing Task . . . 66

5.2.4 Cup Drinking Task 70
5.3 Overall Interpretation of System Performance and Electrode Configuration Effects 74

6 Future Work: Development of the Clinical Trial 77
6.1 Target population: Patients with Chronic Stroke 77
6.2 Study Design 78
6.3 Modifications to the Use of Lazarus and the RehabCam Program for the Rolling Pin Exercise 81

7 Conclusion 83

Bibliography 85

Chapter 1

Rehabilitation and Stroke

A rehabilitation program becomes necessary whenever a patient is affected by conditions that significantly impair functional activities such as motor, cognitive-behavioral, social functions. In this context, stroke represents one of the most common causes of dysfunction, as it compromises functional mobility, balance and gait.

1.1 Stroke

Stroke is one of the leading causes of death and disability worldwide. In 2019, approximately 1240 out of every 100.000 people experienced a stroke [23].

The impact of this condition on Western economies and healthcare systems is strikingly illustrated by recent data from United States, where the annual economic burden has been estimated at around 57 billion USD, including both direct healthcare expenditures and productivity losses [94].

The underlying mechanism of stroke is an interruption of oxygen supply to brain neurons, which leads to necrosis of the affected tissue. Depending on its cause, stroke can be classified into two major types:

- **Hemorrhagic stroke**, caused by intracerebral bleeding (Figure 1.1).
- **Ischemic stroke**, caused by an atherosclerotic plaque or thrombus within cerebral vessels, which may be embolic or non-embolic (Figure 1.1).

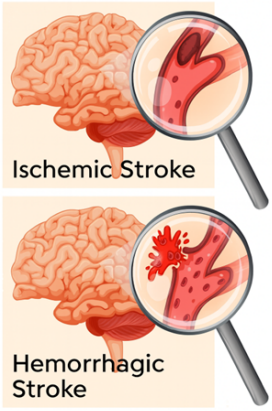

Figure 1.1: Ischemic stroke (above) and hemorrhagic stroke (below).

Diagnosis relies primarily on computed tomography (CT), which allows rapid identification of hemorrhagic stroke but is less sensitive in the very early stages of ischemic stroke. For ischemic events, CT scans are often repeated after 24-48 hours to visualize the lesion zone. A central aim of early imaging is to differentiate between the core, the region of necrotic tissue, and the penumbra, a zone of ischemic but potentially viable cells that may remain salvageable for several hours. Treatment strategies differ according to stroke type. In hemorrhagic stroke, surgery may be required to stop the bleeding. In ischemic stroke, thrombi can be removed by intravenous thrombolytic drugs or by interventional procedures such as MERCI technique, which employs specialized devices to capture, retrieve, and aspirate the clot.

Major risk factors include atherosclerosis, age over 65, family history, and prior stroke. Additional contributors such as hypertension, hypercholesterolemia, diabetes, and smoking further increase the likelihood of an event. Globally, the incidence, mortality, and overall disability burden associated with stroke have increased over the past 20 years, despite advances in acute treatment and prevention. This rise has been most evident in low- and middle- income countries, whereas high-income countries have shown a modest decline in morbidity and mortality [77]. Over the last two decades, reductions in the prevalence of hypertension, hypercholesterolemia and smoking in high-income regions have supported the hypothesis that improved prevention and better management of vascular risk factors, together with effective prophylaxis using antithrombotic or anticoagulant drugs, are driving these diverging trends [85].

Specifically, the reduction in stroke-related mortality and disability in high-income countries is thought to be due more to optimized acute care and anticoagulant prophylaxis than to long-term risk factor control [53, 59].

1.1.1 Consequences of stroke

Despite these improvements, globally the number and severity of activity limitations caused by stroke remain high. The global disease burden attributable to stroke is exceeded only by myocardial infarction and neonatal disorders. With mortality rates decreasing but the number of survivors with often severe and lifelong deficits increasing, no reduction in the overall societal burden of stroke is expected soon. Even today, rehabilitation and long-term care account for the largest share of stroke-related healthcare costs.

The functional consequences of stroke are wide-ranging, affecting many abilities essential for daily life and quality of life. Common symptoms include paralysis (often unilateral), language and speech disorders, spatial disorientation, coordination deficits, sensory disturbances, and visual impairment. Persistent symptoms inevitably lead to long-term functional restrictions, reduced independence, and diminished participation in social life [77].

Paralysis is among the most frequent manifestations and, when lasting, results in loss of autonomy and the need for external assistance [46]. It is often associated with neuropsychological deficits, both cognitive and behavioral, and with pain linked to spasticity and restricted mobility [5, 10]. Even in less severely affected patients, motor deficits significantly contribute to long-term disability, making them a primary target of rehabilitation and research. Paralysis produces immediate and obvious functional limitations that guide the first therapeutic and rehabilitative interventions. Sensory deficits can also indirectly affect stability and gait, for example through hypersensitivity or impaired proprioception, and their recognition may improve therapeutic outcomes [96].

Language disorders are another major issue, with prevalence ranging between 20% and 40%, highest among ischemic stroke cases [24]. They present as difficulties in producing speech and understanding spoken or written language, often resulting in long-term dependence. Beyond their direct impact, aphasia complicates the rehabilitation of other deficits and is associated with longer hospital stays and extended recovery programs [47].

In recent years, cognitive impairments and post-stroke dementia have become increasingly central in both clinical and scientific attention. This is due to the general rise in dementia

prevalence, with vascular dementia representing the second most common form after Alzheimer's disease, as well as evidence from longitudinal studies confirming the high frequency of post-stroke cognitive disorders [9]. Such deficits, ranging in prevalence from 30% to 40% depending on study populations and assessment methods, may include psychomotor slowing and aphasia [6, 70]. Factors such as lesion size and location, baseline cognitive status, and concept of cognitive reserve- the brain's resilience to age- or disease- related damage, influenced by education and mental activity- play crucial roles to prognosis.

Approximately one third of stroke survivors develop neuropsychiatric disturbances such as depression, anxiety, or fatigue [31]. These are rarely evaluated during the acute phase, when clinical stabilization is the main priority, and the typically identified during the rehabilitation through neuropsychological assessments. Patient-reported questionnaires, such as the Patient Health Questionnaire (PHQ-9), have proven valuable tools for screening. Findings regarding the risk for developing neuropsychiatric behavioral disorders after stroke are linked to factors such as age, sex, and pre-existing cognitive deficits.

The negative impact of neuropsychiatric disorders is well documented: they reduce quality of life, hinder recovery of daily functions, increase recurrence risk, and raise mortality. Indeed, the American Heart Association recommends systematic screening for these conditions after stroke to facilitate timely psychological or pharmacological treatment [93]. Routine prescription of antidepressants to all stroke patients has not proven effective in improving overall functionality, reinforcing the need for individualized assessment and tailored interventions [32, 51]. Importantly, post-stroke anxiety and depression are not short-lived conditions but often long-term consequences, requiring continued outpatient management well beyond the rehabilitation phase [21].

1.2 Rehabilitation

Today, the concept of rehabilitation encompassed a wide range of therapeutic activities, which are not necessarily limited to the recovery of motor function. In particular, the Italian Ministry of Health provides the following definition:

"Rehabilitation is a problem-solving and educational process through which a person is helped to achieve the highest possible level of physical, functional, social and emotional well-being, with the least possible restriction of their operational choices, within the limits of their impairment."

Furthermore, according to the Ministry of Health, rehabilitation "constitutes the third pillar of the healthcare system, alongside prevention and treatment, completing the activities aimed at protecting the health of citizens." [61]

The rehabilitation process is primarily structured on two levels:

- **Intensive rehabilitation (or acute rehabilitation):**aimed at the recovery of significant and modifiable disabilities that require a high level of evaluative and/or therapeutic effort.
- **Extensive rehabilitation:** involving a more moderate therapeutic effort with greater assistance, aimed at preventing potential complications in stabilized disabled patients. This level consists of interventions directed at individuals with slowly recovering disabilities who cannot tolerate intensive treatment or who are affected by chronic and progressive disabilities.

1.2.1 Steps of Rehabilitation

To achieve the desired goal, the rehabilitation process is generally divided into four phases:

- **First phase:** focused on the prevention of damage and secondary impairments in high-risk conditions.

- **Second phase:** intensive rehabilitation (acute rehabilitation phase).
- **Third phase:** completion of the recovery process and rehabilitation plan (sub-acute rehabilitation phase).
- **Fourth phase:** maintenance and/or prevention of decline in the motor and functional recovery already achieved (post-acute rehabilitation phase).

These four phases form the foundation of the rehabilitation project, which also requires a therapeutic planning process. The purpose of this process is to help the patient regain sufficient physical to ensure independence and autonomy. Rehabilitation treatments can be further divided into two categories:

- **Individual Rehabilitation Plan (IRP):** a set of proposals developed by the rehabilitation team which, considering the patient's overall needs, impairments, disabilities, residual abilities, as well as environmental limitations and available resources, defines the expected outcomes within specific timeframes. To implement the IRP, the involvement of specialized medical and technical staff is required. For its success, the following are essential:
  - clear and appropriate communication with the patient, family members, and all professionals involved;
  - awareness and understanding of the patient's overall issues, including aspects not directly addressed by specific interventions;
  - adaptation and modification of the protocol, with proper communication to patients and staff, whenever changes occur in the elements on which the plan was based (needs, preferences, impairments, abilities, residual disabilities, environmental/resource limitations, expectations, priorities), or in the event of achieved outcomes, unexpected changes in timing, actions, or previously defined conditions.
- **Facility Rehabilitation Plan**: aimed at ensuring a generally rehabilitative environment through the availability and organization of adequately equipped spaces, structured workflows, and operational procedures. The objective is to provide effective support to maintain and stimulate the functional and relational capacities of all individuals hosted within the facility.

Chapter 2

Functional Assessment and Rehabilitation Protocols for the Upper Limb

The evaluation of motor abilities and their alterations compared to normal physiological conditions is highly valuable in clinical practice, both for diagnostic purposes and for the planning and monitoring of specific rehabilitation treatments.

The onset of pathological process of different origins can lead to altered motor patterns, which combine normal and abnormal movements. These changes have functional repercussions and result in an overall reduction in the individual's autonomy. When such abnormal patterns involve the upper limb, independence is significantly compromised, since the upper limbs are essential for the most day-life interactions with the environment and are therefore fundamental in defining an individual's manual skills.

Assessing upper limb motor function is particularly complex for several reasons. This body segment is anatomically and biomechanically sophisticated, especially due to the involvement of multiple joints (notably the shoulder). Moreover, unlike the lower limb- where walking represents a universal functional task- there is no single representative motor task for the upper limb. For this reason, clinicians typically evaluate upper limb function through a variety of tasks, such as analyzing pointing and reaching movements [76] or the Hand-to-Mouth (HTM) movement, which mimics the action of eating and drinking.

Currently, clinical assessment primarily relies on performance-based tests, which serve as indicators of the system as whole and allow for quantitative evaluation through standardized scales. The assessment usually involves asking the patient to perform a series of predefined movements, based on which the trained clinician assigns and draws conclusions according to the overall results.

2.1 Assessment Scales and Clinical Tests

Specific scales and clinical tests have been developed to evaluate the stage of a disease from a motor perspective. Each scale must meet the following criteria:

- **Applicability:** each assessment scale has its specific field of application, which must be respected unless it has been tested and validated for other contexts.
- **Validity:** there must be a demonstrated correlation between the variables described in the scale and the actual phenomenon being measured.
- **Reproducibility or repeatability:** patients in the same condition should receive the same score, regardless of the evaluator or the environment in which the test is conducted.

- **Sensitivity:** indicates the accuracy with the test are able to capture changes in the clinical condition.

The following sections will present the main scales and clinical tests used to evaluate upper limb motor function.

2.1.1 Scales and Clinical Tests for Assessing Upper Limb Motor Limitations

The most widely used scales and clinical tests to evaluate upper limb motor function are: the Fugl-Meyer Assessment for the Upper Limb (FM-UL), the Wolf Motor Function Test (WMFT), and the Action Research Arm Test (ARAT).

The FM-UL assesses movement of the biceps, triceps, shoulder, elbow, wrist, hand, and fingers during the execution of 33 different tasks. The use of this scale requires various objects (e.g., chair, pencil, ball, etc.). The clinician assigns a score ranging from 0 (inability to perform the movement) to 2 (normal physiological movement). The test takes about 35 minutes, and the maximum score 66 indicates excellent functional mobility.

The WMFT evaluates upper limb movement through 17 motor tasks, 2 of which assess strength and 15 of which are time-based tasks. The test, lasting about 25 minutes, is scored from 0 (no movement ability) to 5 (normal physiological movement). As with the FM-UL, this test also requires the use of various everyday objects (chair, table, pencil, etc.) and has demonstrated high reliability and validity.

The ARAT is based on 19 tasks divided into 4 subtests (grasp, grip, pinch and gross movement), which assess the patient's ability to manipulate objects of different sizes, weight, and shapes (Figure 2.1). Administration takes about 10 minutes, and each task is scored from 0 (unable to perform the task) to 3 (normal physiological movement).

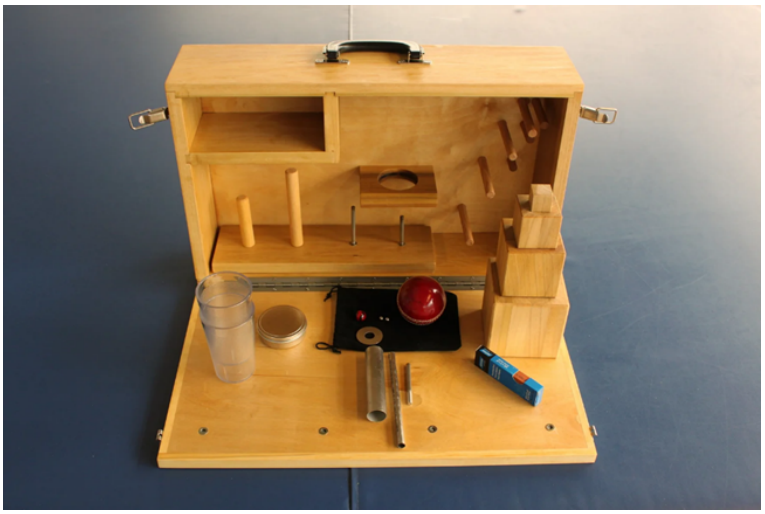

Figure 2.1: ARAT kit for test administration. Reproduced from [33]

2.2 Instrumental Tests for Upper Limb Assessment

In addition to the clinical tests described earlier, instrumental tests are also used to evaluate upper limb motor ability. These can take different forms, with some examples provided below:

- Box and Block Test (BBT)
- Hand Grip Strength Test (HGS)

- Nine Hole Peg Test (9HPT)

The BBT measures unilateral gross manual dexterity. It is inexpensive and easy to use. The test employs a wooden box measuring 53.7 cm long, 25.4 cm wide, and 8.5 cm high, containing 150 wooden blocks, each side of 2.5 cm. When the box is open, it reveals two compartments separated by a 15.2 cm- high divider (Figure 2.2). To conduct the test, the box is placed lengthwise in front of the patient, with the blocks positioned in the compartment on the side of the hand being tested. The patient's task is to transfer as many blocks as possible, one at time, from one compartment to the other within 60 seconds.

Figure 2.2: Execution of the BBT. Reproduced from [3]

In cases of unilateral upper limb impairment, such as after stroke, the healthy limb is tested first, followed by the paretic one. The BBT score corresponds to the number of blocks transferred within the designated 60 seconds. Typical scores for healthy individuals range between 47 and 80 blocks with the dominant hand and between 44 and 85 blocks with the non-dominant hand [62].

The HGS test is used to assess grip strength, i.e., the force generated by the hand and forearm muscles. The main tool is the dynamometer, which can be of three types: mechanical with analog display, mechanical with digital display, or hydraulic. For the test, the patient should be seated with the shoulder adducted and in neutral position, the elbow flexed at 90°, and the wrist positioned between 0° and 30° dorsiflexion and 0° and 15° ulnar deviation (Figure 2.3). To ensure reliable results, the test is repeated three times, with 30-50 seconds of rest between trials. The final score is determined by either the average or the highest value among the three attempts.

Figure 2.3: Execution of the HGS Test. Reproduced from [72]

The 9HPT measures fine manual dexterity. It is relatively inexpensive and simple to use. The test employs a rectangular board with nine holes and nine pegs (Figure 2.4)

Figure 2.4: Kit used for performing the 9HPT. Reproduced from [71]

The patient's task is to pick up the pegs from a container. As with the BBT, when unilateral impairment is present, the healthy limb is tested first, followed by the paretic limb. The evaluation is based on the time recorded with a stopwatch to complete the task: the shorter the time, the better performance. Healthy individuals typically complete the test in 14-37 seconds with the dominant hand and 16-30 seconds with the non-dominant hand [62].

These tests, although extremely useful for evaluation purposes, present some limitations. They are, in fact, not sensitive to small variations in motor function and are often unable to detect changes resulting from pharmacological or rehabilitative treatments. Moreover, they don't provide detailed information on the duration of individual movements or on movement kinematics (such as joint angles, displacements, velocities, and accelerations). Another limitation is that they don't allow the detection of fatigue phenomena, except through prolonged execution of motor tasks. For these reasons, it has become increasingly common to integrate such assessments with instrumental tests, which rely on advanced technologies and are able to provide

quantitative information on the kinematics and dynamics of the movement under study. Among the main tools used for this type of evaluation are inertial sensors and motion capture systems based on optoelectronic stereophotogrammetry, which is currently regarded as the gold standard in human movement analysis. For the evaluation of the upper limb motor function, the HTM test is one of the most widely used in three-dimensional motion analysis. This test assesses upper limb functionality during the execution of an activity like eating: lifting the hand from the table, bringing it to the mouth, and then returning to the initial resting phase by touching the table again. The HTM is easy to perform yet complex when it comes to identifying motor impairments in patients with movement disorders. Therefore, to summarize the information derived from this test, researchers typically use synthetic indices, which condense the information contained in the entire kinematic dataset into just a few parameters [15], thereby highlighting deviations from reference normality.

2.3 Traditional Rehabilitation of the Upper Limb

Stroke- as already mentioned in previous chapter- is highly disabling condition, particularly if rehabilitation interventions aren't initiated promptly. A patient with suspected stroke must be immediately admitted to hospital for an accurate diagnosis of the location, nature, and cause of brain damage. This allows the reduction of possible complications with pathology and enables the immediate initiation of most appropriate treatments. Physical therapy should begin as soon as the patient shows the first signs of motor recovery, with the aim of improving balance, mobility, and muscle strength through mobilization exercises. If this isn't done, in the case of the upper limb, patients tend to perform daily activities primarily using the unaffected arm while avoiding the use of the impaired one [2, 75]. This often results in complete disuse of the affected arm [75]. Since most simple daily activities- such as eating, washing, dressing, and writing- involve the hands and upper limbs, the inability to use one arm can lead to further loss of function and consequently, a reduction in movements essential for everyday life, thereby compromising the patient's autonomy [48]. As a result, this may increase feelings of depression, anxiety, sleep disturbances, and helplessness, foster a lifestyle of dependency on others, lower self-esteem, and even cause physiological pain [13], ultimately having a negative impact on quality of life [102]. Scientific literature consistently recognizes the fundamental role of rehabilitation therapies as tools that allow patients to recover- at least partially- the motor functions compromised by their condition. These treatments can be broadly divided into two main categories:

- Active-passive rehabilitation
- Passive rehabilitation

The first is recommended when the musculature is weak but still functional, requiring the support of a physiotherapist to perform certain functionals exercises. The second, instead, is applied when patients are completely unable to carry out motor activity. Another possible way to classify rehabilitation is based on the type of exercise involved. In this regard, it is possible to distinguish among:

- **Multiple exercising concepts**, which include methods consisting of several exercises designed to stimulate different muscle groups of the patient.
- **Isolated concepts**, in which rehabilitative techniques are aimed at acting on a single specific muscle group.
- **Task oriented training approaches**, in which rehabilitation exercises are designed to help patients recover movements related to activities of daily living.

The most widely used motor rehabilitation approaches after stroke include Constraint-Induced Movement Therapy (CIMT) and the Bobath method. CIMT belongs to the category of task-oriented methods for the upper limb. This rehabilitative approach requires the patient to use the paretic limb while simultaneously restricting the use of the unaffected one, to perform exercises designed to restore dexterity and fine motor skills. Treatment is typically initiated about three months after the stroke event, with the best outcomes achieved through intensive sessions of around six hours per day during the first week of therapy.

The Bobath method, instead, falls under the "multiple exercising" category and consists of active-assistive exercises. It also includes specific upper limb activities, such as the Affolter grasp, a guided exercise in which the patient performs daily tasks- for example washing hand or holding cutlery as if to eat- under the supervision and assistant of physiotherapist.

2.4 Rehabilitation Treatment with Functional Electrical Stimulation

FES represents one of the most significant innovations in neurological rehabilitation that integrates physiological knowledge with biomedical technology to recreate motor patterns that are useful in the patient's daily life.

When combined with voluntary motor intent, FES promotes neuroplastic processes that are highly similar to those activated during conventional rehabilitation. By repeatedly delivering stimulation that enables functional motor patterns, FES promotes neuroplasticity at both cortical and spinal levels, thereby supporting the recovery of impaired neural pathways or the development of alternative circuits. As a result, FES not only acts as mechanical aid to execute movements but also as therapeutic strategy capable of progressively enhancing the patient's residual motor capacity. Clinical evidence has demonstrated that regular FES-based training improves motor performance, reduces spasticity, and fosters greater independence in activities of daily living. This justifies the use of FES as a valid and effective complement- or, in some cases, an early substitute- for traditional rehabilitation, especially in the early stages of recovery when voluntary motor activity is absent or severely limited. However key physiological differences remain. FES induces muscle contractions by electrically stimulating motor nerves, resulting in synchronous and non-selective recruitment of motor units. This contrasts with the natural recruitment order of voluntary contractions, where smaller, fatigue-resistant motor units are activated first, followed by larger ones as needed [56]. During FES therapy, in fact, large- diameter axons- which supply the larger motor units- are preferentially recruited, since their wider spacing between nodes of Ranvier results in larger induced trans-membrane voltage changes and thus lower activation thresholds. In addition, the sensory feedback provided by FES tends to be more intense and less finely graded than that produced by voluntary movement, potentially influencing how the brain interprets and adapts to these signals [98]. As a result, while FES can effectively engage central motor circuits- especially when paired with patient intention- it still produces a different neuromuscular output compared to voluntary exercise.

From a physiological standpoint, FES relies on the integrity of lower motor neurons and neuromuscular junctions, which typically remain functional in most central neurological disorders. When an electrical stimulus is applied through an electrode, it generates an electric field that depolarizes the neural membrane. Once the depolarization reaches the threshold, an action potential is elicited and propagated along the axon and ultimately triggering contraction of the associated muscle fibers [69]. The strength of FES lies in its ability to modulate such contractions in a reproducible, selective, and coordinated manner, thereby transforming isolated muscle activation into complex, functional movements such as grasping, standing, or walking.

Muscle contraction under FES is primarily by three stimulation parameters: frequency (fs), amplitude (I), and pulse duration (PW). Low frequencies result in twitch-like contractions, whereas higher frequencies lead to smooth contractions through temporal summation. Increasing

amplitude or pulse width recruits additional motor units via spatial summation. However, excessive use of high frequencies or strong parameters can accelerate the onset of muscle fatigue, one of the major limitations of FES. For this reason, clinical protocols employ combinations of parameters that balance functional effectiveness with fatigue minimization, thereby ensuring that stimulation can be used effectively in repeated rehabilitation sessions.

From a technological perspective, several system configurations have been developed, differing mainly in electrode type and placement.

Electrical activation of neuromuscular tissue always requires at least two electrodes to produce a current flow, typically arranged in monopolar or bipolar configurations. In monopolar systems, a single remote return electrode serves multiple active electrodes placed near target nerves or motor points, thus reducing the total number of electrodes and leads. In contrast, bipolar configurations use one return electrode for each active electrode, increasing the number of leads but allowing more localized and selective stimulation [29].

Surface systems are the most common: they use electrodes placed on the skin over motor points, offering a non-invasive, simple, and relatively inexpensive solution (Figure 2.5a). Their limitations include variability in electrode positioning, inconsistent responses and potential discomfort on intact skin. Percutaneous systems, by contrast, employ intramuscular electrodes that pass through the skin, enabling selective and reproducible activation of deeper muscles, through requiring careful maintenance of the insertion sites (Figure 2.5b). Finally, fully implanted systems represent the most advanced option: electrodes and stimulators are surgically implanted, providing stable and highly selective activation without external wires (Figure 2.5c). While these systems improve usability and long-term performance, they require invasive procedures and sophisticated technology.

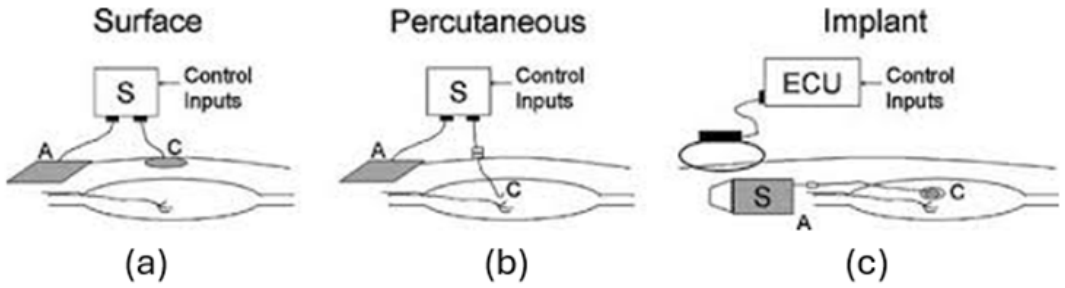

Figure 2.5: Configurations of FES systems: (a) surface, (b) percutaneous and (c) implanted. Reproduced from [69]

An additional engineering consideration is waveform design. Biphasic, charge-balanced pulses are most used to minimize the risk of tissue damage and electrode corrosion.

Stimulators may be designed to regulate either voltage or current. With voltage-regulated stimulation, the stimulator output is a fixed voltage, and thus the magnitude of current delivered to the tissue depends on the impedance at the electrode - tissue interface (Ohm's law). In the case of surface electrodes, impedance at the electrode-skin interface tends to increase as the electrode dries out or loses full contact with the skin. As impedance rises, the current delivered by a voltage-stimulator decreases, which in turn reduces the risk of excessive current density and skin burns. For this reason, voltage-regulated stimulation is commonly used in surface FES applications. However, the motor response is more variable with voltage regulation, as the effective current depends on changes in electrode impedance.

By contrast, current-regulated stimulation directly controls the amount of current delivered, regardless of variations in tissue load. This ensures that the charge per stimulus pulse remains

consistent and within safe limits, making current-regulated waveforms particularly suitable for implanted electrodes. Furthermore, current regulation increases the likelihood of obtaining stable and reproducible muscle responses over time.

By integrating advanced engineering with clinical practice, FES has established itself as an indispensable component of modern neurorehabilitation, with its role expected to expand further as scientific knowledge and technological innovation continue to progress [69].

2.4.1 Open-loop and Closed-Loop FES systems

It is crucial to differentiate between the major types of FES that have been developed to improve motor recovery. FES systems are commonly classified into two main categories depending on their mode of control: open-loop FES systems and closed-loop FES systems. Each approach provides different mechanisms for motor rehabilitation, varying in terms of patient involvement, feedback integration, and the degree of neuroplastic engagement.

Open-loop FES systems were the first to be applied clinically in neurorehabilitation. In these systems, stimulation is delivered through preprogrammed defined by the therapist, and patients cannot directly influence or modulate the stimulation based on their own feedback (Figure 2.6a). Moe and Post [38] first introduced open-loop FES in hemiplegia patients, and subsequent developments by Kralj et al. [43] expanded its application to individuals with other neurological disorders. Its strengths lie in its simplicity and reliability, making it easy to apply in controlled settings. However, the main limitation is its passive nature: because the stimulation does not adapt to the patient's voluntary effort or neural feedback, the opportunities for reinforcing motor learning and long-term neuroplastic changes are limited. Despite these constraints, open-loop FES has played a fundamental role in the history of neurorehabilitation, demonstrating that electrical stimulation can effectively support functional tasks such as grasping, reaching, or locomotor activity.

In contrast, closed-loop FES systems represent a significant advancement by integrating patient feedback into the stimulation process. These systems establish a feedback loop that allows electrical stimulation to be modulated in real time, depending on either cortical activity or muscular activation. The two most widely investigated closed-loop paradigms are brain-computer interface (BCI)-based FES and electromyogram (EMG)-controlled FES.

BCI-FES, also referred to as electroencephalogram (EEG)-FES, uses EEG to capture the patient's brain activity and translate it into control signals for the stimulator [19, 52](Figure 2.6b). A common paradigm is motor imagery (MI), in which patients imagine movements of their paretic limbs without executing them physically. MI has been shown to activate neural circuits that underlie real motor actions, promoting functional reorganization and neuroplasticity [8,99]. During rehabilitation, EEG recordings of MI events are processed by a computer-based system that generates a corresponding electrical stimulation pattern, which in turn elicits the intended movement in the affected muscles. This coupling of motor intention and movement outcome provides multisensory feedback that strengthens cortical reorganization and accelerates recovery. Their greatest advantage is that they actively engage the patient's attention and intention, making them powerful tools for harnessing neuroplasticity.

EMG-controlled FES systems represent another form of closed-loop stimulation, in which the feedback signal comes not from cortical activity but from muscular activity itself (Figure 2.6c).

EMG signals reflect the electrical currents generated during muscle contractions and provide real-time information about neuromuscular activity [1]. In EMG-controlled systems, voluntary muscle activity is detected and used to trigger or modulate FES, so that stimulation is applied only when the patient initiates a movement [34, 73]. This integration of voluntary effort and stimulation-induced contraction enhances motor learning, accelerates functional recovery, and reduces the likelihood of overstimulation, cramps, and fatigue [40]. Importantly, EMG-controlled systems ensure that the patient remains an active participant in the rehabilitation

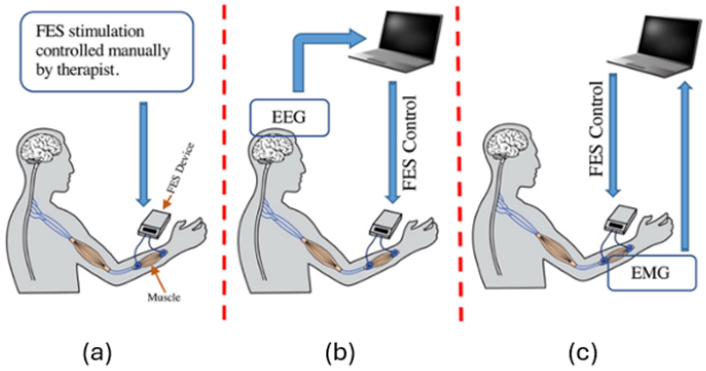

Figure 2.6: Control strategies in FES: (a) open-loop FES controlled manually by the therapist; (b) closed-loop BCI-FES using EEG to trigger stimulation; (c) closed-loop EMG-FES where muscle activity modulates stimulation in real time. Reproduced from [41]

process, which is essential for fast motor relearning and long-term functional gains.

Together, open-loop and closed-loop systems illustrate the technological and therapeutic progression of FES in neurorehabilitation. Open-loop FES demonstrated the feasibility of using patterned electrical stimulation to restore basic functional movements but lacked adaptive responsiveness to patient feedback. Closed-loop systems, whether BCI- or EMG- controlled, introduced dynamic interaction between the patient and the stimulator, maximizing neuroplasticity and rehabilitation outcomes.

While open-loop systems remain valuable for their simplicity and reliability, closed-loop approaches represent the future of FES, offering personalized, feedback-driven therapies that hold the potential to significantly improve the quality of life of patients.

2.4.2 Clinical Application of Open-Loop FES for Upper Limb Rehabilitation After Stroke

A large body of research has evaluated the clinical potential of open loop FES for restoring motor function in post-stroke patients, particularly in the upper limbs. Nakipoglu Yuzer and colleagues [103] conducted a randomized controlled trial (RCT) on 30 hemiplegic patients, applying two-channel stimulation through four surface electrodes to spastic wrist flexors. Results demonstrated a significant reduction in spasticity and improvement in clinical scores, supporting the role of FES as an effective tool to counteract hypertonia.

Makowski and collaborators [55] expanded on functional applications by examining hand opening in patients with impaired voluntary control. Their findings showed that while voluntary effort alone was insufficient due to flexor coactivation, combing FES with reaching and hand-opening stimulation significantly increased functional hand opening (3.8-8.8 cm), even when patients exerted minimal or no effort. This highlights the ability of FES to overcome abnormal muscle synergies and enhance functional reach-to-grasp patterns.

Further evidence was provided by Meadmore and co-workers [58], who delivered stimulation to the shoulder, elbow, and wrist muscles in five patients across 18 sessions. Functional outcomes were assessed using FMA and the ARAT, both of which showed a mean improvement of 4.4 points. These results suggest that even low-cost hardware integrated with advanced FES controllers can contribute to measurable reductions in motor impairment.

Sun and his team [88] investigated the feasibility of high-intensity therapy by applying FES to support upper limb functional activities in 22 stroke patients. With over 90% of the sessions

successfully completed by 17 participants, this study highlighted the capabily of FES to deliver structured, task-specific rehabilitation at intensities that surpass conventional face-to-face therapy.

A novel approach was introduced by Niu and his group [67], who employed programmable FES devices to generate stimulation patterns based on muscle synergies recorded from health individuals. Applied first to three patients and later expended to a second group, this method yielded significant improvements in FMA scores (28.6% $\pm$ 13.7%), demonstrating the potential of synergy-based FES in restoring coordinated movements. Building on this work, Chou and colleagues [14] designed an automated system to match electrically induced and voluntary residual movements. Patients showed more consistent compound movements with reduced root mean square (RMS) errors, reinforcing the added value of synchronization strategies. Martín-Odriozola and collaborators [57] reported the application of the Fesia Grasp device, a commercial open-loop stimulator specifically developed for hand dexterity rehabilitation. In their case study of a 69-year-old post-ischemic stroke patient, the device enabled meaningful functional recovery in hand use, supporting the translational potential of open-loop systems into clinical devices. Finally, Niu and co-workers [68] further validated the synergy-based approach in a task-oriented training (TOT) protocol with 16 patients. The group receiving FES demonstrated significantly higher FMA scores than the sham group, indicating the clinical efficacy of open-loop stimulation in structured rehabilitation programs. Overall, open-loop FES systems have proven effective in reducing spasticity, facilitating functional hand opening, improving proximal and distal motor control, and supporting high-intensity and task-oriented rehabilitation. While outcomes vary depending on protocol design and patient condition, a pooled analyses of three studies [58,67,68] including 17 stroke patients demonstrated a significant improvement in upper limb function as measured by FMA.

Specifically, the meta-analysis reported a Mean Differences (MD) of 5.6 [95% Confidence Interval (CI): 3.77-7.5, $p < 0.001$], indicating a robust and clinically meaningful effect of open-loop FES. Importantly, the results were statically homogeneous ($I2 = 0$, $p = 0.657$), suggesting consistency across the included trials and strengthening confidence in the reliability of the findings [41]. These results demonstrate that despite their simplicity, open-loop systems remain a clinically valuable tool for upper limb recovery after stroke, particularly when applied with innovative paradigms such as synergy-based control or commercial devices tailored for hand rehabilitation.

2.4.3 Clinical Application of Closed-Loop BCI-FES for Upper Limb Rehabilitation After Stroke

Unlike open-loop systems, closed-loop approaches integrate real-time feedback, ensuring that stimulation is dynamically linked with patient's neural activity. Among these, BCI-controlled FES systems have emerged as an optimal strategy, providing a direct interface between the brain and the stimulation device, thereby enhancing patient participation and engagement during stroke rehabilitation [63]. A typical BCI-FES consists of three main modules: the BCI unit (Figure 2.7b), which records EEG signals; the interface that translates EEG patterns into stimulation commands (Figure 2.7c); and the FES module that delivers electrical impulses to the impaired muscles (Figure 2.7d). In many implementations, the setup also integrates a virtual reality (VR) (Figure 2.7a) paradigm to provide immersive training environment. During therapy, patients are exposed to a VR task, such as hand flexion or extension, and are asked to imagine performing the displayed motion. This MI produces specific EEG signals performing that are processed by the BCI unit. The interface then generates trigger commands to control both ON/OFF states and the parameters of the stimulation, which in turn activities the relevant muscles and facilitates the intents movements. To make the system effective, patients usually undergo a training phase to learn how to generate distinct neural patterns through repeated mental practice, thus enabling reliable classification of motor imagery events [63].

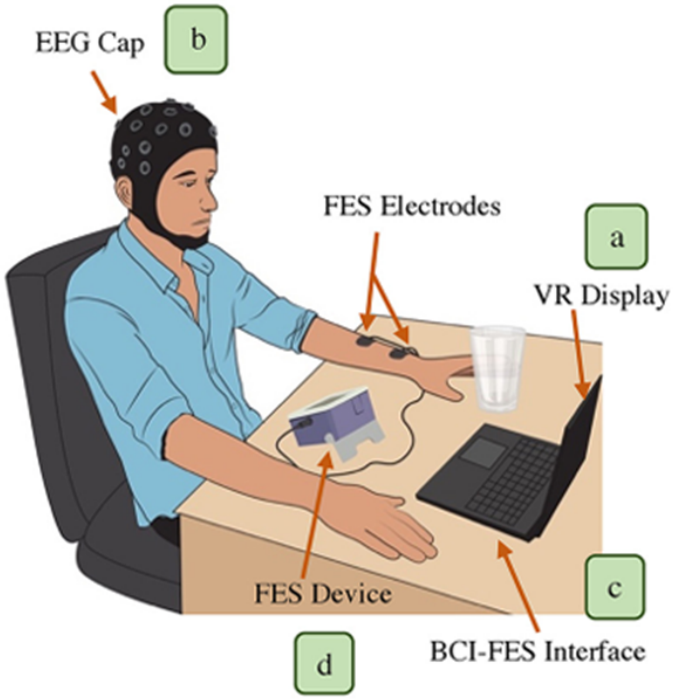

Figure 2.7: Closed-loop BCI-FES system consisting of (a) a VR display, (b) an EEG cap for brain signal acquisition, (c) a BCI-FES interface running on the computer to process EEG data, and (d) an FES device delivering stimulation through electrodes placed on the patient's forearm. Reproduced from [41]

The clinical application of BCI-FES has been extensively studied in RCTs. Cincotti and colleagues [16] conducted an RCT aimed at restoring hand grasping movements, using outcome measures such as the FMA, Medical Research Council (MRC) scale, and European Stroke Scale (ESS). Results demonstrated that patients receiving BCI-FES therapy exhibited significantly better motor recovery compared to those treated with conventional open-loop FES. Similarly, Li and collaborators [49] focused on stroke survivors with severe upper limb paralysis, reporting a MI classification accuracy of 77% and significantly improved rehabilitation outcomes in the BCI-FES group. Kim and co-workers [42] also validated the positive influence of BCI-FES in upper extremity recovery, confirming its superiority over traditional physical training. Further evidence was provided by Miao and Chen [11, 60], who emphasized the clinical benefits of BCI-FES in promoting motor activity restoration and enhancing upper limb function.

Beyond RCTs, several feasibility studies have demonstrated the practical applicability of BCI-FES systems. Daily and co-workers [18] developed a customized system and tested it on a stroke survivor with impaired finger extension. During the initial session, classification accuracies 97% for attempted movements and 83% for imagined movements achieved. Progressive improvements were observed across sessions, and after nine training sessions, the patient regained complete finger extension. Likewise, Mukaino and collaborators [64] reported the case of a stroke survivor treated with BCI-controlled neuromuscular stimulator, showing that this intervention promoted cortical plasticity and functional recovery.

Commercially available systems have also entered the clinical landscape. The RecoveriX system (g.tec), designed specifically for wrist dorsiflexion rehabilitation, exemplifies the translation of BCI-FES technology into practical use [36]. Multiple studies have validated its effectiveness reported classification accuracies of up to 95% and significant improvements in upper limb function in stroke survivors [12, 37, 74, 81, 84]. These findings highlight not only the technical

robustness of the system but also its ability to deliver clinically meaningful motor recovery outcomes.

Taking together, evidence from both controlled trials and feasibility studies demonstrates that BCI-FES systems offer a powerful closed-loop strategy for post-stroke rehabilitation. By linking cortical activity, motor intention, and FES, these systems actively engage the patient's brain in the rehabilitation process, promote cortical plasticity, and lead to substantial improvements in motor function. This conclusion is further reinforced by a recent meta-analysis of six studies [11, 49, 64, 84] including 99 patients, which reported a significant improvement in FMA scores ($MD = 5.37$, 95% CI $(4.2 - 6.6)$, $p < 0.001$), with homogeneity across studies ($I2 = 0$, $p = 0.198$) [41]. As such, BCI-controlled FES represents one of the most promising therapeutic modalities in modern neurorehabilitation.

2.4.4 Clinical Application of closed-Loop EMG-FES for Upper Limb Rehabilitation After Stroke

An EMG-controlled system typically comprises three modules: an EMG sensing unit (Figure 2.8b), an EMG-FES interface (Figure 2.8c), and the stimulator module (Figure 2.8d). Some designs also integrate VR components (Figure 2.8a) to provide immersive and task-oriented rehabilitation sessions. Therapy generally begins with calibration, during which EMG thresholds and maximal stimulation levels are set individually for each patient.

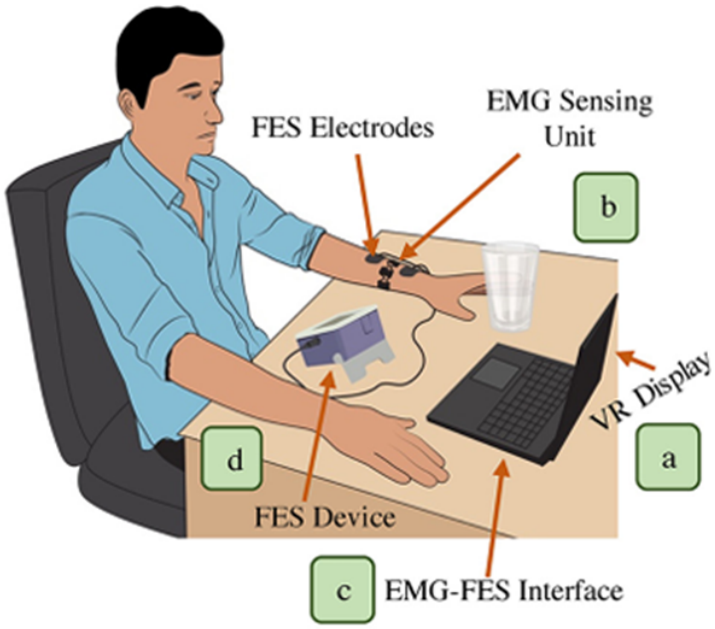

Figure 2.8: Closed-loop EMG-FES system consisting of (a) a VR display providing visual feedback, (b) an EMG sensing unit acquiring muscle activity, (c) an EMG-FES interface running on the computer to process the recorded signals, and (d) an FES device delivering electrical stimulation through electrodes placed on the patient's forearm. Reproduced from [41]

.

During training, the patient attempts a specific movement (for example, wrist extension), and the EMG unit records the myoelectric activity. Once the predefined threshold is reached, the system not only triggers the FES but also scales the stimulation intensity to match the voluntary contraction, thus producing a coordinated movement that combines voluntary and electrically induced muscle activity. This adaptive feedback loop ensures that stimulation levels vary according to the patient's real-time muscular effort, reinforcing motor learning mechanisms.

Several clinical studies and RCTs have investigated the efficacy of EMG-controlled FES in upper limb rehabilitation. Shindo and colleagues [86] conducted an RCT using the myoelectric-controlled stimulator developed by Muraoka and his team [65]. Over three weeks of training (five sessions per week), stimulation was applied to the paretic extensor digitorum communis muscles during finger extension tasks. Improvements were evaluated using FMA and the ARAT, and results showed that EMG-controlled stimulation produced greater functional improvements compared to control groups.

Further advances came from the group of Thorsen, who developed the MeCFES system [89, 91]. In an RCT involving 11 stroke survivors, EMG electrodes placed on wrist and finger extensors controlled stimulation for extension tasks. The experimental group demonstrated significant improvements in upper limb function measured by ARAT [90]. Building on these results, Thorsen's team conducted the first large multicenter RCT on TOT with MeCFES, involving 68 stroke survivors across several rehabilitation centers [39]. The results confirmed that MeCFES-assisted TOT was both safe and effective, showing clear functional improvements without adverse events. More recently, an updated wearable and portable version, named FITFES, has been developed to support task-oriented training in ambulatory settings. Although still in the prototype phase, initial feasibility testing has shown promising usability [17].

Additional mechanistic insights were provided by Hara and colleagues [35], who examined the relationship between brain cortical prefusion (BCP) in the sensorimotor cortex (SMC) and functional outcomes during EMG-FES therapy. Using near-infrared spectroscopy (NIRS), they observed increased activation of the SMC during therapy, which correlated with significant improvements in FMA and HGS scores. These findings provide neurophysiological evidence that EMG-controlled FES promotes cortical plasticity and contributes to functional recovery.

Overall, clinical investigations demonstrate that closed-loop EMG-FES systems offer an effective and safe rehabilitation strategy for stroke survivors, particularly for upper limb recovery. By coupling voluntary muscle activation with adaptive stimulation, these systems enhance patient engagement, promote cortical reorganization, and lead to measurable functional improvements. From early EMG-trigged approaches to advanced EMG-controlled systems like MeCFES and FITFES, the evidence indicates that technology represents a promising direction for post-rehabilitation, with the potential to become a standard component of task-oriented therapy programs. This conclusion is further supported by a meta-analysis of three EMG-controlled FES studies [35, 39, 86] involving 60 patients, which reported a substantial increase in FMA scores [$MD = 14.14$, 95% CI (11.72-16.6), $p < 0.001$]. Importantly the data were homogeneous ($I2 = 0$, $p = 0.006$), underscoring the consistency of findings across trials and reinforcing the clinical value of EMG-FES in promoting upper limb motor recovery [41].

Chapter 3

The Lazarus FES device

Lazarus is a closed-loop EMG-controlled FES device, in which the stimulation intensity is regulated by the Average Threshold Crossing (ATC), a parameter extracted in real time from the EMG signal of the target muscle. The device can be employed for upper-limb rehabilitation as well as for lower-limb rehabilitation.

The Lazarus device is operated via dedicated software that can run on any standard PC, allowing the clinician to control the system and manage the patient database.

Its architecture consists of the Apollux unit (Figure 3.1a), the programmable open-loop FES stimulator Hasomed RehaMove2 (Figure 3.1c), stimulation channels (Figure 3.1d) and a PC running the control software (Figure 3.1b), which uses Bluetooth dongle to receive ATC data.

For stimulation, commercially available electrodes can be employed, while standard electrocardiogram (ECG) electrodes are used for EMG acquisition.

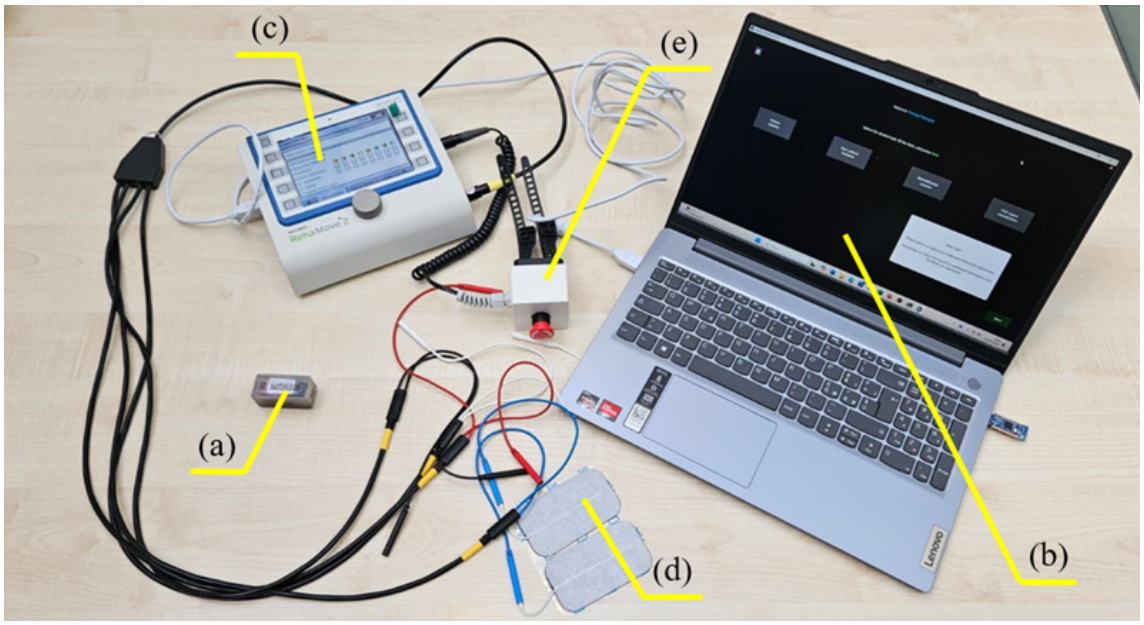

Figure 3.1: The Lazarus device is composed of: (a) the Apollux unit, (b) the Lazarus control software running on the physiotherapist's PC, (c) the open-loop FES system HASOMED RehaMove2, (d) the stimulation channels, and (e) the emergency button.

The device can be operated either directly by the patient for self-stimulation or by the physiotherapist, who guides the patient's movement as desired.

3.1 Apollox Unit

The Apollux unit is a compact, wearable, and bio-inspired sEMG platform that implements the ATC paradigm to sense, process and wirelessly transmit muscular information with very low energy cost while preserving clinically meaningful features of muscle activation. ATC reframes sEMG acquisition around three converging principles: (i) bio-inspiration, whereby neural communication through spikes mimicked by representing quantitative information as series of digital pulses; (ii) event-based design, which activates processing only upon meaningful threshold-crossing events, thereby minimizing unnecessary computation and energy consumption; and (iii) information synthesis, in which feature extraction is performed directly on the sensor node, drastically reducing data transmission load and enabling edge computing. Concretely, once the sEMG is amplified and filtered, every threshold crossing is treated as an informative event, and the number of crossings in an observation window defines the ATC parameter (3.1):

$$E = \frac{\#TC_{events}}{T_{window}} \tag{3.1}$$

where the $\#TC_{events}$, which represents the total number of observed threshold-crossing (TC) events detected relative to a certain threshold, and T_{window}, which denotes the observation time window. This parameter scales with contraction intensity and has been shown to fit sEMG particularly well compared with classic features such as Zero-Crossing (ZC) and Wilson Amplitude (WAMP), with strong force correlations close to those of Absolute Rectified Value (ARV); the correlation remains acceptable (> 0.9) even with substantial event loss, supporting ATC's robustness as a low-power surrogate of force estimation and enabling coarse force-level discrimination when thresholds are optimized per subject [7, 78, 92].

Building on this signal model, the hardware architecture co-designs conditioning and feature extraction so that threshold-crossing (TC) generation occurs directly in the analog front-end (AFE), shifting feature extraction from software into hardware. This would been impossible using descriptors such as ZC or WAMP, which require full sampling of the sEMG signal and subsequent processing only after digitization. By contrast, ATC can be implemented directly in hardware because the TC signal is quasi-digital in nature and can be counted through the standard input/output interfaces of the microcontroller, without the need for any additional analog-to-digital (ADC) conversion circuity. This functionality has been realized through both the design of an application-specific integrated circuit (ASIC) and the development of a printed circuit board (PCB) based on commercial off-the-shelf components [30, 83].

The block diagram in Figure 3.2 illustrates the architecture of the AFE of the Apollux unit for sEMG acquisition and threshold-crossing extraction. The system relies on three electrodes: two differential sensing electrodes (VE1 and VE2) and one reference electrode (VER). At the input stage, both sensing channels are equipped with protection circuits to guard against overvoltage and electrostatic discharges, followed by impedance decoupling units. The main objectives at this stage are to ensure the amplifier inputs the correct impedance, effectively isolating them from the electrode-skin impedance, and to preserve the integrity of the sEMG signal. The signals are then filtered through a differential high-pass filter (DHPF) with a 30 Hz cutoff, designed to attenuate motion artifacts and low-frequency disturbances without compromising the physiological sEMG bandwidth.

The conditioned signals are fed into the first amplification stage, which employs an instrumentation amplifier (InAmp) with a fixed gain of 500. This stage ensures high common-mode rejection, thereby reducing environmental and power -line interferences. A low-pass filter (LPF) with a cutoff at 70 Hz is integrated in the feedback path of the InAmp to suppress low-frequency noise components and stabilize the baseline. The VER is stabilized through a dedicated driving circuit, which can operate either as a simple buffer or as Driven Right Leg (DRL) circuit. The DRL configuration actively injects an inverted version of detected common-mode signal back into the body effectively minimizing common-mode noise and further improving signal quality.

The second amplification stage consists of a programmable gain amplifier (PGA), which provides additional selectable gains of x 1, x 2, x 3, x 4 or x 5 . This design allows the system to adapt to different muscles and electrode placements, where signal amplitudes may vary significantly. Each gain path ensures that only the dynamic components of the sEMG are amplified, thus preventing baseline drift from suturing the amplifier. Following amplification, a Sallen-Key low-pass filter with a cutoff frequency of 400 Hz defines to the physiological sEMG range to function as an anti-aliasing filter in case the signal is digitized by an ADC. The final block of the chain is the voltage comparator, which transforms the analog sEMG waveform into a quasi-digital threshold-crossing (TC) signal. The comparator threshold is set via a digital-to-analog converter (DAC), allowing dynamic adjustment depending on the subject's resting baseline and environmental noise conditions. A built-in hysteresis of approximately 30 mV converts the comparator into a Schmitt trigger, thereby preventing spurious events caused by oscillations of the signal around the threshold. The output of this stage consists of two distinct signals: the raw conditioned sEMG, available for conventional analysis, and the TC signal, which can be directly fed to a microcontroller for real-time event counting without the need for additional analog-to-digital conversion. The digital core of the Apollux unit is built around the

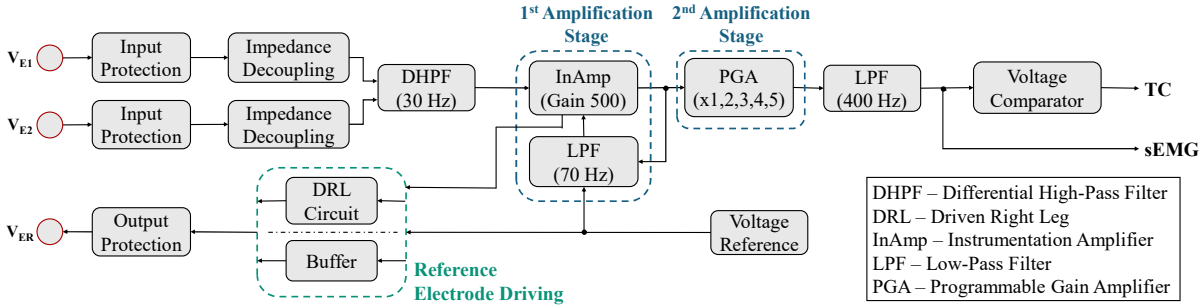

Figure 3.2: Block diagram of the AFE of Apollux unit for sEMG acquisition and threshold-crossing (TC) extraction. Reproduced from [79]

.

Apollo3 Blue microcontroller, which integrates an ARM Cortex-M4F processor optimized for low-power operation and concurrent task management. This unit is responsible for both feature extraction and wireless communication, and it interfaces directly with the AFE. To support versatile operation, several additional peripherals are included: a UART-to-USB converter for debugging and firmware bootloading, two I2C connectors for chained inter-board communication, a digital-to-analog converter (DAC) used to finely calibrate the detection threshold, and a USB-compatible battery charging circuit that enhances wearability by enabling autonomous operation. Communication with external devices is enabled either via a UART-to-USB bridge or through BLE transmission via the integrated antenna (Figure 3.3). All of these parts are orchestrated through FreeRTOS, which allows seamless real-time management of ATC event continuing and Bluetooth 4.2 data transmission.

A critical part of this digital architecture is the automatic threshold calibration, which ensures robust detection of TC events under varying physiological and environmental conditions. Since the ideal threshold should be set just above the resting sEMG baseline to detect genuine muscular activations while rejecting noise, the firmware executes an adaptive routine structured as a finite state machine. As shown in Figure 3.4, the process begins with a conservative high threshold (1.8 V) and progressively decreases it in large steps (-150 mV) until an event is observed. Once an event is detected, the algorithm checks for confirmation to discard spurious spikes; if confirmed, the threshold is temporarily raised ($+200$ mV) to start fine tuning. Subsequent states refine the calibration with smaller (-10 mV), again requiring double confirmation

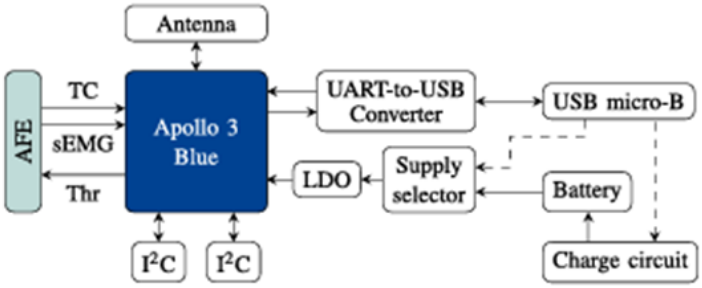

Figure 3.3: Schematic block of the digital part: Apollo3 Blue represents the central core of the system, which processes the signals from the AFE and manages wireless communication. Reproduced from [79]

.

of events to ensure robustness against transient noise. Finally, once a stable baseline is established, the threshold is raised slightly (+40 mV) to account for comparator's hysteresis, and the calibration terminates. This multi-step routine guarantees that the system dynamically adapts to noise fluctuations, electrode placement variability, and inter-subject differences without user intervention.

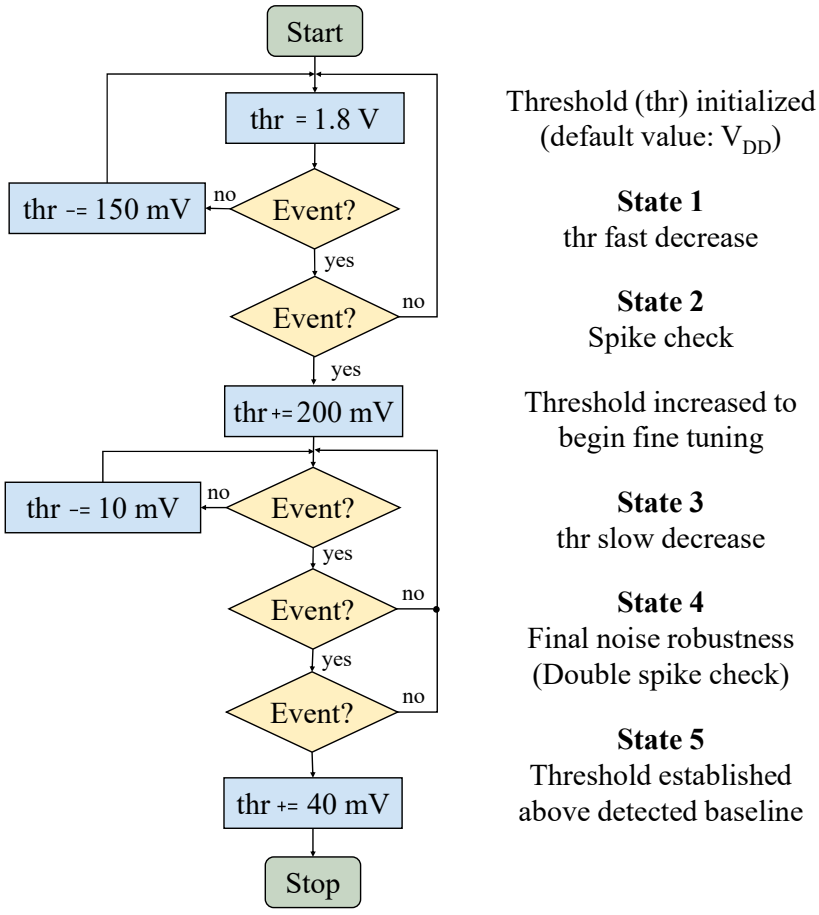

Figure 3.4: Firmware routine for threshold auto calibration. Reproduced from [79]

.

Once the calibration is completed, the ATC evaluation is triggered by enabling interrupts the microcontroller pin connected to the TC signal. Each TC event generates an interrupt service routine call, incrementing a counter. At the end of the user-defined observation window (130 ms), the total event count is stored as the ATC parameter, and the counter is reset. By using this quasi-digital TC signal, the system avoids continuous analog-to-digital conversion, significantly reducing both computational load and energy consumption. In the present implementation, the main clock frequency is configured at 24 MHz, reduced from the default 48 MHz, since the application does not require higher rates.

The Apollux unit adopts a compact, wearable architecture built on a standard four-layer PCB (20.5 x 33.2 x 9.5 mm) expressly organized to segregate sensitive analog circuitry from noisy digital domains. The entire AFE is placed on the bottom layer, while the top layer hosts the digital subsystem- Apollo3 Blue Microcontroller unit (MCU) module, power-supply control, battery charger, and I/O interfaces- so that the inner layers can be dedicated to signal routing and solid power/ground planes. This stack-up reduces electromagnetic coupling, improves return paths, and stabilizes the reference rails, which is crucial when the AFE is operating at high gains. For the MCU, the design integrates SparkFun's Artemis module (10 x 15 mm), which packages the Ambiq Apollo3 Blue into a small footprint eith a proven layout, easing firmware development, simplifying assembly. Height-saving planar connectors are used for battery, debug, electrodes, I2C and reset, keeping the z-profile low and the wearable form factor unobtrusive. Both JTAG and a USB micro-B port are included to allow in-system programming, debugging, and direct wired communication during development and testing (Figure 3.5). The board is en-

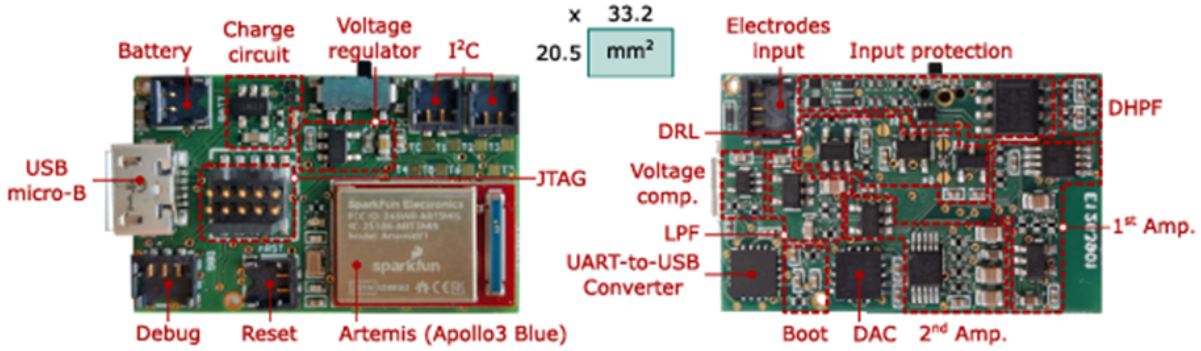

Figure 3.5: PCB of the Apollux unit. Reproduced from [79]

.

closed in a purpose-designed 3D-printed case that completes the wearable system by integrating a rechargeable battery and electrode connectors. The finished device measures 57.8 x 25.2 x 22.1 mm (Figure 3.6). To minimize cabling and improve ergonomics, the three electrodes (and their connectors) are positioned directly beneath the PCB, mechanically secured by the battery holder so the assembly sits stably over the target muscle. A dedicated opening exposes the USB micro-B connector, allowing the battery to be recharged without disassembling the unit. With adhesive wet electrodes the device adheres directly to the skin without additional straps.

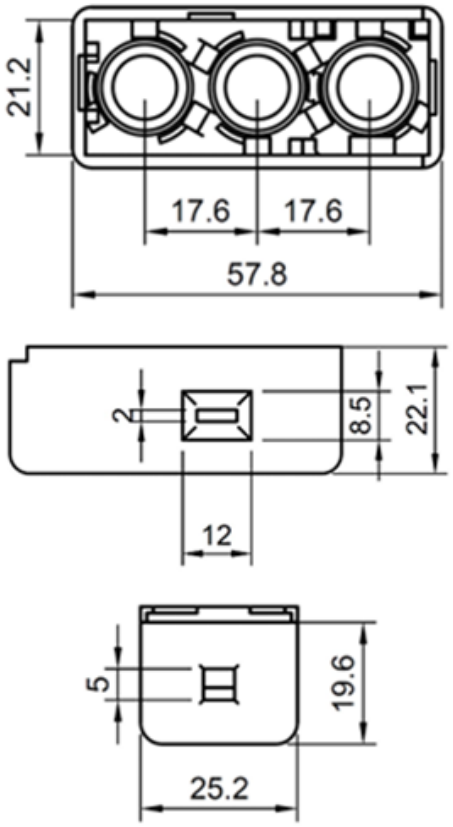

Figure 3.6: Design specification of the 3D-printed case of the Apollux unit. Reproduced from [79]
.

Thanks to the embedded Bluetooth Low Energy (BLE) interface, the device requires only a minimal external setup to operate: a commercial USB dongle (Nordic nRF52840) or any BLE-equipped host can act as the receiver, providing a straightforward bridge between the wearable node and the user interface on a PC [79].

3.2 Steps of the Rehabilitation Process Using Lazarus and Patient Database Registration

The rehabilitation therapy with the Lazarus device consists of the following steps:

1. Patient registration within the Lazarus software database;
2. Creation of the rehabilitation pattern;
3. Calibration of the device on the patient;
4. Execution of the rehabilitation therapy.

When a new patient uses the Lazarus device for the first time, they must be registered in the database through the dedicated interface of the control software. The software, developed in Python and running on physiotherapist's computer, provides a function called "New Patient Inclusion". Once this option is selected, the physiotherapist is prompted to enter the social security number (Figure 3.7).

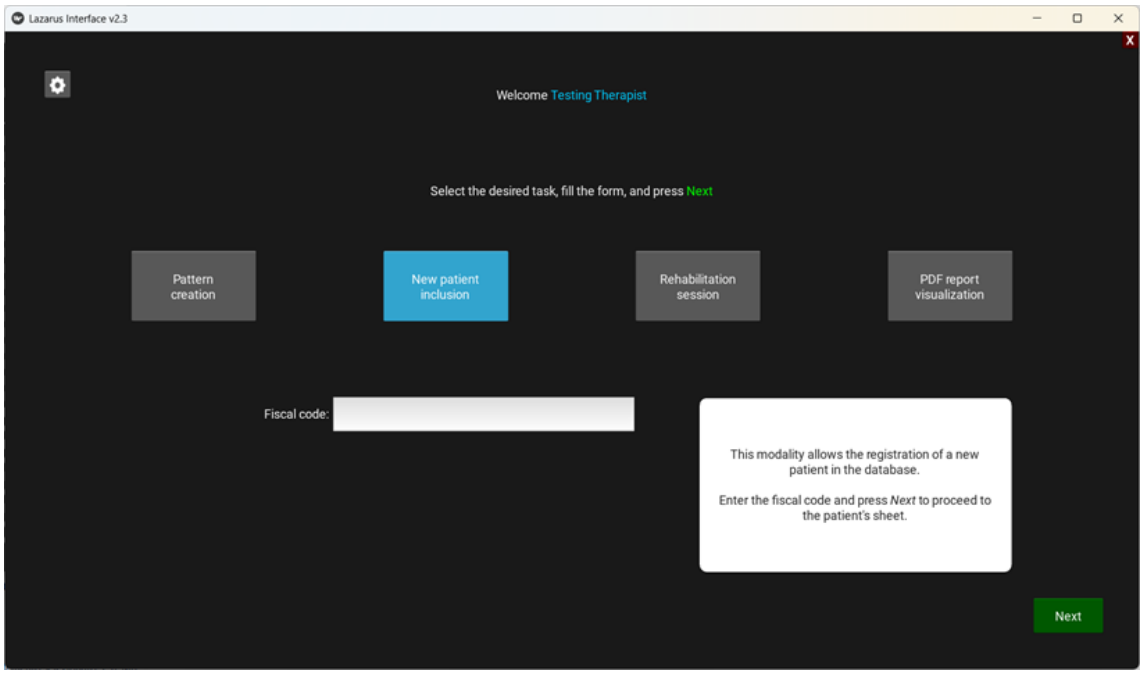

Figure 3.7: Initial interface of Lazarus Control Software, and the field in which the physiotherapist must enter the social security number.

The process then proceeds to the next interface, where the remaining personal details must be completed, including first and last name, and email address. Additional, non-mandatory information can also be recorded, such as the reason for the visit, the patient's medical history, therapist's notes, and the recommended treatment plan (Figure 3.8).

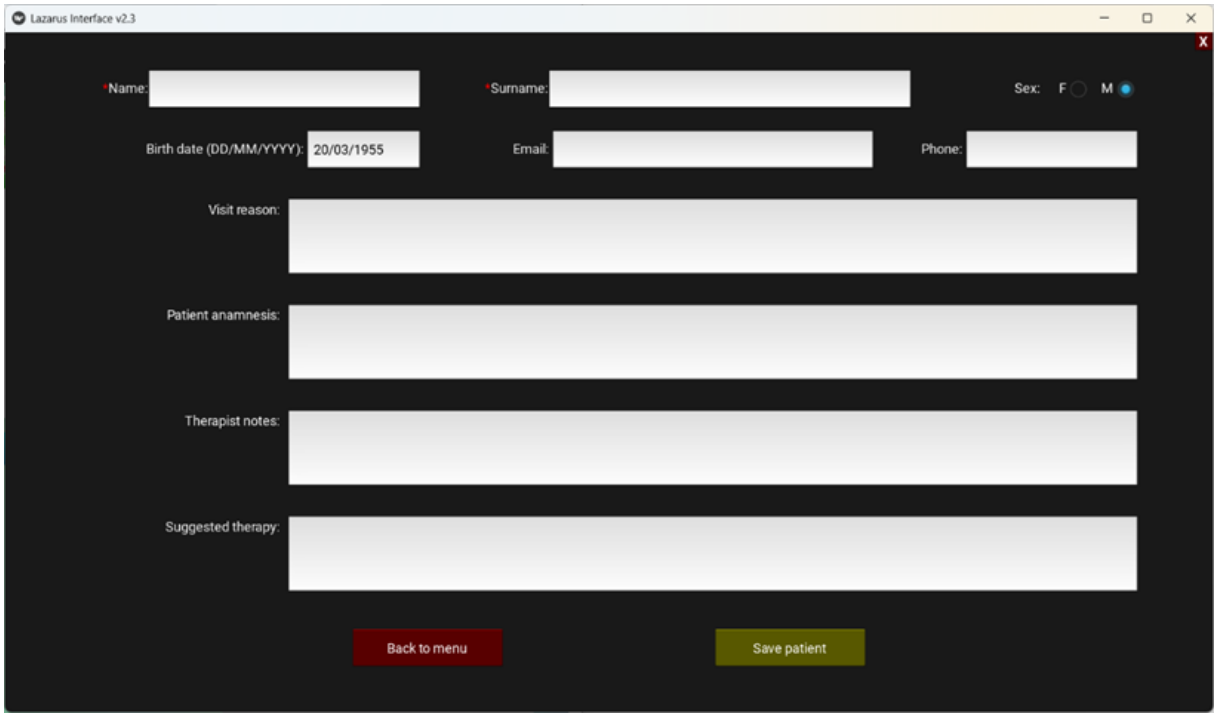

Figure 3.8: The interface where the physiotherapist completes the patient's registration by entering the remaining details.

3.2.1 Creation of Rehabilitation Pattern and Calibration Phase

When the physiotherapist wants to generate a pattern for a specific muscle or muscles to be rehabilitated, they must click on the "pattern creation" option from the home screen of the control software. Once this is done the system will ask for the name of the movement to be rehabilitated (Figure 3.9). The entire pattern creation process can be carried out either with a single Apollux- resulting in a single-channel configuration- or with multiple Apollux units- enabling a multi-channel configuration.

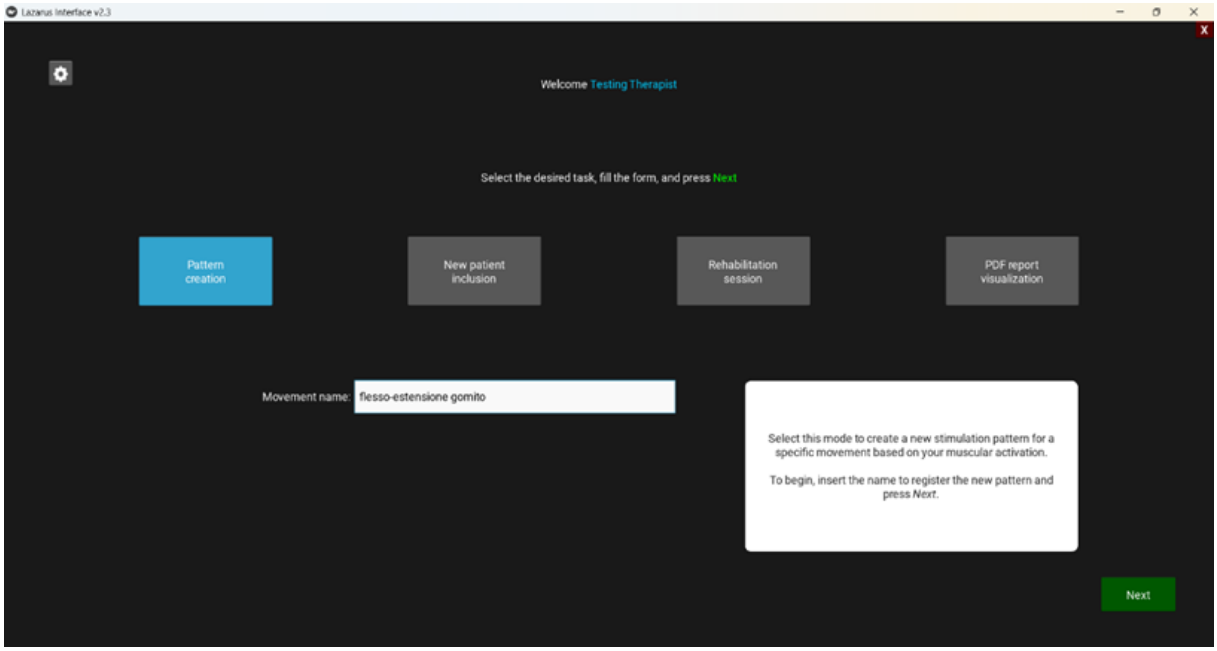

Figure 3.9: Home screen of the software, where the physiotherapist initiates the pattern creation process and enters the name of the movement to be rehabilitated.

Before starting the ATC acquisition, the system must connect to the Apollux unit or units currently in use. At this stage, the physiotherapist must specify both the stimulation channel to which the acquired signal will be assigned and the muscle from which the ATC signal is being recorded (Figure 3.10).

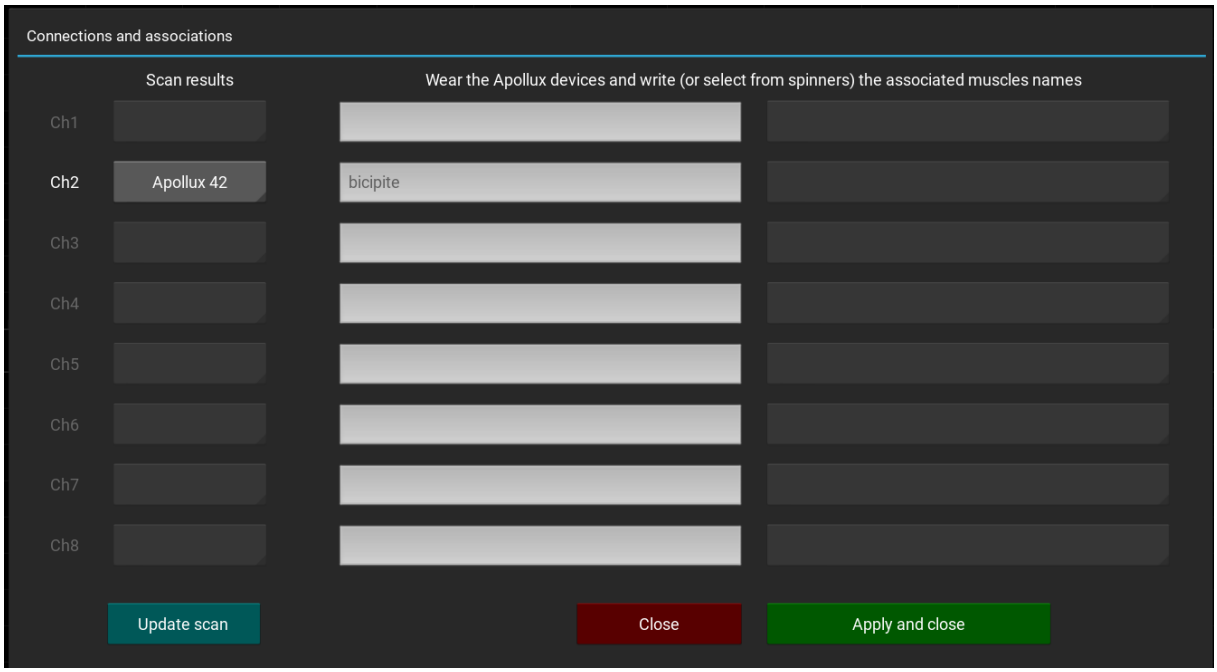

Figure 3.10: Window where the physiotherapist assigns the Apollux unit to a stimulation channel and specifies the name of the movement to be stimulated.

After that, the ATC is acquired from the target muscle or muscles. To complete the pattern creation process, the rehabilitation movement must be repeated several times (Figure 3.11). This can be done either by the patient or by the therapist. The resulting raw data will consist of multiple ATC curves placed side by side, representing the muscle or muscles activation pattern.

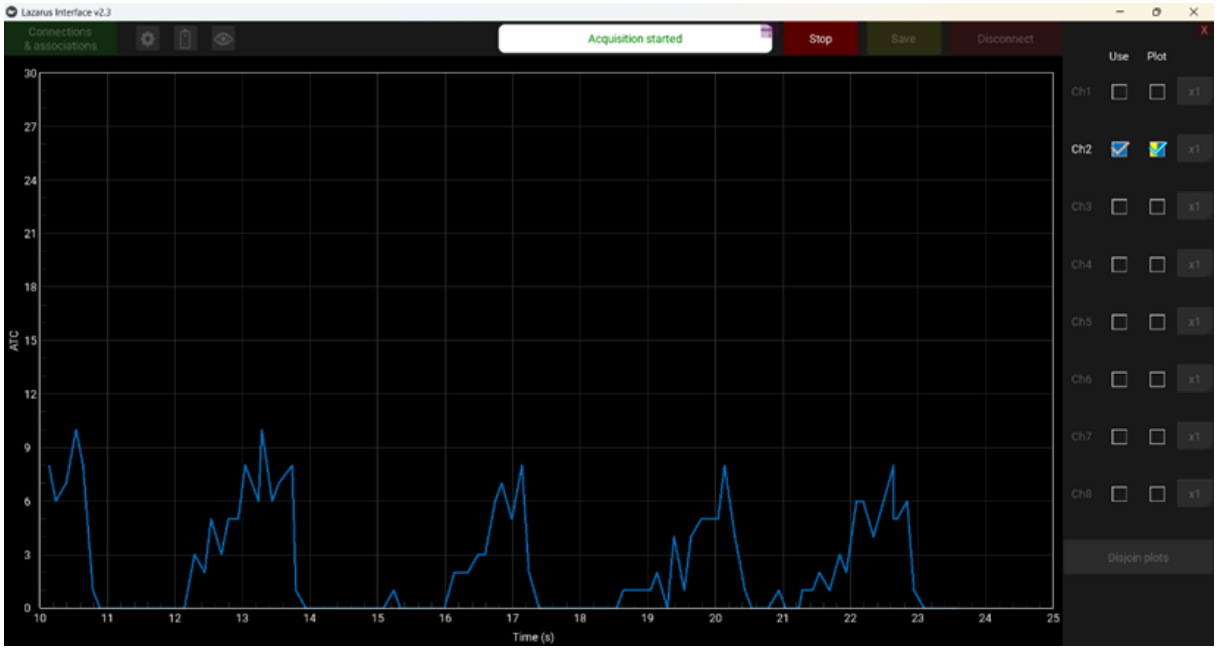

Figure 3.11: Raw ATC signal recorded during the pattern creation phase.

Subsequently, the raw data must be processed to extract meaningful information and generate the muscle or muscles activation profile required for the next phases. The Profile Extraction

(PE) pipeline begins with the smoothing of the raw ATC signals, which despite being intrinsically robust [78], can still be influenced by the background noise and spurious threshold-crossing events. To mitigate these effects, each acquisition channel undergoes median filtering (Figure 3.12b), thereby regularizing the signal and minimizing unwanted fluctuations. Once the signals are smoothed, the algorithm performs movement segmentation (Figure 3.12c) by monitoring the data streams in real time to detect functional contractions. A movement can be identified either as individual activity, when a single channel shows continuous non-zero ATC values or at least one significant peak, or group activity, when multiple channels are simultaneously activated beyond a predefined Group Factor Threshold (GFT), which quantifies inter-channel synergy. Each detected contraction is segmented into a movement matrix, where rows represent channels and columns correspond to time samples, and the movement is considered complete when group activity is no longer observed for a set number of iterations. Following segmentation, the algorithm applies an irregular movement rejection step (Figure 3.12d), based on the assumption that repetitive voluntary tasks should yield reproducible activation patterns. All segmented movements are compared through a Similarity Index computed from channel-wise-cross-correlations weighted by channel contributions. Movements with similarity below 0.7 are discarded as irregular, and this process is repeated until only consistent and reproducible patterns remain. In the final stage, the remaining movements are aligned (Figure 3.12e) and combined to extract the profile. Alignment is achieved by selecting the most consistent movement as reference, cross-correlating all others against it, and shifting them accordingly, with zero-padding applied to equalize their lengths. The aligned matrices are then stacked into a three-dimensional array, from which the final multi-channel profile is extracted by applying the median (Figure 3.12f) across repetitions. The result is a stable and biomimetic representation of muscular activity that enables accurate and reproducible calibration of FES, particularly in multi-channels applications.

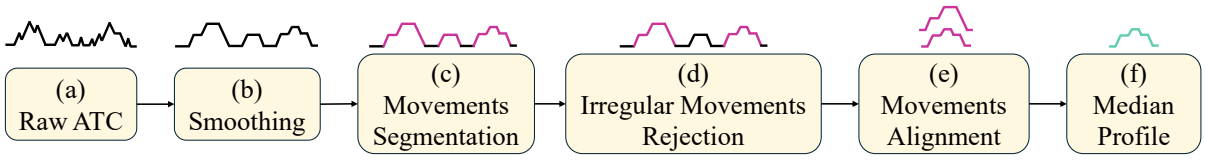

Figure 3.12: Schematic representation of the Profile Extraction (PE) pipeline, which starts from the raw ATC signal that is first (b) smoothed, then (c) segmented into movement repetitions, followed by the (d) rejection of irregular or inconsistent movements, after which the valid repetitions (e) are aligned and finally combined through a median operation. Reproduced from [45]

In Figure 3.13a, the median ATC profile is shown, derived from the signals depicted in Figure 3.11. This phase is essential to determine the maximum ATC value, which is directly associated with the muscle contraction of a specific muscle in the given patient during a particular movement. After the pattern creation phase, the process continues with the patient calibration stage, during which each patient receives a pyramidal-shaped stimulation pattern closely resembling the previously extracted median ATC profile. This step is necessary to determine the maximum current intensity required by the patient to perform the target movement. To achieve this, the operator first starts the procedure from the home sceen shown in Figure 3.9, by clicking on Rehabilitation Session, selecting the patient to be rehabilitated from the database, choosing Patient calibration activity, and then selecting the specific movement to be calibrated. A clearer view of the interface is provided later in Figure 3.15.

The patient then receives a series of stimulations starting from a predefined maximum current value (8 mA by default in the device), with the maximum value being gradually increased in steps of 2 mA for each subsequent stimulation (Figure 3.13b). The operator must stop the

sequence of pulses as soon as the patient is able to perform the target exercise. At the beginning of this phase, the operator can also adjust the stimulation parameters such as frequency (fs) and pulse width (PW), which are recommended to be set at the minimum values reported in the literature, namely 20 Hz for the frequency and 150 μs for the PW [87].

(a)

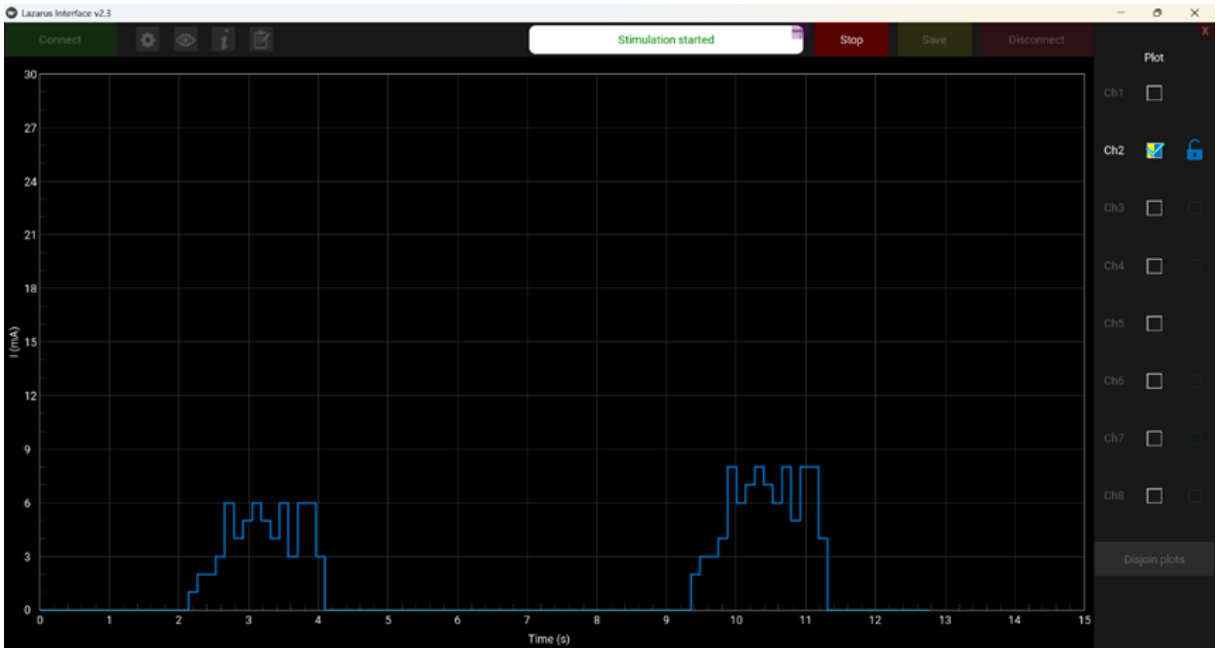

(b)

Figure 3.13: The (a) median ATC profile obtained from the data presented in Figure 3.11 and (b) pyramidal-shaped stimulation pattern delivered to the patient during the calibration phase.

After both the pattern creation and patient calibration phases have been completed, the system generates a lookup table for the specific patient and exercise. This table links the maximum ATC value- used as the column index of the matrix- with the maximum current intensity identified during the calibration. Figure 3.14 provides a practical example of this

concept with four channels: for each channel, the table associates the maximum ATC value obtained during the pattern creation phase with the corresponding maximum current value determined during the calibration phase.

Maximum ATC

15	10	13	7
Ch 1	Ch 2	Ch 3	Ch 4

Maximum current (mA)

42	18	12	24
Ch 1	Ch 2	Ch 3	Ch 4

Fes current Matrix (mA)

Ch 1	0	0	3	6	9	12	15	18	21	24	27	30	33	36	39	42
Ch 2	0	0	2	4	6	8	10	12	14	16	18	-	-	-	-	-
Ch 3	0	0	1	2	3	4	5	6	7	8	9	10	11	12	-	-
Ch 4	0	0	4	8	12	16	20	24	-	-	-	-	-	-	-	-
	0	1	2	3	4	5	6	7	8	9	10	11	12	13	17	15

Figure 3.14: Lookup table example with four channels, showing the maximum ATC values from pattern creation (orange) linked to the maximum current values from calibration (purple) and the corresponding FES current matrix. Reproduced from [80]

3.2.2 Rehabilitation Session using the Lazarus device

Once all the previous phases have been completed, the physiotherapist can start the actual rehabilitation session using ATC- based therapy control. To access this mode, the therapist must open the Rehabilitation Session section, select the patient who will perform the movement, choose the type of movement, and then start the Online Session Activity (Figure 3.15)

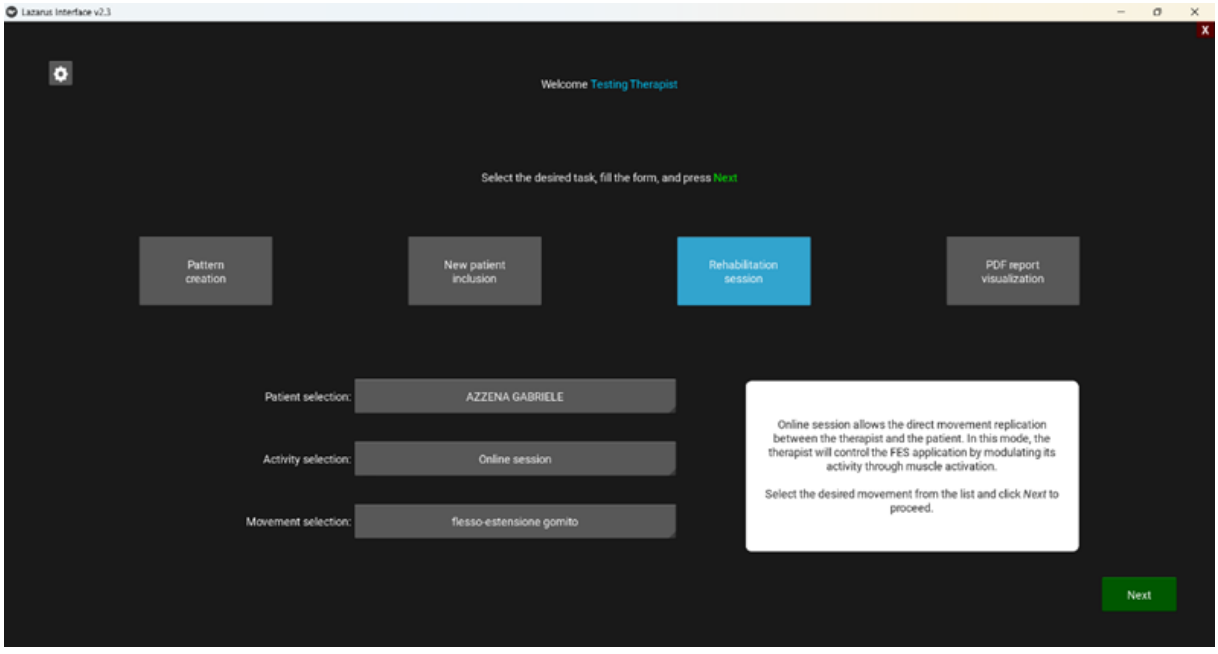

Figure 3.15: Screen from which the physiotherapist can access the Rehabilitation Session section, select the patient and the type of movement to be performed.

After this step, the therapist must select the Apollux or Apollux units in use and place them on muscles from which the signals were recorded during the pattern creation phase. Similarly to what was shown previously in Figure 3.10, for example, the therapist has to connect an Apollux unit to the biceps muscle, as indicated by the physician during the pattern creation, and assign it to stimulation channel 2, which delivers the stimulation to the patient.

When the physiotherapist clicks Apply and Close, the actual rehabilitation session begins. During this phase, two real-time graphs are displayed: one showing the ATC signal detected from the target muscle-either from the patient or from the therapist, depending on the selected operating mode- and the other showing the amount of current, expressed in milliamperes (mA), delivered to patient's arm (Figure 3.16).

Figure 3.16: Example of the rehabilitation interface displaying, in real time, the ATC signal from the target muscle and the stimulation current delivered to the patient's arm.

To associate each measured ATC value with a corresponding current intensity, the device relies on the lookup table generated at the end of the calibration phase. Each time a new BLE packet arrives containing data from n channels the values are appended to an n x 4 matrix (ATC matrix), which also stores the three most recent ATC windows. A row-median operation is then applied to obtain a robust ATC estimate, effectively filtering out noise. Since the ATC matrix is updated with every new ATC window, this procedure acts as moving median. The result is an n x 1 array, whose values are interpreted as indices pointing to the corresponding stimulation intensities in the FES Current Matrix. Once the new amplitude of the stimulation is defined through this algorithm, an FES data packet is constructed and transmitted to the stimulator. An example of this process with four channels is shown in Figure 3.17, similar to the one previously presented in Figure 3.14.

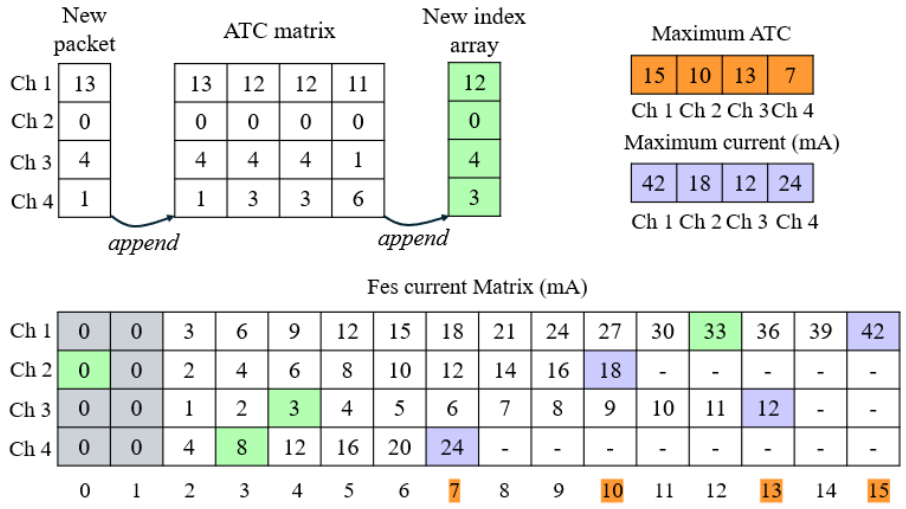

Figure 3.17: Example of the algorithm applied to a four-channel configuration, where ATC values are mapped to stimulation intensities in the FES Current Matrix.

3.3 Limitations of the Lazarus Device

The Lazarus presents two main limitations:

1. There is a lack of feedback mechanisms to monitor the quality of therapy.
2. It is not possible to automatically or objectively adjust stimulation parameters during the therapy session [87]. In fact, the Lazarus requires the therapist to manually control the remaining stimulation parameters, fs and PW, through a dedicated interface before the beginning of the rehabilitation session (Figure 3.18).

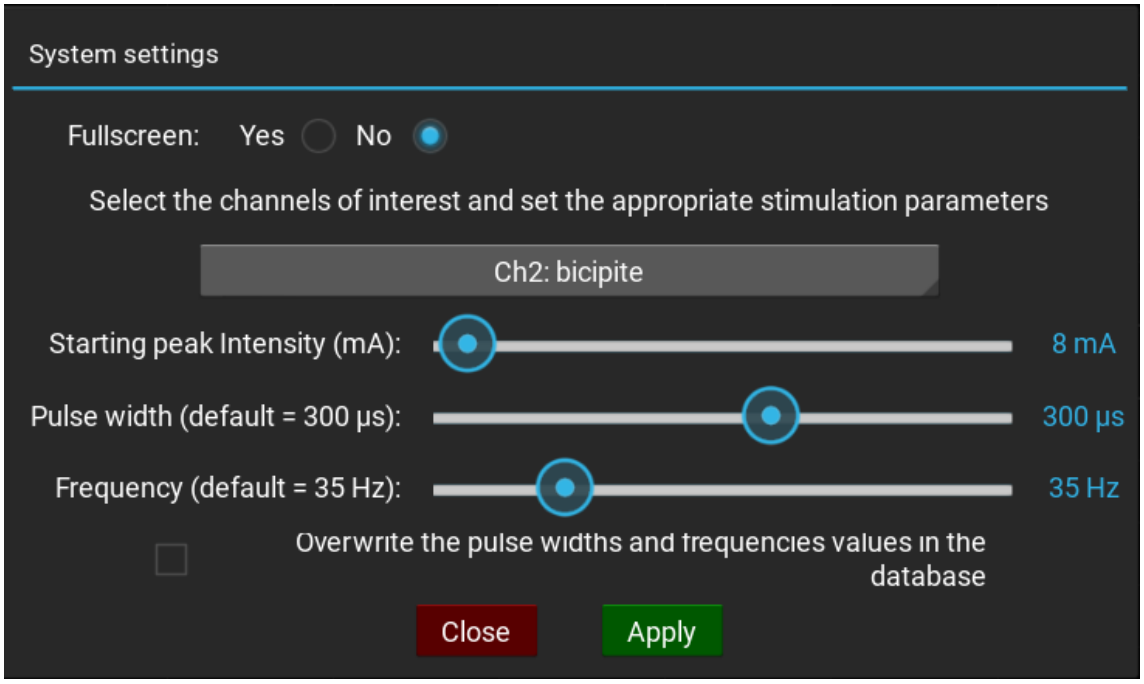

Figure 3.18: Interface of the Lazarus device, where the therapist manually adjusts the stimulation parameters- frequency (fs) and pulse width (PW).

Regarding the first limitation, the Lazarus, like almost all instruments typically used in rehabilitation, don't provide objective feedback on the quality of the delivered treatment, once again leaving this evaluation to subjective clinical assessment.

As highlighted by the second limitation, the effectiveness of the therapy depends on the therapist's ability to choose the most appropriate values of the parameters. This approach inevitably makes the therapy highly subjective, since parameter selection relies exclusively on the therapist's personal experience and clinical judgment.

To address these issues, this thesis introduces RehabCam, an innovative software solution designed to integrate with the Lazarus device. RehabCam assists the physiotherapist by suggesting optimal stimulation parameters and, at the end of each rehabilitation session, generates a PDF report summarizing all key metrics required to objectively assess session quality.

Chapter 4

RehabCam: an Assistive Software for the Lazarus Device and Preparatory Tests for the Trial

RehabCam is an innovative software solution, developed in Python, that integrates two simple RGB webcams into the Lazarus device setup. Each webcam is directed toward on of the patient' s arms (left or right) and computes key metrics for movement analysis, which are then used to compare the motion of two arms in real time (Figure 4.1 a and Figure 4.1 b). If discrepancies are detected between these metrics, the system suggests updating the stimulation parameters (f_s and PW); otherwise, the parameters remain unchanged. These key metrics are also used to assess the overall quality of the rehabilitation session.

Figure 4.1: The set-up of the Lazarus system integrated with RehabCam, showing (a) the webcam monitoring the right arm and (b) the webcam monitoring the left arm.

To perform movements analysis, the system employs a convolution neural network (CNN), specifically the YOLOv8 Pose model developed by Ultralytics, which provides an efficient real-time approach for estimating joint positions [54]. For this application, joint positions are represented as 2D coordinates, which are sufficient to extract the parameters required for movement analysis. The choice of YOLOv8 was motivated by its speed, accuracy and scalability [100]. The network used for this purpose was pre-trained and validated on the large-scale COCO8-pose dataset, which contains a wide variety of labeled human poses, enabling robust detection of body parts and their relationships [95]. Thanks to its efficiency, the network operates in real time, requiring only a few ms to identify key positions such as those of the shoulder, elbow, and

wrist, which are the joints utilized in this work (Figure 4.2).

Figure 4.2: Example of shoulder, elbow and wrist key points along with their connections extracted using the YOLOv8-Pose model.

4.1 RehabCam Homepage and Patient Registration

The software homepage provides three options: starting a rehabilitation session, managing patients, and exiting the system (Figure 4.3).

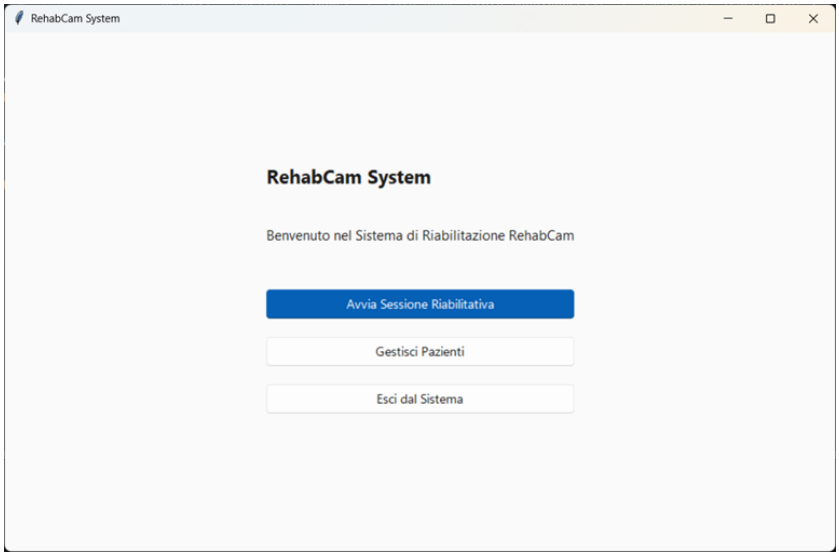

Figure 4.3: Homepage of the RehabCam software, showing the main options available to the clinician.

The first step for the clinician is to register the patient within RehabCam by clicking on Manage Patients. This interface displays all patients already registered in the system, and from here the clinician can add a new patient, edit an existing one, or remove a patient from the database (Figure 4.4). This step is fundamental, as the system generates a unique ID for each patient in order to identify their movement data for every exercise, which are stored in a locally saved database on the therapist's computer.

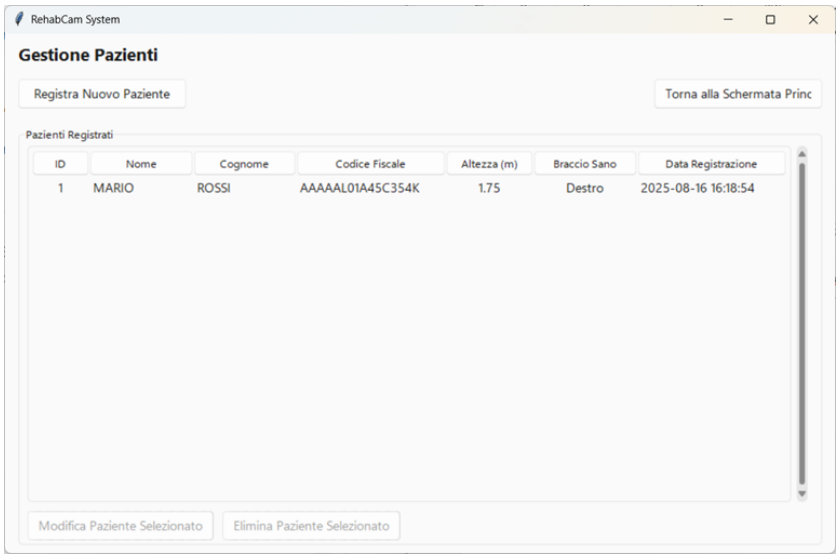

Figure 4.4: Screen where the clinician can edit the patient database, including viewing, modifying, and deleting registered patients.

After registering the patient, the therapist can start the rehabilitation session by clicking the Start Rehabilitation Session button on the main screen (Figure 4.3). Once selected, the interface checks whether the required webcam is properly connected and whether the neural network has been correctly loaded. If these conditions are met, the therapist can choose the patient who will receive the therapy, the type of exercise to be performed, the duration of the session, and assign each webcam to the corresponding arm. In addition, the interface provides feedback on exercise execution, displaying a small message below each exercise to indicate whether it has been successfully performed (Figure 4.5).

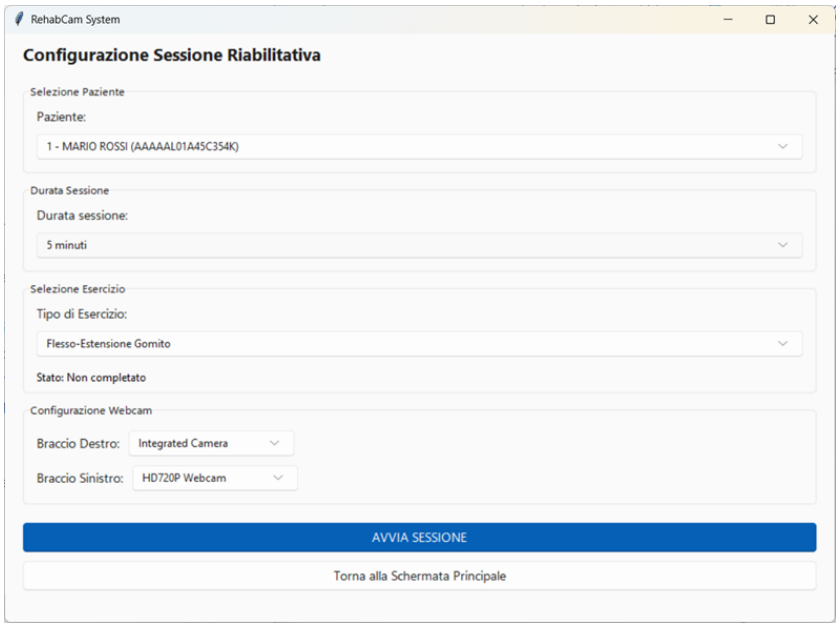

Figure 4.5: Screen where the clinician can edit the patient database, including viewing, modifying, and deleting registered patients.

4.2 Key Movement Parameters Computed by the RehabCam software

The key movement parameters calculated by the RehabCam software are the relative height of the wrist with respect to the elbow (Figure 4.6a),the wrist velocity, the timing of the movements and the angle between the upper arm and the forearm (Figure 4.6b) .

To calculate these quantities the system uses the coordinates extracted by the YOLOv8-Pose network, which are expressed in pixels. YOLO provides these coordinates in a reference system with its origin at the top-left corner of the image. They are then converted into relative reference system with its origin at the elbow, as shown in Figure 4.6a.

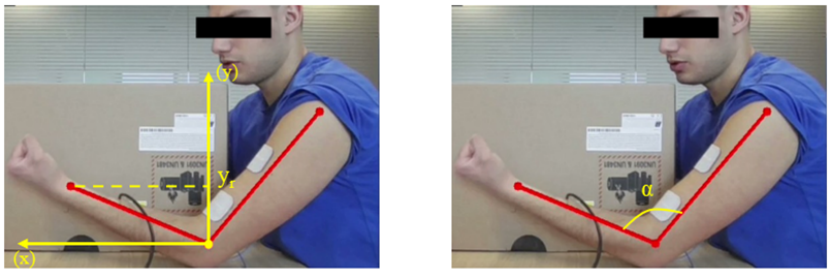

(a) (b)

Figure 4.6: A graphical example of (a) relative height and of (b) the angle between the upper arm and the forearm calculated by the RehabCam software.

For this computation, the wrist coordinates are used directly, while the elbow and shoulder coordinates are taken as the average of their values over the preceding frames, including the most recent one returned by the network. From these relative coordinates, the relative height, which is calculated as follows 4.1:

$$y_r = |y_w - y_e| \tag{4.1}$$

where y_r denotes the relative height of the wrist with respect to the elbow, y_w is the y-coordinate of the wrist, and y_e is the y-coordinate of the elbow. The absolute value is applied because the images of two arms have inverted coordinates signs; thus, to enable comparison, all values are considered as positive. In this formulation the coordinates are expressed in pixels, although from the operator's perspective it would be more meaningful to represent them in standard measurement units, such as centimeters. To achieve this, the distance calculated in pixels is multiplied by a conversion factor, which is defined as follows 4.2:

$$K_{cm} = \frac{(l_m \times 100)}{l_P} \tag{4.2}$$

where l_m denotes the anthropometrically estimated forearm length, expressed in centimeters by multiplying the patient' s height by an anthropometric factor [101] and then scaling by 100, while l_p represents the pixel-based distance between the elbow and the wrist, computed as the Euclidian distance between these two points. For the calculation of the angle in degrees between the upper arm and the forearm, the following formula is used 4.3:

$$\alpha_t = \cos^{-1}\left(\frac{\vec{p_t} \cdot \vec{q}}{|\vec{p_t}|\,|\vec{q}|}\right) \tag{4.3}$$

where $\vec{p_t}$ is the vector from the elbow to the wrist, and $\vec{q}$ is the vector from the elbow to the shoulder. The term $\vec{p_t} \cdot \vec{q}$ represents the dot product of these two vectors, while $|\vec{p_t}| \cdot |\vec{q}|$ denotes the product of their magnitudes, and the two vectors $\vec{p_t}$ and $\vec{q}$ are computed as follows 4.4, 4.5:

$$\vec{p_t} = e_{x,y} - w_{x_t,y_t} \tag{4.4}$$

$$\vec{q} = e_{x,y} - s_{x_t,y_t} \tag{4.5}$$

Along with the angle and wrist height relative to the elbow, the wrist velocity is also computed as follows 4.6:

$$v_w = \frac{d_w}{\Delta t} \tag{4.6}$$

where d_w is the Euclidean distance between the wrist positions in the current frame and the previous one, multiplied by the scale factor K_{cm}, calculated as in equation 4.2, and divided by 100 to convert the distance into meters, and finally divided by the time interval between the two frames.

The height (in centimeters), the angle (in degrees), and the velocity (in meters per second) are recorded for each frame in dedicated text files, organized by the main phases of the software workflow and separately for each patient's arm. The acquisition time of each frame, expressed in seconds, is also stored, allowing the calculation- through post-processing of the extracted variables- of wrist movement timings such as rise time, fall time, and total movement duration. Unlike the other parameters, these timing values are not displayed on screen in real-time during the execution of the rehabilitation.

4.3 Rehabcam Rehabilitation Steps

The Rehabcam system follows three main steps:

1. **Scale factor estimation**;
2. **Extraction of the minimum and maximum angle for normalization in the stimulation parameter control implementation**;
3. **Execution of rehabilitation session**.

In the first step, the therapist must verify the reliability of the measurements provided by the system. During this phase, with the patient resting their forearms on the table, the therapist checks that the two webcams are correctly positioned by comparing the angle values, which should be as similar as possible. The patient is then asked to raise both arms as much as possible, which helps detect an incorrect scale factor K_{cm}. If an error in scale factor estimation is identified, the operator can recalculate it by clicking the Recalibrate button; otherwise, they can proceed to the next step by selecting Next (Figure 4.7).

Figure 4.7: Interface of RehabCam software where the therapist can either recalibrate the scale factor or proceed to the next phase of the workflow.

The next phase consists of extraction of the maximum and the minimum angle from a single repetition performed by the patient while carrying out a simple elbow flexion-extension movement. The final step is the rehabilitation session, where the actual control of stimulation parameters takes place. In this phase, the RehabCam software is used in combination with the Lazarus device, set to rehabilitation mode as described in section 3.2.2. The developed algorithm runs in parallel on both arms and uses the derivate of the arm elevation signal, which is expected to be positive above certain threshold, as the first trigger. When this condition is met, a state variable is updated to indicate the beginning of a potential repetition. After this event, the algorithm searches for the minimum joint angle until the value starts to increase again. When this occurs, the algorithm identifies the descending phase of the movement through two parallel conditions serving different purposes: the first one activates another state variable confirming that a valid repetition has taken place, based on the detection of a negative derivative of the elevation signal; the second condition instructs the system to stop searching for the minimum angle, as the descending phase has begun, and it is based on the derivative of the angle evolution between two consecutive frames. Once this process is complete, the minimum angle is normalized using min-max scaling, computed from the maximum and minimum values extracted in the previous step. At the end of each repetition, if the stimulated arm does not move, or if its movement is too limited and falls outside a predefined tolerance threshold of the normalized minimum angle, computed with respect to the value reached by the healthy arm that controls the contraction, the system suggests updating the stimulation parameters. Conversely, if the stimulated arm reaches a normalized minimum angle lower than that of the controlling arm, or if it remains within the threshold, the repetition is considered valid and successfully completed. All of these operations are managed through dedicated control variables that are assigned specific values to communicate state transitions and ensure proper synchronization between both arms throughout the execution of the algorithm. The algorithm is also illustrated in graphical view through a block diagram in Figure 4.8.

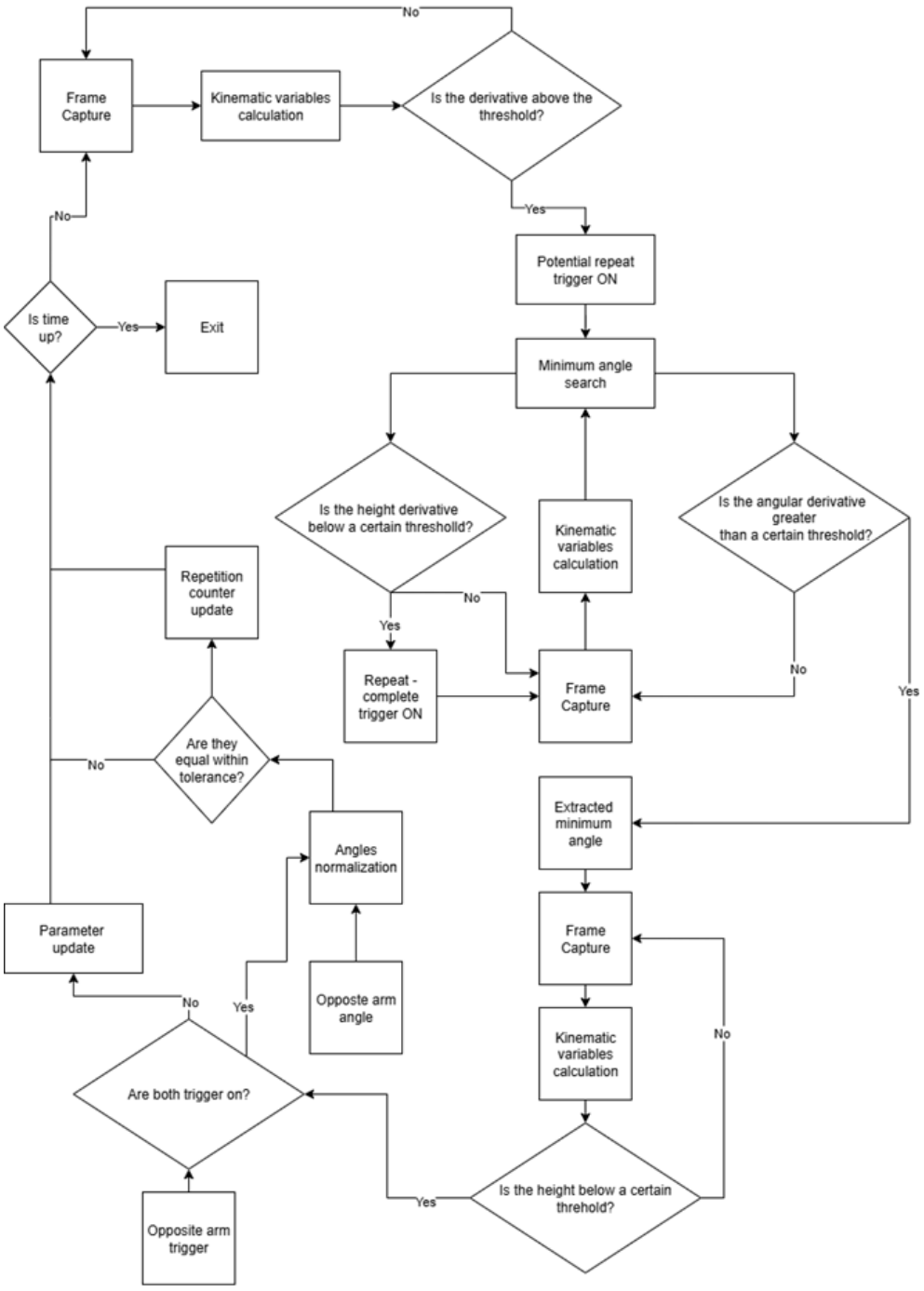

Figure 4.8: Block diagram of the algorithm for comparing the movement between the two arms.

The adaptation process of fs and PW first increases the PW by 50 μs for each repetition in which the movements of the two arms are not comparable, up to a maximum of 450 μs. Once this limit is reached, the PW is reset to the initial value of 150 μs, while the frequency is increased by 10 Hz. The control strategy always starts with low stimulation parameters, namely a frequency of 20 Hz and a PW of 150 μs. The block- diagram illustrating the parameter update mechanism is presented in Figure 4.9.

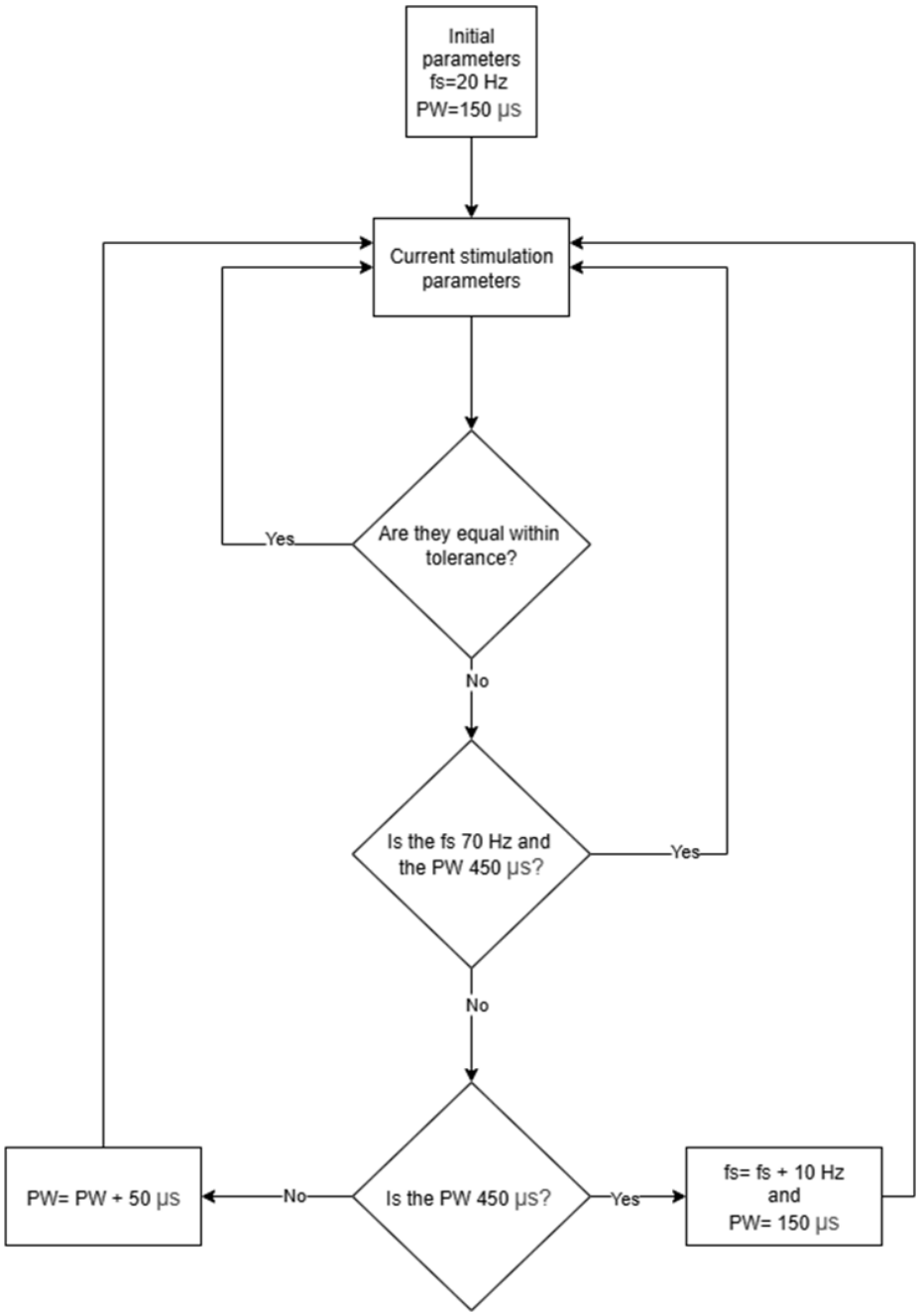

Figure 4.9: Block diagram of the parameter-update algorithm.

Each time the system recommends an update, a pop-up notification is shown to the therapist (Figure 4.10), who must pause the rehabilitation session of the Lazarus device to adjust the parameters as illustrated in the pop-up. This process described previously continues until the target rehabilitation time, defined at the beginning of the session, is reached.

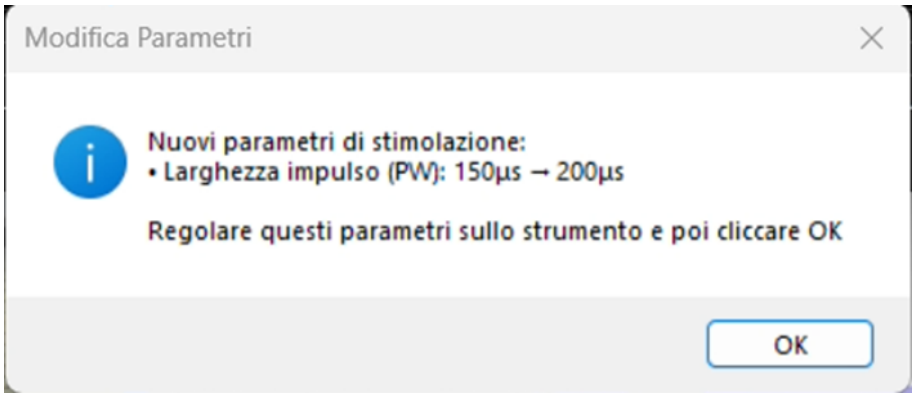

Figure 4.10: Example of a pop-up notification that alerts the therapist to update the stimulation parameters.

During the session, the system also tracks the number of repetitions performed by the patient and continuously updates, in real time, the wrist velocity, the relative height with respect to the elbow, and the angle between the upper arm and the forearm (Figure 4.11).

Figure 4.11: Example of the interface used during a rehabilitation session.

The explanation provided above refers to the use of the Lazarus device in the mode where the patient self-stimulates one arm through contractions of the other. However, the device can also be operated in therapist-patient mode. The only difference is that the extraction of the maximum and the minimum movement angles must be performed on the therapist' s arm, or more generally, always on the arm responsible for controlling the stimulation through its contractions. At the end of the rehabilitation session, the software processes the data collected during the therapy and generates a PDF report that provides the physiotherapist with a quantitative description of the session. The extracted metrics will be described in detail in the following sections.

4.4 Experimental Testing of the Lazarus Device Integrated with RehabCam

To evaluate the system composed of the Lazarus device used in combination with the RehabCam software, a dedicated experimental protocol was developed. The protocol consisted of task-oriented exercises designed to promote the recovery of daily life gestures. The selected exercises were:

- elbow flexion-extension with the wrist in both pronation and supination;

- drinking from a cup and placing it back;

- putting on and removing eyeglasses;

- opening and closing a box.

Each of these exercises lasts five minutes, resulting in a total session duration of 20 minutes for each subject. For this purpose, two electrode configurations were developed, selected according to the subject's comfort during the execution of the different exercises. In the first configuration, two rectangular electrodes are placed on one arm of the subject (Figure 4.12a), while a single Apollux unit is positioned on the opposite arm (Figure 4.12b), resulting in single-channel stimulation.

(a) (b)

Figure 4.12: Electrode placement for the first configuration: (a) stimulation electrodes and (b) Apollux unit.

The second configuration uses four square electrodes, placed on the biceps of one arm, which correspond to a two-channel stimulation setup (Figure 4.13a). In this case, two Apollux units are positioned on the opposite arm: one placed on the biceps brachii and the other on the brachialis muscle (Figure 4.13b).

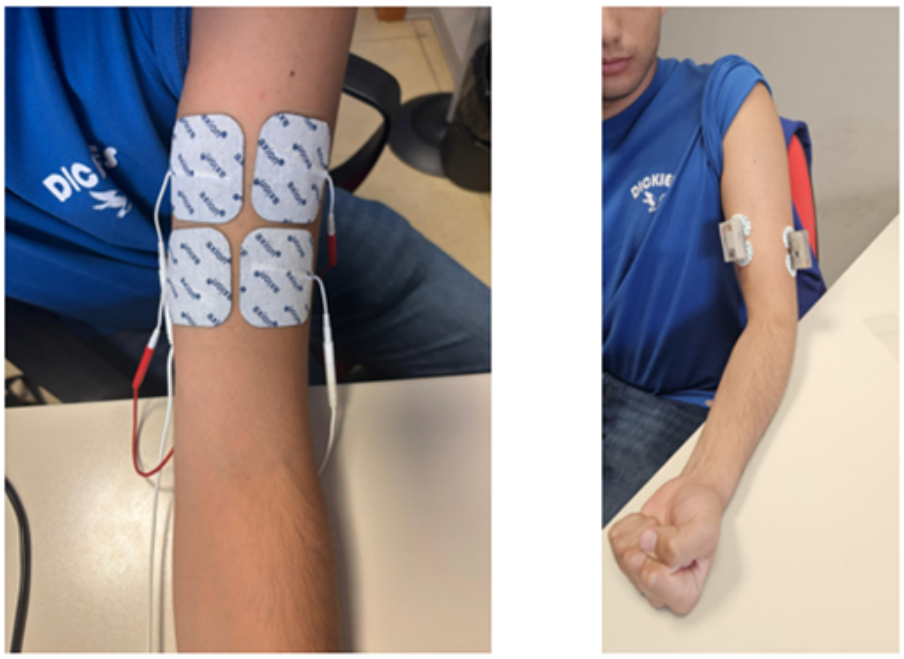

(a) (b)

Figure 4.13: Electrode placement for the second configuration: (a) stimulation electrodes, which are activated through diagonally corresponding stimulation channels, and (b) Apollux units.

Data acquisition for these exercises was carried out at the Department of Electronics and Telecommunications (DET) of Politecnico di Torino. The study involved nine participants, specifically four male and five female. The demographic and anthropometric characteristics of the participants are provided in Table 4.1.

Variable	**Value**
Age (years)	26.44 ± 4.59
Weight (kg)	61.11 ± 8.46
Height (cm)	169.44 ± 8.97
Sex	4 M, 5 F

Table 4.1: Anthropometric table showing data from participants in the experimental

4.5 Data processing

The data extracted during the rehabilitation session are post processed using Python and organized into tables, with each row corresponding to an exercise performed by a patient. The variables listed below are derived for these tables, included in the rehabilitation session report, and calculated separately for the right and left arm:

- **Average rise time (s):** calculated as the mean of all rise times, where each rise time is defined as the difference between the instant the arm reached its maximum height and the instant a repetition begins;
- **Average fall time (s):** calculated as the mean of all fall times, where each fall time

is defined as the difference between the instant a repetition end and the instant the arm reaches its maximum height;

- **Total repetition mean time (s):** calculated as the average duration of all repetitions, where each repetition time is defined as difference between the end instant and the start instant of the repetition;

- **Absolute minimum angle (degrees):** defined as the absolute minimum angle reached by each patient for each exercise;

- **Absolute maximum angle (degrees):** defined as the absolute maximum angle reached by each patient for each exercise;

- **Average minimum angle (degrees):** calculated as the mean of all minimum angles reached across repetitions, for each patient and each exercise;

- **Average maximum angle (degrees):** calculated as the mean of all maximum angles reached across repetitions, for each patient and each exercise;

- **Normalized mean peak height (Dimensionless):** calculated as the mean of all peaks across the repetitions divided by the length of each patient forearm;

- **Average velocity (m/s):** calculated as the mean of the patient's velocities, obtained by isolating the velocity values within each repetition, for every exercise and each patient.

- **Number of repetitions (Dimensionless):** The highest repetition count recorded for each patient for each exercise;

- **Optimal parameters (fs expressed in Hz and PW expressed in μs):** defined as the best stimulation parameter sets identified for each patient and each exercise. The optimal set is determined as the one that enables the highest number of consecutive repetitions; in case of a tie between multiple sets, the one allowing the smallest minimum angle to reached is selected. This quantity is calculated for the arm receiving the stimulation;

The angular variables extracted correspond to the internal elbow angle measured by the RehabCam software. To obtain the external angle, which represents the conventional reference for flexion-extension joint angle analysis, each value was computed as 180° minus the internal angle. In addition, graphical plots of the trajectories were generated to provide a visual representation of the movements. These trajectories are shown as a point cloud including all frames between the initial and final frame of each repetition. From this point cloud, an ideal trajectory was also derived: a circumference centered at the elbow, with a radius equal to the average distance of all points from the elbow (Figure 4.14).

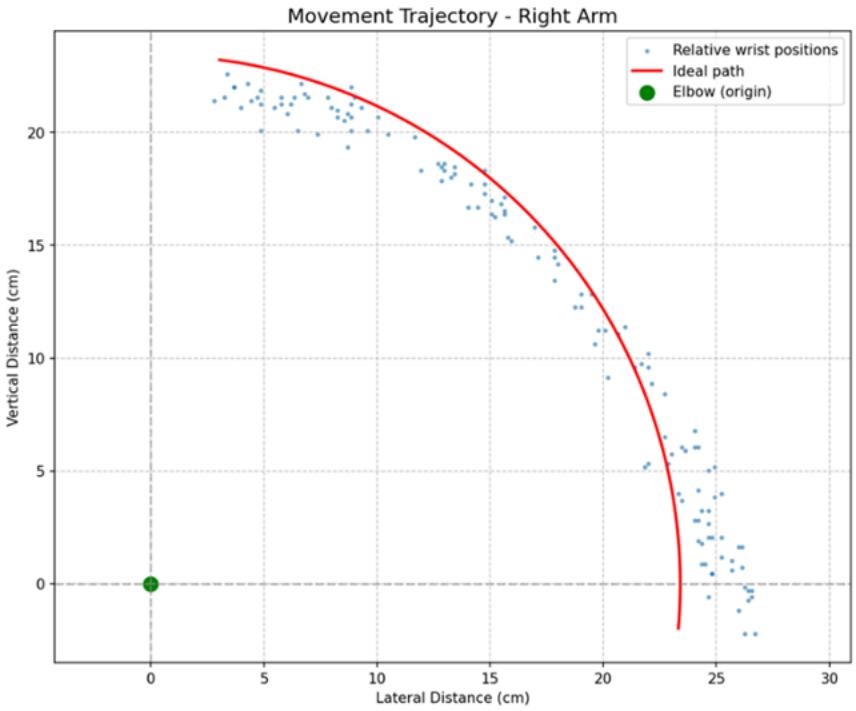

Figure 4.14: Example of the ideal trajectory, recorded trajectory points, and the elbow origin of a patient during the elbow-flexion exercise.

To assess the quality of the exercise performed during the session, an error parameter was computed with respect to the ideal trajectory. This parameter was calculated as the mean distance of each wrist point from the ideal trajectory, normalized by the forearm length, which was obtained as the mean distance between the elbow and wrist throughout the entire exercise duration. Once these values were calculated for each patient and each exercise and entered into the table, the mean and standard deviation (SD) were computed as descriptive statistics for each analysis group.

Chapter 5

Results and discussion

This chapter presents and discusses the main obtained results from the analysis of the parameters described in the previous chapter 4, based on the trials carried out by the participants. In particular, the data were compared and used to verify the correct functioning in terms of functional output of the developed system, and will also be used to qualitatively assess the performance of the program in terms of parameter updates.

5.1 Qualitative Analysis of Parameter Updates

Now the functioning of the RehabCam software is analyzed from a qualitative perspective, in order to verify whether the program operates correctly. As explained in the previous chapter 4, the RehabCam program intervenes in four specific cases:

1. when the normalized minimum angle of the limb receiving the stimulation falls outside the tolerance threshold compared to the same angle of the arm generating the stimulation, leading to an increase in the stimulation parameters;

2. when the arm receiving the stimulation does not move, resulting in an increase in the stimulation parameters;

3. when the normalized minimum angle value of the limb receiving the stimulation is lower than that of the limb controlling the stimulation, the number of repetitions is increased;

4. when the normalized minimum angle of the limb receiving the stimulation falls in the tolerance threshold, causing the repetitions to increase.

Regarding the first case, the example shown in Figure 5.1 is illustrative. In Figure 5.1a, the movement is detected by applying a threshold to the derivative of the height. Subsequently, the minimum angle of both the arm controlling the stimulation and the one being stimulated is identified (Figure 5.1b). After normalization (Figure 5.1c) and comparison, the parameter update is applied- specifically the PW- as described in the previous chapter. In this case, the PW increases by 50 μs, from an initial value of 200 μs to 250 μs, while the stimulation frequency remains constant at 20 Hz.

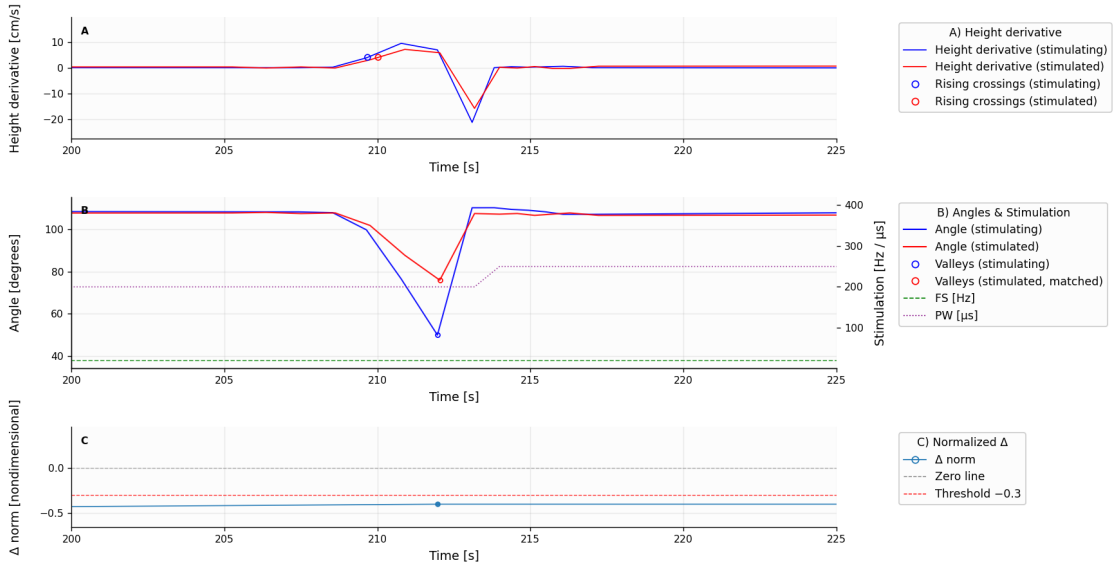

Figure 5.1: (a) Detection of the movement, (b) identification of the minimum angles, (c) comparison between normalized angles and (b) parameter update: PW increases from 200 μs to 250 μs, while fs remains constant at 20 Hz.

In the second case, the program detects movement only from the derivative of the limb controlling the stimulation, while the stimulated arm remains still (Figure 5.2a). As the system recognizes motion solely in the controlling limb and not in the stimulated one, it results in an increase of the stimulation parameters (Figure 5.2b).

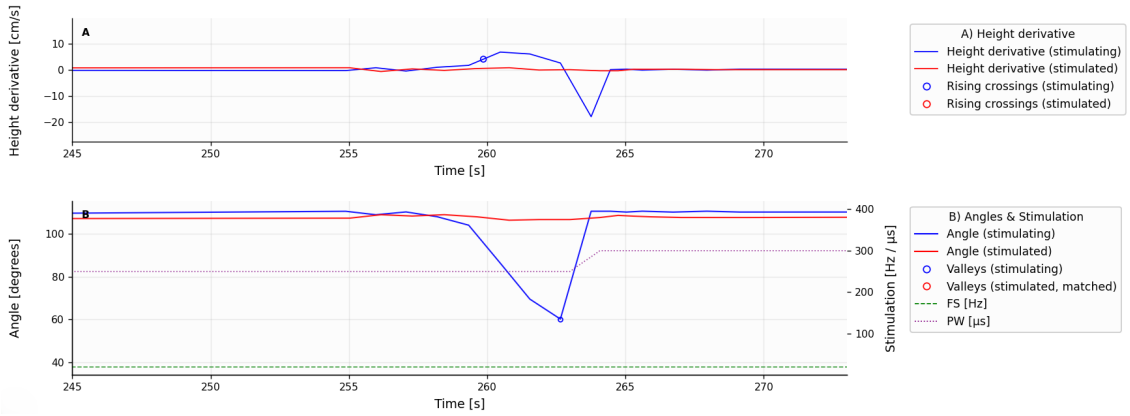

Figure 5.2: (a) Detection of the movement only in the limb controlling the stimulation, while the stimulated arm remains still, (b) leading to an increase in the stimulation parameters.

In the third case, the system detects the repetition by applying a threshold to the height derivative (Figure 5.3a) and then activates the mechanism for identifying the minimum angle (Figure 5.3b). After this step, the detected angles are normalized and compared between the limb receiving the stimulation and the limb controlling it (Figure 5.3c). As shown by the normalized angle values, the stimulated limb exhibits a greater range of motion, which results in an increase in the number of repetitions (Figure 5.3b).

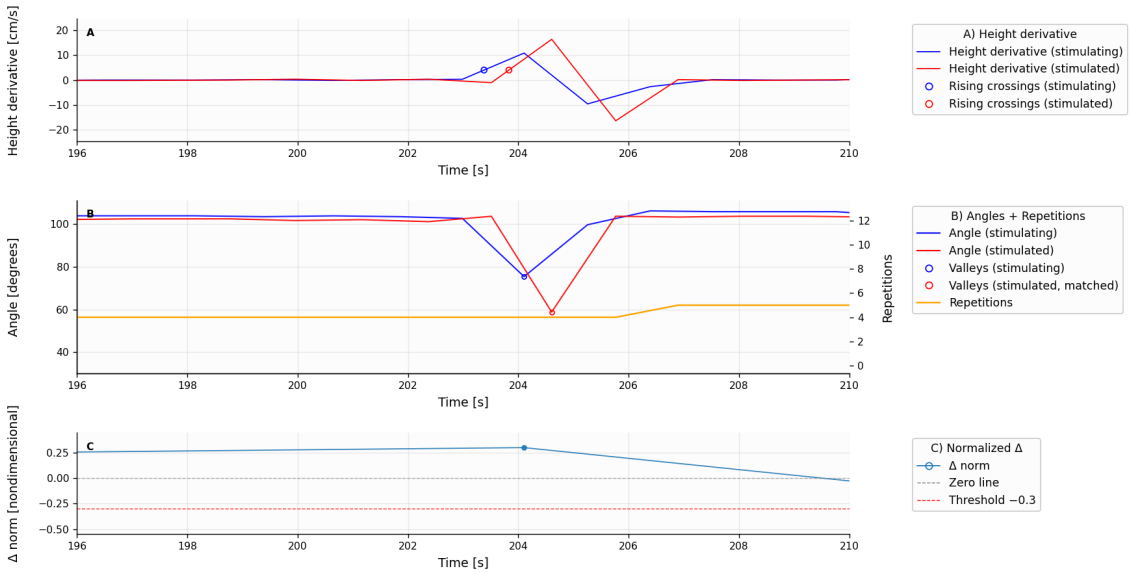

Figure 5.3: (a) Detection of the repetition, (b) identification and (c) normalization of the minimum angles, and (b) increases in repetitions due to greater movement of the stimulated limb.

Finally, in the final case, as shown in Figure 5.4, the program first analyses the derivative of the height, from which it identifies the start of the repetition (Figure 5.4a). From that point onward, the entire algorithm described in the previous chapter 4 is executed, allowing the detection of the minimum angle for both the limb that controls the stimulation and the one that receives it. The difference between the normalized minimum angles is then calculated, and as illustrated in Figure 5.4c, this difference falls within the defined tolerance threshold. Consequently, the program correctly assigns the repetitions, as shown in Figure 5.4b.

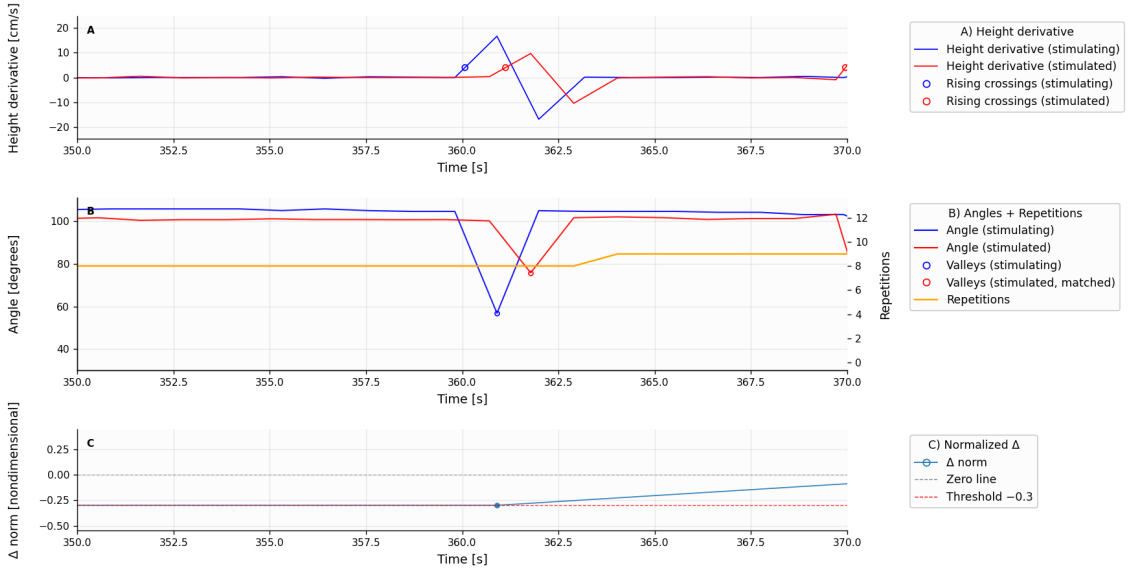

Figure 5.4: The program identifies the (a) start of the repetition from the height derivative, computes the (b) minimum angles of the stimulating and stimulated limbs, and verifies (c) that their normalized difference remains within the tolerance threshold.

However, the RehabCam program is not free from limitations. Since the control process is based on the derivative, the system may sometimes trigger a parameter update unnecessarily,

simply because the initial trigger that activates the algorithm is not detected. This issue becomes more evident in exercises that require finer motion control - such as the one in which the patient must put on the glasses -where the velocity condition is harder to meet. An example of this situation is shown in Figure 5.5, where the movement of the two arms falls within the acceptable threshold. Nevertheless, due to the low derivative value, the movement is not recognized, leading the system to update the parameters instead of increasing the repetition counter.

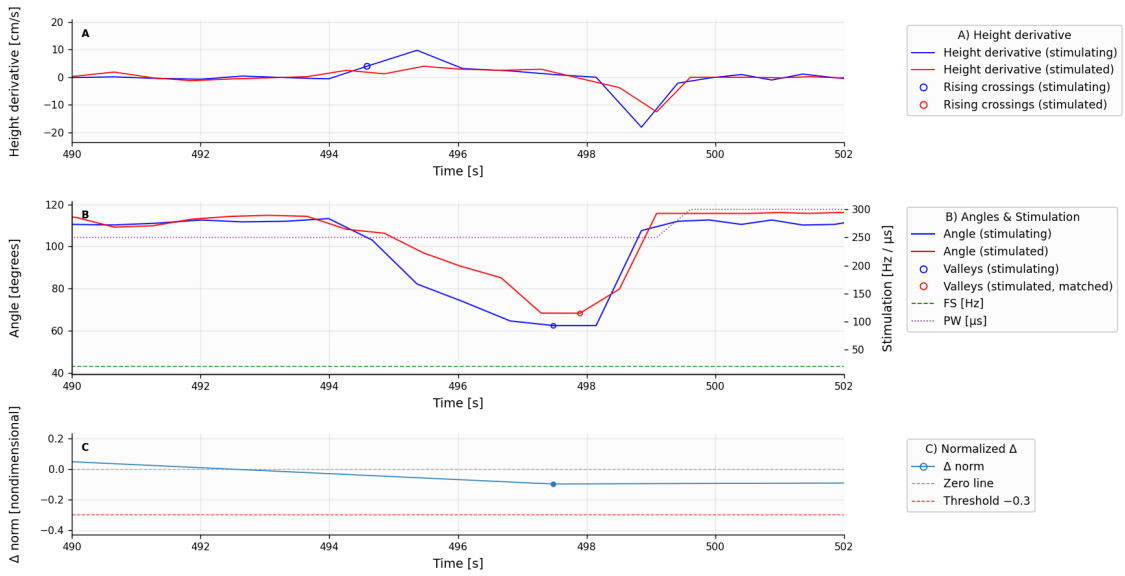

Figure 5.5: Example of the glasses exercise, where the arm movements fall within the acceptable threshold, but the low derivative value prevents motion detection, causing a parameter update instead of an increase in the repetitions.

5.2 Quantitative Analysis of Motion

A detailed analysis of the parameters extracted and explained in the previous chapter 4 is now presented to assess the effectiveness of the integrated use of the Lazarus device and the RehabCam software with respect to functional output. This analysis is performed for each exercise and for two separate groups: patients who carried out the exercises with two electrodes and those who used four.

5.2.1 Elbow Flexion-Extension in Pronation and Supination

The table below summarizes the main movement parameters considered for the subsequent analysis (Table 5.1).

Variable name	# electrodes	Arm type	Mean ± SD
Error parameter (dimensionless)	2	Stimulated arm	6.86 ± 1.33
	2	Controlling arm	6.25 ± 3.52
	4	Stimulated arm	6.37 ± 2.37
	4	Controlling arm	4.77 ± 1.55

continue on next page

Variable name	# electrodes	Arm type	Mean ± SD
Normalized peak height (dimensionless)	2	Stimulated arm	0.81 ± 0.12
	2	Controlling arm	0.90 ± 0.10
	4	Stimulated arm	0.82 ± 0.08
	4	Controlling arm	0.75 ± 0.13
Absolute maximum angle (°)	2	Stimulated arm	53.30 ± 0.76
	2	Controlling arm	54.75 ± 15.50
	4	Stimulated arm	61.32 ± 13.54
	4	Controlling arm	58.60 ± 12.22
Mean maximum angle (°)	2	Stimulated arm	56.82 ± 1.93
	2	Controlling arm	59.24 ± 13.25
	4	Stimulated arm	64.52 ± 12.56
	4	Controlling arm	63.67 ± 10.30
Absolute minimum angle (°)	2	Stimulated arm	141.51 ± 5.91
	2	Controlling arm	149.23 ± 24.37
	4	Stimulated arm	146.20 ± 4.09
	4	Controlling arm	138.27 ± 5.64
Mean minimum angle (°)	2	Stimulated arm	129.76 ± 11.07
	2	Controlling arm	135.81 ± 20.59
	4	Stimulated arm	133.12 ± 6.74
	4	Controlling arm	123.85 ± 9.02
Mean descent time (s)	2	Stimulated arm	0.97 ± 0.14
	2	Controlling arm	1.11 ± 0.45
	4	Stimulated arm	1.26 ± 0.38
	4	Controlling arm	1.28 ± 0.29
Mean ascent time (s)	2	Stimulated arm	1.79 ± 0.46
	2	Controlling arm	2.31 ± 0.56
	4	Stimulated arm	2.01 ± 0.63
	4	Controlling arm	2.12 ± 0.74
Mean total time (s)	2	Stimulated arm	2.76 ± 0.32
	2	Controlling arm	3.42 ± 1.00
	4	Stimulated arm	3.26 ± 0.68
	4	Controlling arm	3.40 ± 0.76
Mean velocity (m/s)	2	Stimulated arm	0.16 ± 0.03
	2	Controlling arm	0.15 ± 0.04
	4	Stimulated arm	0.12 ± 0.01
	4	Controlling arm	0.10 ± 0.02

continue on next page

Variable name	# electrodes	Arm type	Mean ± SD
Max repetition (dimensionless)	2	both	31.50 ± 3.54
	4	both	21.00 ± 6.66
Frequency stimulation (Hz)	2	both	20.00 ± 0.00
	4	both	20.00 ± 0.00
Pulse width (µs)	2	both	150.00 ± 0.00
	4	both	266.67 ± 93.10

Table 5.1: Kinematic variables (mean ± SD) by arm type and group, the number of repetitions (mean ± SD) and the stimulation parameters (mean ± SD) — flexion-extension exercise.

The results show a typical flexion-extension pattern of the elbow in healthy participants, with a full and symmetrical range of motion consistent with the reference values in literature. This pattern was observed in both the two- and four electrode groups, indicating that the number of electrodes did not substantially affect the overall movement profile. The joint excursion observed falls within the functional range described by Zwerus et al. [104], where the physiological range is approximately 148°-155°, depending on sex (Figure 5.7a). For both groups, the absolute maximum angle and the mean maximum angle were highly comparable between the controlling and the stimulated arms, suggesting that participants maintained a consistent starting position throughout the experimental session (Figure 5.6a and Figure 5.6b). The mean minimum angles reached approximately 130° for each arm in both groups (Figure 5.7b), further indicating an adequate range of motion to perform more complex functional tasks such as the glasses, box and cup exercises, as described by Vasen et al. [97]. Moreover, the fact that the absolute minimum angle exceeded the mean minimum angle in both groups suggests that participants did not maintain peak performance throughout the entire session for that exercise (Figure 5.7a and Figure 5.7b).

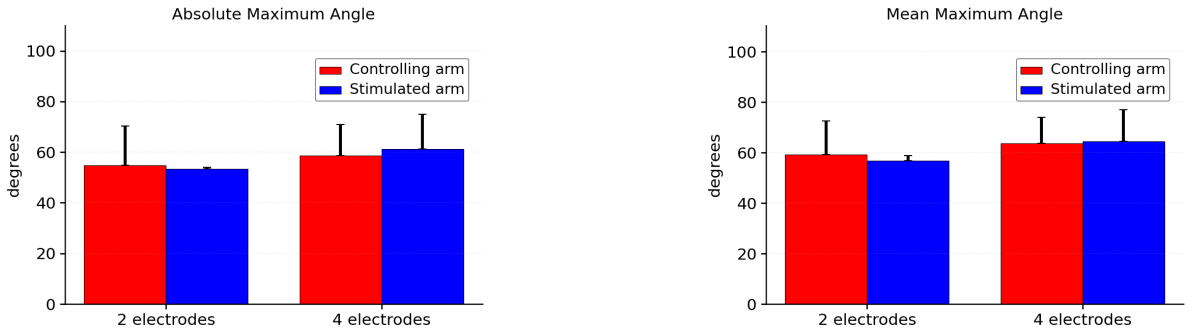

(a) (b)

Figure 5.6: (a) Average and (b) absolute maximum angles (mean ± SD) by arm type and group-flexion-extension exercise.

These favorable joint results are further supported by the analysis of normalized mean peak height, as each arm- across both configurations- achieved a value of at least 0.75 for this exercise (Figure 5.8).

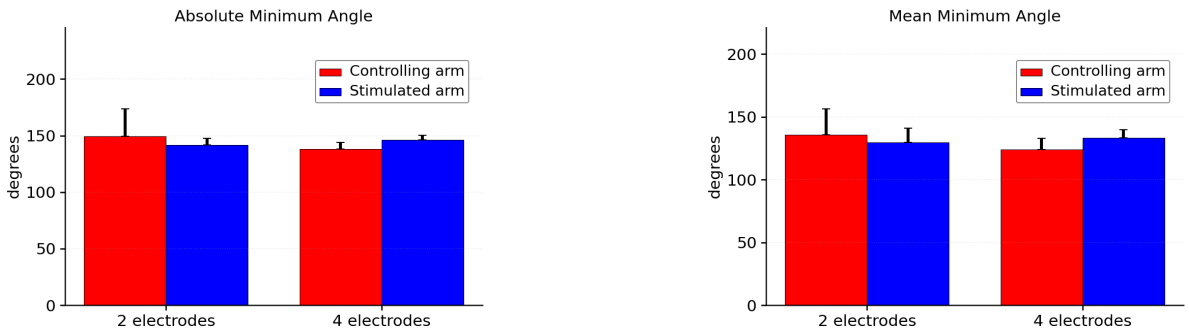

(a) (b)

Figure 5.7: (a) Average and (b) absolute minimum angles (mean ± SD) by arm type and group- flexion-extension exercise.

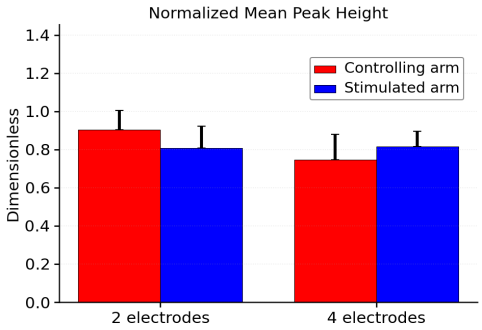

Figure 5.8: Normalized Mean Peak Height (mean ± SD) by arm type and group- flexion-extension exercise.

The trajectory error remained low in all cases for both groups. As expected, the controlling arm exhibited smaller deviations from the ideal path than the stimulated arm, likely because voluntary movements are more precise and continuously adjusted, whereas electrically induced movements tend to be more impulsive due to the sudden current peaks (Figure 5.9).

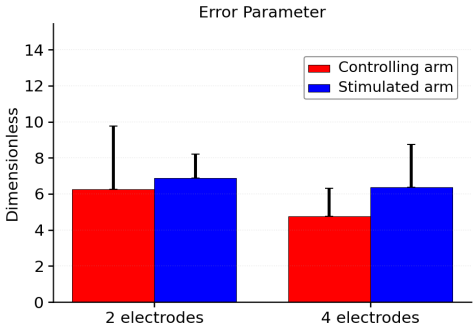

Figure 5.9: Error parameter (mean ± SD) by arm type and group- flexion-extension exercise.

This interpretation is reinforced by the timing and velocity data: in both electrode configurations, the stimulated arm moved faster (Figure 5.11b) and completed the task in a shorter time

than the controlling arm (Figure 5.10a, Figure 5.10b, Figure 5.11a). Nevertheless, the overall movement remained controlled, with lower velocities and longer durations compared with those reported in studies where subjects performed everyday activities such as drinking from a glass [66].

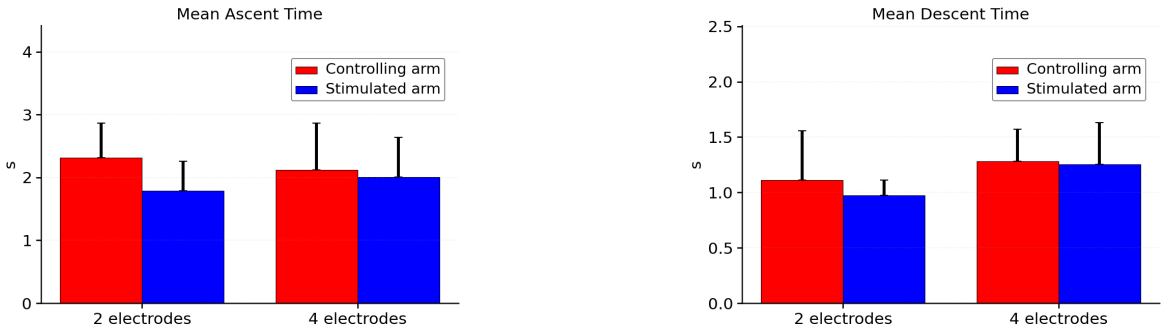

(a) (b)

Figure 5.10: (a) Mean ascending, (b) descending (mean ± SD) by arm type and group- flexion-extension exercise.

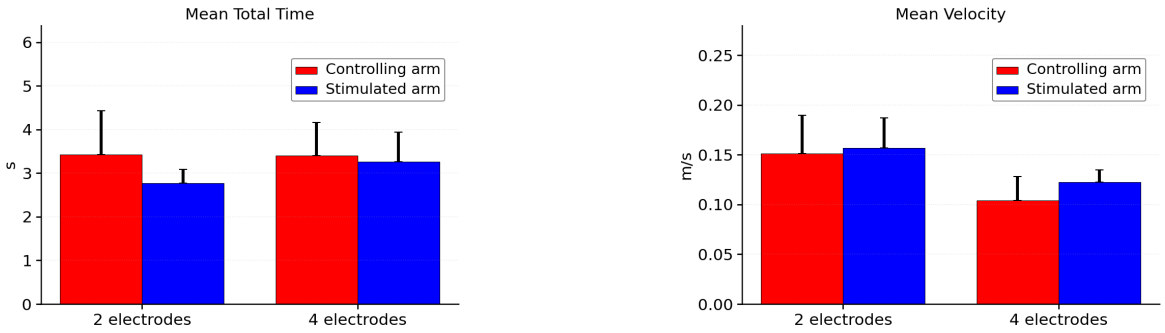

(a) (b)

Figure 5.11: (a) Mean total movement times, and (b) mean velocity (mean ± SD) by arm type and group- flexion-extension exercise.

A comparison between the two electrodes configurations reveals that the two-electrode setup produces slightly better functional outcomes in terms of movement velocity, whereas the results for the other variables are largely comparable between configurations. Participants using this configuration tended to complete the tasks more quickly. In contrast, the four-electrode setup appeared to be more fatiguing, as indicated by slower movements and longer execution times observed. This concept is further supported by the observation that the maximum number of repetitions was higher with two electrodes than with four (Figure 5.12).

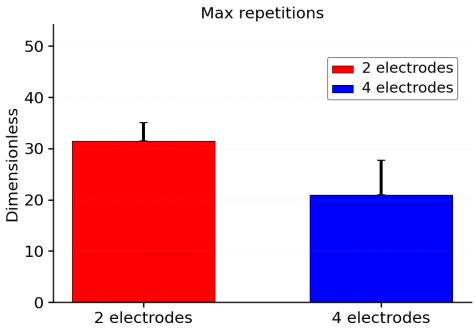

Figure 5.12: Maximum number of repetitions (mean ± SD) compared between the two electrode groups - flexion-extension exercise.

A confirmation of the probably greater effort required to performed the exercise by subjects with four electrodes can be observed in the fact that the stimulation parameters are higher for this group compered to those with only two electrodes. This indicates that higher parameters are needed to recruit a sufficient number of muscle fibers to complete the exercise (Figure 5.13).

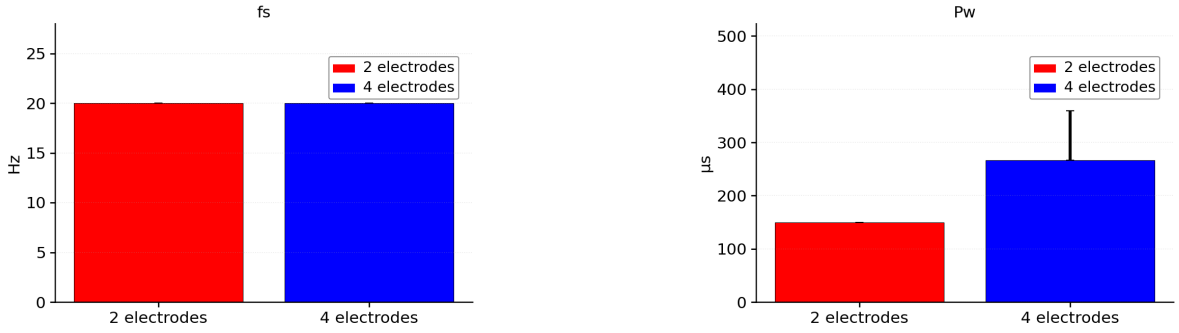

(a) (b)

Figure 5.13: Bar charts of the stimulation parameters (a) fs and (b) PW in the two groups (2 vs 4 electrodes) - flexion-extension exercise.

5.2.2 Eyeglasses Donning and Removal Task

The table below provides an overview of the main movement parameters used for the subsequent analysis (Table 5.2).

Variable name	**# electrodes**	**Arm type**	**Mean ± SD**
Error parameter (dimensionless)	2	Stimulated arm	6.25 ± 2.55
	2	Controlling arm	4.46 ± 1.31
	4	Stimulated arm	6.16 ± 1.49
	4	Controlling arm	6.01 ± 2.58
Normalized peak height (dimensionless)	2	Stimulated arm	0.90 ± 0.03
	2	Controlling arm	0.93 ± 0.12

continue on next page

Variable name	# electrodes	Arm type	Mean ± SD
	4	Stimulated arm	0.90 ± 0.10
	4	Controlling arm	0.89 ± 0.08
Absolute maximum angle (°)	2	Stimulated arm	45.02 ± 4.12
	2	Controlling arm	43.54 ± 1.51
	4	Stimulated arm	56.42 ± 6.12
	4	Controlling arm	55.74 ± 8.19
Mean maximum angle (°)	2	Stimulated arm	47.98 ± 4.84
	2	Controlling arm	48.84 ± 0.60
	4	Stimulated arm	61.90 ± 6.63
	4	Controlling arm	60.56 ± 9.15
Absolute minimum angle (°)	2	Stimulated arm	129.90 ± 2.33
	2	Controlling arm	135.19 ± 5.82
	4	Stimulated arm	138.48 ± 3.55
	4	Controlling arm	136.07 ± 7.75
Mean minimum angle (°)	2	Stimulated arm	122.67 ± 3.76
	2	Controlling arm	128.23 ± 1.25
	4	Stimulated arm	130.25 ± 4.01
	4	Controlling arm	128.34 ± 7.21
Mean descent time (s)	2	Stimulated arm	1.32 ± 0.12
	2	Controlling arm	1.32 ± 0.17
	4	Stimulated arm	2.31 ± 0.93
	4	Controlling arm	2.35 ± 0.64
Mean ascent time (s)	2	Stimulated arm	2.16 ± 0.13
	2	Controlling arm	2.10 ± 0.36
	4	Stimulated arm	3.56 ± 1.46
	4	Controlling arm	3.71 ± 1.39
Mean total time (s)	2	Stimulated arm	3.48 ± 0.01
	2	Controlling arm	3.43 ± 0.19
	4	Stimulated arm	5.87 ± 2.06
	4	Controlling arm	6.06 ± 1.94
Mean velocity (m/s)	2	Stimulated arm	0.14 ± 0.01
	2	Controlling arm	0.15 ± 0.01
	4	Stimulated arm	0.09 ± 0.03
	4	Controlling arm	0.08 ± 0.03
Max repetition (dimensionless)	2	both	30.00 ± 1.41
	4	both	22.00 ± 6.00
Frequency stimulation (Hz)	2	both	20.00 ± 0.00

continue on next page

Variable name	# electrodes	Arm type	Mean ± SD
	4	both	20.00 ± 0.00
Pulse width (µs)	2	both	225.00 ± 35.36
	4	both	170.00 ± 44.72

Table 5.2: Kinematic variables (mean ± SD) by arm type and group, the number of repetitions (mean ± SD) and the stimulation parameters (mean ± SD) — glasses exercise.

In this case all metrics appear very similar between conditions. As in the previous task, the mean minimum angles reached values around 130° for both the controlling and stimulated arms, which corresponds to the joint flexion required for many activities of daily living [97]. Both the absolute and mean minimum angles were nearly identical, indicating consistent joint performance across repetitions. This suggests that participants were able to reliably reproduce the same movement pattern in both electrode configurations and for both arms (Figure 5.15). Moreover, as can be seen from the similarity between the absolute and mean maximum angle values, the initial position during the session was the same (Figure 5.14).

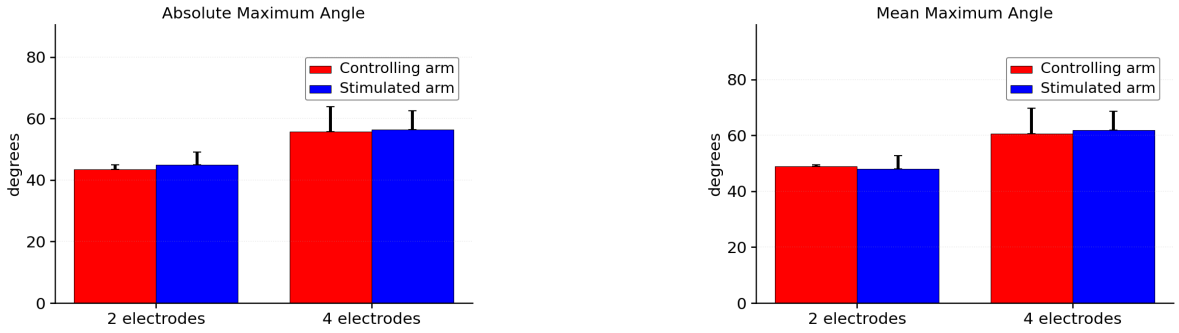

(a) (b)

Figure 5.14: (a) Average and (b) absolute maximum angles (mean ± SD) by arm type and group- Eyeglasses exercise.

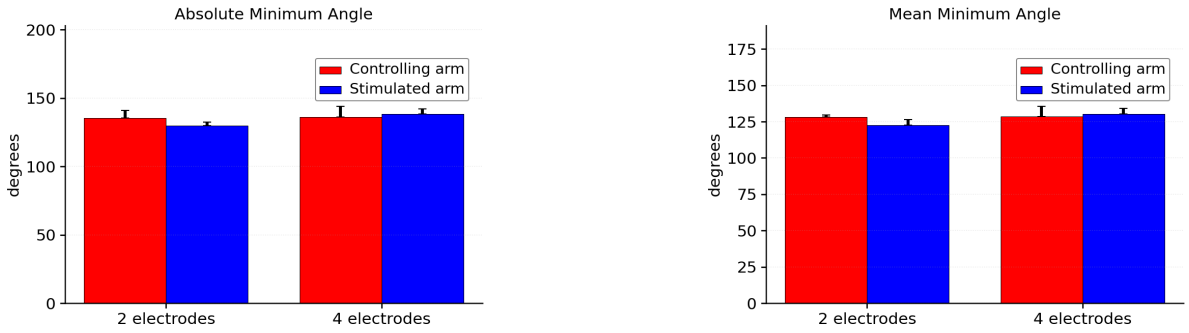

(a) (b)

Figure 5.15: (a) Average and (b) absolute minimum angles (mean ± SD) by arm type and group- Eyeglasses exercise.

The normalized mean peak height further supports this observation, showing the same trend observed in both the mean and absolute minimum angles for both electrode configurations (Figure 5.16).

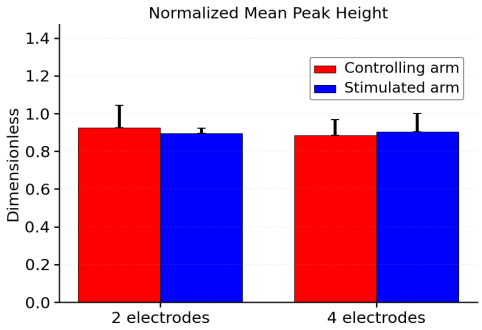

Figure 5.16: Normalized Mean Peak Height (mean ± SD) by arm type and group- Eyeglasses exercise.

Coordination quality also appears high, as the velocity values between the controlling and stimulated arms were almost identical, with minimal differences in both SD and mean across both electrode configurations. The same pattern was observed for the average ascent, descent, and total movement times, confirming that the motion dynamics were highly similar between the two limbs, both in terms of joint output and temporal execution, across both electrode configurations. As observed in the flexion-extension task, these time and velocity values are higher than those typically reported in the literature for comparable functional exercises [66]. Interestingly, while the four-electrode configuration produced generally higher time values for both arms, whereas the two-electrode configuration consistently resulted in lower movement times. This suggests that the exercise was easier to perform with two electrodes (Figure 5.17 and Figure 5.18).

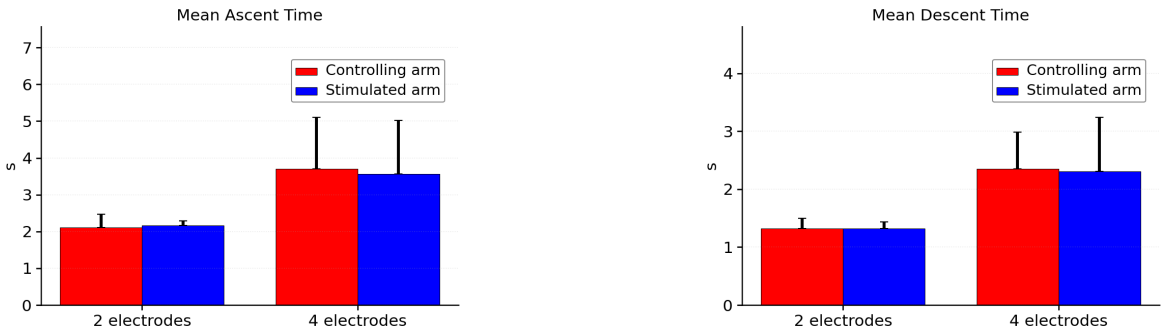

(a) (b)

Figure 5.17: (a) Mean ascending, (b) descending (mean ± SD) by arm type and group- Eyeglasses exercise.

The trajectory error analysis support this interpretation: errors for both arms remained low and comparable, but tended to increase in the four-electrode configuration, reinforcing the idea that the two-electrode condition allowed participants to execute the task greater ease and precision (Figure 5.19).

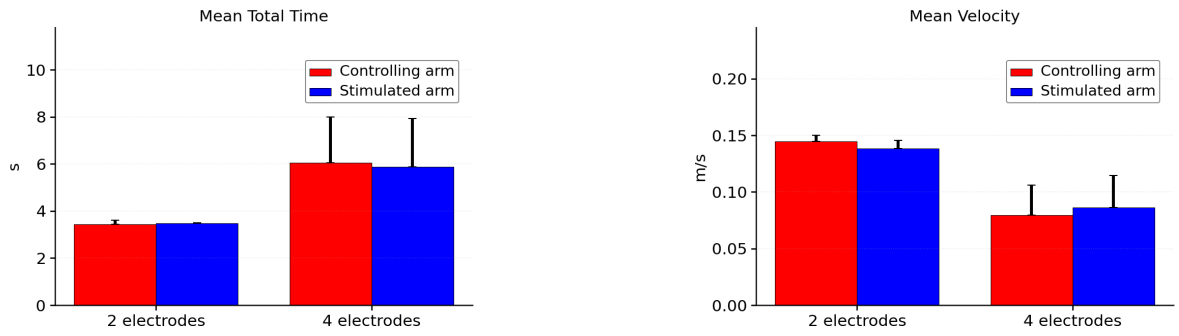

(a) (b)

Figure 5.18: (a) Mean total movement times, and (b) mean velocity (mean ± SD) by arm type and group- Eyeglasses exercise.

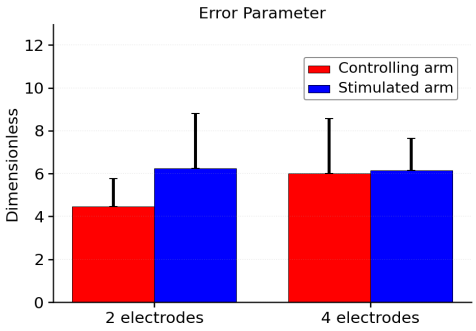

Figure 5.19: Error parameter (mean ± SD) by arm type and group- Eyeglasses exercise.

As in the previous task, participants with two electrodes completed a higher number of repetitions than those with four electrodes, further indicating that the two-electrode configuration is less fatiguing and more manageable (Figure 5.20).

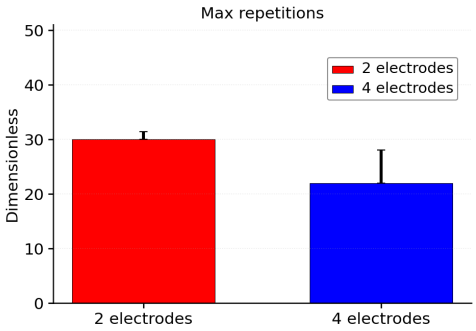

Figure 5.20: Maximum number of repetitions (mean ± SD) compared between the two electrode groups - Eyeglasses exercise.

These superior performances in the two electrode condition appear related to the fact that the PW was on average higher in this configuration than in the four-electrode setup. This may suggest that, despite the increased challenge, participants were able to successfully complete the repetitions without failure, rather relying on parameter adjustments to compensate (Figure

5.21).

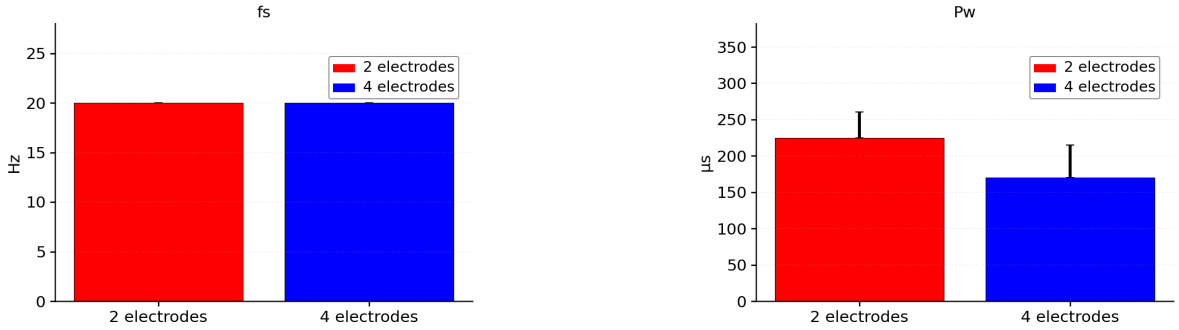

(a) (b)

Figure 5.21: Bar charts of the stimulation parameters (a) fs and (b) PW in the two groups (2 vs 4 electrodes) - Eyeglasses exercise.

5.2.3 Box Opening and Closing Task

The main movement parameters considered for the subsequent analysis are summarized in Table 5.3

Variable name	**# electrodes**	**Arm type**	**Mean ± SD**
Error parameter (dimensionless)	2	Stimulated arm	5.61 ± 1.34
	2	Controlling arm	5.63 ± 1.48
	4	Stimulated arm	6.21 ± 3.39
	4	Controlling arm	5.32 ± 1.92
Normalized peak height (dimensionless)	2	Stimulated arm	0.80 ± 0.06
	2	Controlling arm	0.94 ± 0.10
	4	Stimulated arm	0.81 ± 0.15
	4	Controlling arm	0.83 ± 0.08
Absolute maximum angle (°)	2	Stimulated arm	52.78 ± 11.75
	2	Controlling arm	51.05 ± 16.11
	4	Stimulated arm	57.52 ± 10.37
	4	Controlling arm	56.34 ± 14.03
Mean maximum angle (°)	2	Stimulated arm	56.86 ± 11.74
	2	Controlling arm	58.94 ± 14.55
	4	Stimulated arm	62.62 ± 9.93
	4	Controlling arm	60.91 ± 14.22
Absolute minimum angle (°)	2	Stimulated arm	147.52 ± 15.77
	2	Controlling arm	146.38 ± 6.77
	4	Stimulated arm	136.33 ± 17.32

continue on next page

Variable name	# electrodes	Arm type	Mean ± SD
	4	Controlling arm	132.04 ± 15.09
Mean minimum angle (°)	2	Stimulated arm	138.38 ± 17.11
	2	Controlling arm	132.24 ± 6.14
	4	Stimulated arm	126.29 ± 17.43
	4	Controlling arm	121.36 ± 15.86
Mean descent time (s)	2	Stimulated arm	1.49 ± 0.61
	2	Controlling arm	1.10 ± 0.16
	4	Stimulated arm	1.57 ± 0.73
	4	Controlling arm	1.48 ± 0.76
Mean ascent time (s)	2	Stimulated arm	2.05 ± 0.21
	2	Controlling arm	2.25 ± 0.50
	4	Stimulated arm	2.92 ± 1.16
	4	Controlling arm	2.98 ± 0.93
Mean total time (s)	2	Stimulated arm	3.53 ± 0.77
	2	Controlling arm	3.35 ± 0.66
	4	Stimulated arm	4.49 ± 1.79
	4	Controlling arm	4.46 ± 1.54
Mean velocity (m/s)	2	Stimulated arm	0.12 ± 0.04
	2	Controlling arm	0.14 ± 0.03
	4	Stimulated arm	0.09 ± 0.03
	4	Controlling arm	0.09 ± 0.03
Max repetition (dimensionless)	2	both	27.33 ± 1.53
	4	both	18.83 ± 6.52
Frequency stimulation (Hz)	2	both	20.00 ± 0.00
	4	both	20.00 ± 0.00
Pulse width (µs)	2	both	183.33 ± 28.87
	4	both	183.33 ± 60.55

Table 5.3: Kinematic variables (mean ± SD) by arm type and group, the number of repetitions (mean ± SD) and the stimulation parameters (mean ± SD) — box exercise.

For the box exercise, the functional output achieved the values reported by Vasen et al. in both the electrode configurations, with a functional output around 130° [97]. Compared to the glasses exercise, a slight decrease in performance was observed , with a difference of approximately 10° between the absolute and mean minimum angles. However, this small discrepancy still indicates excellent repeatability of the movement pattern. The equivalence between the absolute and mean maximum angles highlights that the starting joint position was consistent and maintained throughout the entire duration of the exercise, as observe in previous tasks for both arms in both electrode configurations. The difference between the mean minimum angles of the controlling and stimulated arms remained low - around 6° - further confirming consistent execution across repetitions (Figure 5.22 and Figure 5.23).

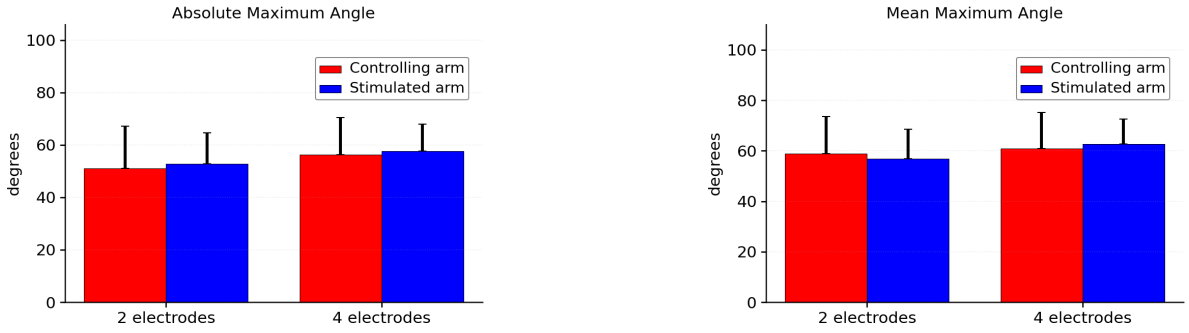

(a) (b)

Figure 5.22: (a) Average and (b) absolute maximum angles (mean ± SD) by arm type and group- Box exercise.

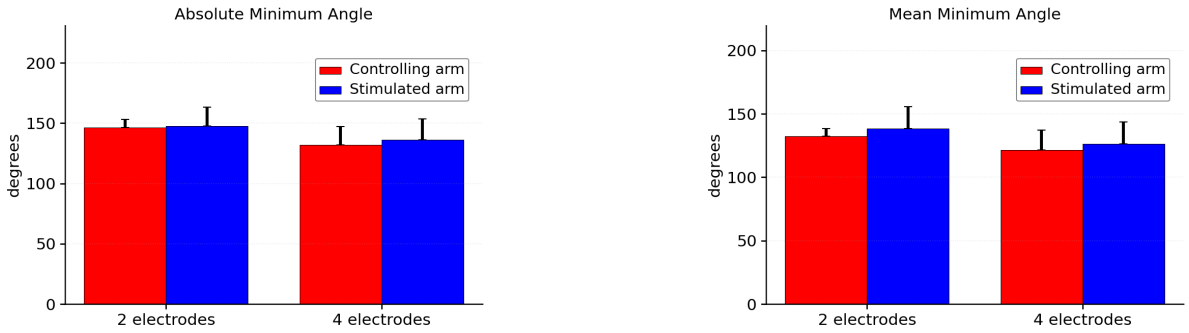

(a) (b)

Figure 5.23: (a) Average and (b) absolute minimum angles (mean ± SD) by arm type and group- Box exercise.

The high level of coordination suggested by these angular values is also evident in the average time parameters (ascent, descent and total time) and in the mean velocity, both showing minimal differences between the controlling and the stimulated arms across both configuration electrodes (Figure 5.24 and Figure 5.25).

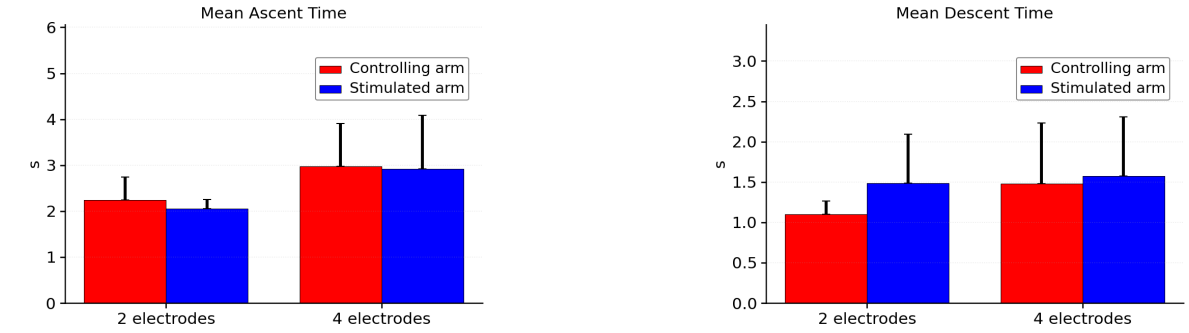

(a) (b)

Figure 5.24: (a) Mean ascending, (b) descending (mean ± SD) by arm type and group- Box exercise.

Moreover, the trajectory errors relative to the ideal path were quite similar between the two electrode configurations (2 and 4). In fact, both the movement velocity and execution times

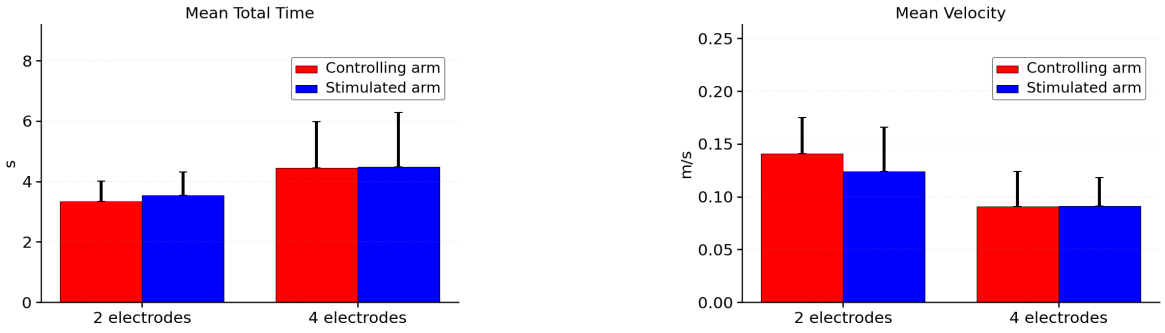

(a) (b)

Figure 5.25: (a) Mean total movement times, and (b) mean velocity (mean ± SD) by arm type and group- Box exercise.

were very similar, highlighting strong resemblance between the movements produced by the two arms (Figure 5.26).

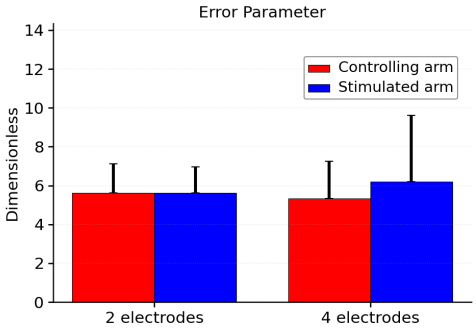

Figure 5.26: Error parameter (mean ± SD) by arm type and group- Box exercise.

In this case, the normalized peak height and the minimum angle values did not coincide. This discrepancy may be attributed to instances in which the scaling factor was not correctly calibrated by the operator (Figure 5.27).

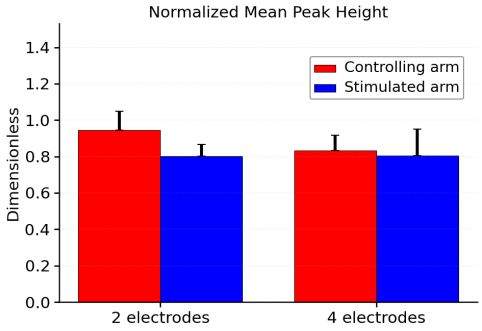

Figure 5.27: Normalized Mean Peak Height (mean ± SD) by arm type and group- Box exercise.

It is worth noting, however, that the number of repetitions performed with the 4-electrode setup was lower. This reduction likely reflects decreased stimulation tolerance associated with

the higher number of active electrodes, which may have limited the participant's endurance during the task (Figure 5.28).

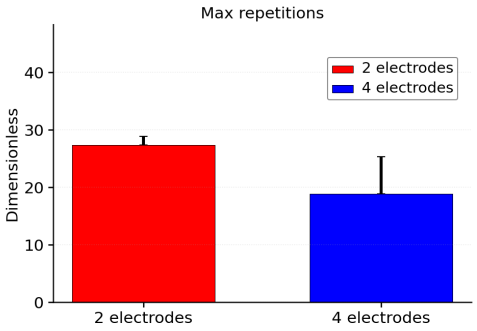

Figure 5.28: Maximum number of repetitions (mean ± SD) compared between the two electrode groups - Box exercise.

Finally, no significant differences were detected between the two electrode configurations with respect to the stimulation parameters, as clearly illustrated in Figure 5.29.

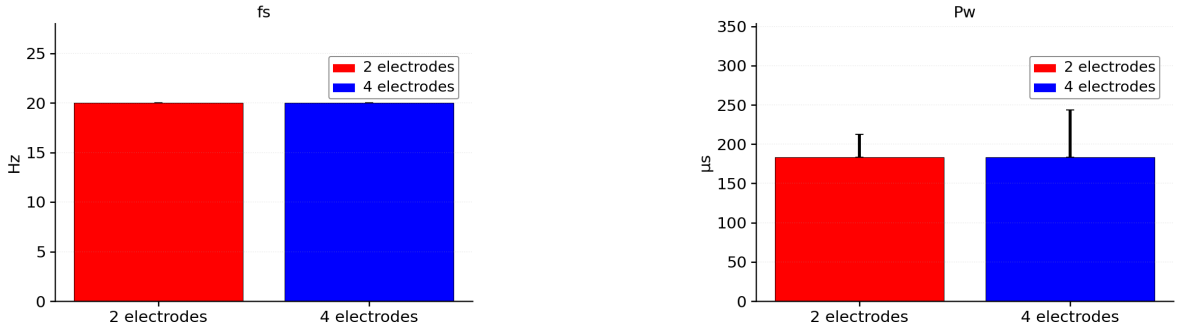

(a) (b)

Figure 5.29: Bar charts of the stimulation parameters (a) fs and (b) PW in the two groups (2 vs 4 electrodes) - Box exercise.

5.2.4 Cup Drinking Task

The key movement parameters included in following analysis are listed in Table 5.4

Variable name	**# electrodes**	**Arm type**	**Mean ± SD**
Error parameter (dimensionless)	2	Stimulated arm	5.27 ± 0.84
	2	Controlling arm	5.69 ± 0.92
	4	Stimulated arm	6.14 ± 2.11
	4	Controlling arm	5.40 ± 2.63
Normalized peak height (dimensionless)	2	Stimulated arm	0.83 ± 0.15
	2	Controlling arm	0.95 ± 0.05

continue on next page

Variable name	# electrodes	Arm type	Mean ± SD
	4	Stimulated arm	0.88 ± 0.12
	4	Controlling arm	0.90 ± 0.09
Absolute maximum angle (°)	2	Stimulated arm	63.20 ± 6.55
	2	Controlling arm	55.95 ± 19.42
	4	Stimulated arm	49.11 ± 4.84
	4	Controlling arm	46.27 ± 6.06
Mean maximum angle (°)	2	Stimulated arm	66.89 ± 6.53
	2	Controlling arm	62.55 ± 16.05
	4	Stimulated arm	52.53 ± 5.09
	4	Controlling arm	51.60 ± 4.33
Absolute minimum angle (°)	2	Stimulated arm	146.01 ± 4.98
	2	Controlling arm	144.67 ± 17.93
	4	Stimulated arm	138.31 ± 11.63
	4	Controlling arm	130.83 ± 7.32
Mean minimum angle (°)	2	Stimulated arm	134.72 ± 5.24
	2	Controlling arm	135.09 ± 14.16
	4	Stimulated arm	127.24 ± 12.31
	4	Controlling arm	122.92 ± 7.76
Mean descent time (s)	2	Stimulated arm	0.97 ± 0.11
	2	Controlling arm	1.00 ± 0.16
	4	Stimulated arm	1.56 ± 0.79
	4	Controlling arm	1.41 ± 0.65
Mean ascent time (s)	2	Stimulated arm	2.43 ± 0.36
	2	Controlling arm	2.44 ± 0.55
	4	Stimulated arm	2.56 ± 0.50
	4	Controlling arm	2.68 ± 0.58
Mean total time (s)	2	Stimulated arm	3.40 ± 0.48
	2	Controlling arm	3.44 ± 0.71
	4	Stimulated arm	4.13 ± 0.85
	4	Controlling arm	4.09 ± 0.97
Mean velocity (m/s)	2	Stimulated arm	0.12 ± 0.02
	2	Controlling arm	0.14 ± 0.03
	4	Stimulated arm	0.11 ± 0.01
	4	Controlling arm	0.11 ± 0.04
Max repetition (dimensionless)	2	both	25.50 ± 3.54
	4	both	24.80 ± 4.49
Frequency stimulation (Hz)	2	both	20.00 ± 0.00

continue on next page

Variable name	# electrodes	Arm type	Mean ± SD
	4	both	20.00 ± 0.00
Pulse width (µs)	2	both	250.00 ± 70.71
	4	both	160.00 ± 22.36

Table 5.4: Kinematic variables (mean ± SD) by arm type and group, the number of repetitions (mean ± SD) and the stimulation parameters (mean ± SD) — cup exercise.

In the cup exercise, the functional joint performance was good, with the mean minimum angles reaching approximately 135° for both arms in both electrode configurations [97]. As in the previous tasks, the absolute and mean maximum angles were nearly identical, indicating that the starting position was consistently maintained across repetitions. Regarding the minimum angles, the difference between the mean and absolute minimum angles was about 10° for both electrode configurations, reflecting stable and repeatable movement patterns. When comparing the two arms- the one controlling and the one being stimulated- the mean minimum angles were almost identical in both configurations (Figure 5.30 and Figure 5.31).

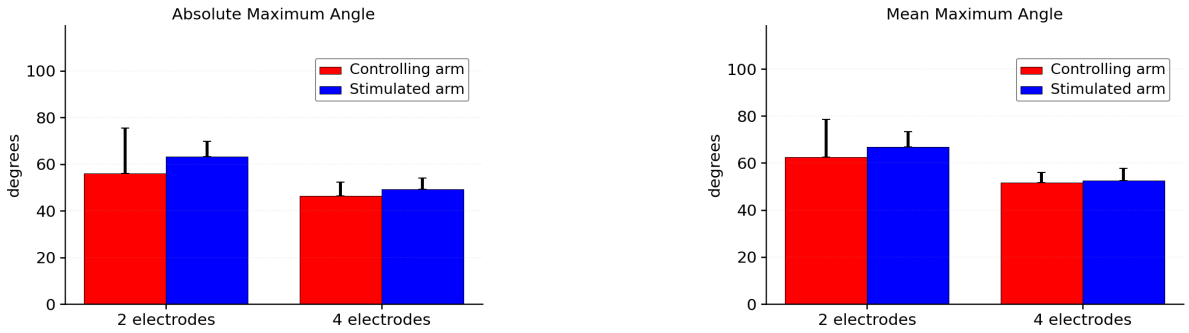

(a) (b)

Figure 5.30: (a) Average and (b) absolute maximum angles (mean ± SD) by arm type and group- Cup exercise.

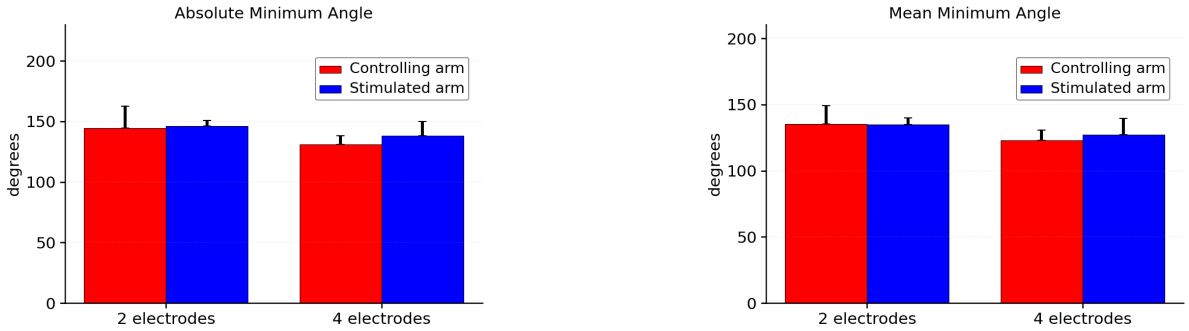

(a) (b)

Figure 5.31: (a) Average and (b) absolute minimum angles (mean ± SD) by arm type and group- Cup exercise.

Overall, the bilateral coordination was very good, as confirmed by the average time parameters (ascent, descent, and total duration) and mean velocity, which were highly similar both

between the two arms and between the two electrode configurations (Figure 5.32 and Figure 5.33).

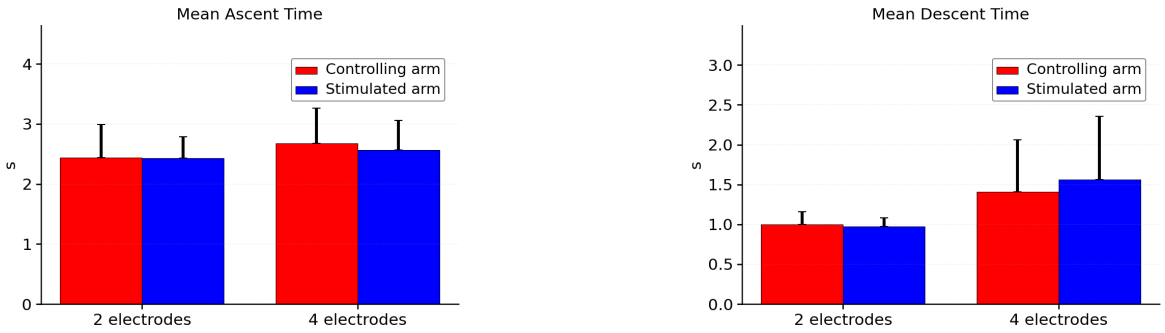

(a) (b)

Figure 5.32: (a) Mean ascending, (b) descending, (mean ± SD) by arm type and group- Cup exercise.

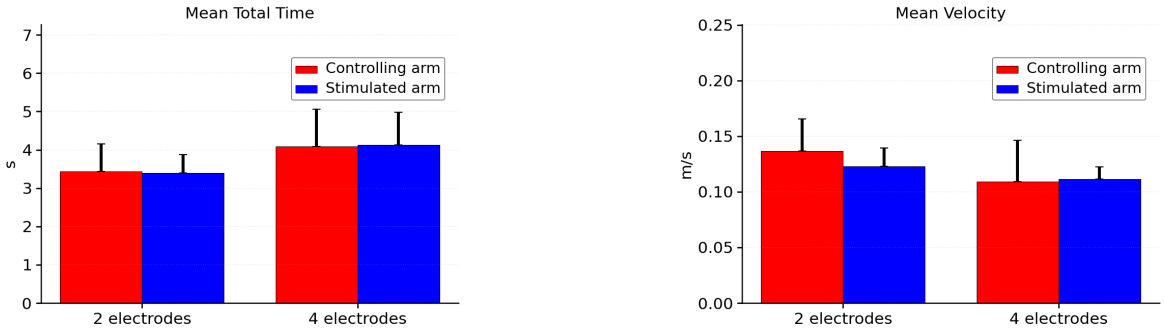

(a) (b)

Figure 5.33: (a) Mean total movement times, and (b) mean velocity (mean ± SD) by arm type and group- Cup exercise.

In this task, therefore, the two electrode setups demonstrated very similar overall performance, as also reflected by the number of repetitions, which differed by only three repetitions on average between configurations (Figure 5.34).

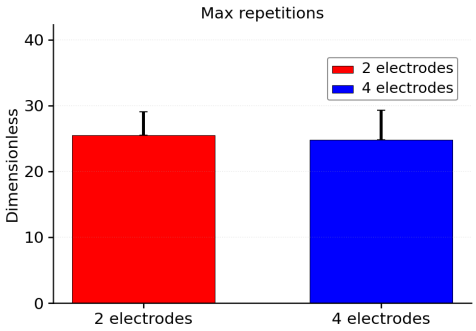

Figure 5.34: Maximum number of repetitions (mean ± SD) compared between the two electrode groups - Cup exercise.

Once again, the normalized mean peak height values differed from the information inferred from the mean minimum joint angles, as previously observed in the box exercise. This discrepancy is likely due to an incorrect calibration by the operator like in the previous exercise (Figure 5.35).

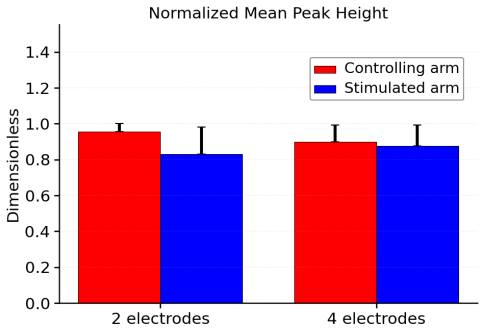

Figure 5.35: Normalized Mean Peak Height (mean ± SD) by arm type and group- Cup exercise.

In this case, it is evident that when using the two-electrode setup, larger pulse-width parameters were employed (Figure 5.36).

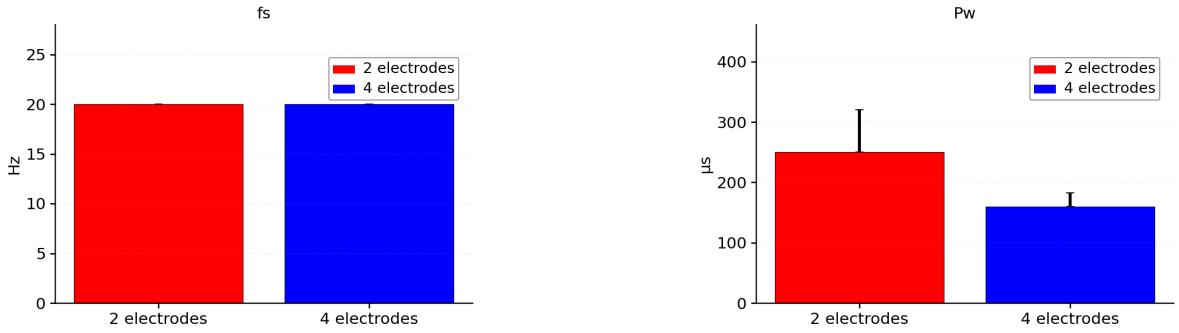

(a) (b)

Figure 5.36: Bar charts of the stimulation parameters (a) fs and (b) PW in the two groups (2 vs 4 electrodes) - Cup exercise.

5.3 Overall Interpretation of System Performance and Electrode Configuration Effects

From a qualitative perspective, the program was examined across the four conditions in which it intervenes to modulate the stimulation parameters. Figures 5.1,5.2,5.3,5.4, illustrate how the system correctly identifies movement through the height derivative, detects the minimum angles of both arms, applies normalization, and then updates the stimulation parameters-PW and fs- or the number of repetitions depending on what is required. However, as shown in Figure 5.5, the reliance on the derivative may occasionally lead to missed triggers, particularly during fine motor tasks (such as the eyeglasses exercise), resulting in unnecessary parameter updates.

Overall, the combined analysis of the four exercises highlights several main observations that coherently describe both system behavior and participant performance. In all tasks, the movements generated were physiological, repeatable, and aligned with reference values reported in the literature, demonstrating good coordination between the controlling and stimulated limbs

(Figures 5.6, 5.7, 5.14, 5.15, 5.22, 5.23, 5.30, 5.31). Differences between the two electrode configurations did not hinder task execution, through clear trends emerged: the two-electrode setup consistently proved evidently less fatiguing and more functional than the four electrode configuration, as shown by the higher number of repetitions performed (Figures 5.12,5.20,5.28,5.34), shorter execution times, and more favorable movement velocities in several exercises (Figures 5.10,5.11,5.17,5.18, 5.24,5.25, 5.32, 5.33). In general, the stimulated arm tended to move faster than the controlling arm, likely due to the impulsive nature of electrical muscle recruitment, as observed in the elbow flexion-extension analysis (Figure 5.11) or at least consistent in the other exercises, which involved specific functional tasks where coordinated movement speed between the two arms was essential (Figures 5.18,5.25, 5.33). At the same time, trajectory and movement precision displayed minimal discrepancies between the two arms. In the functional tasks, the trajectory errors remained particularly small and comparable across configurations, indicating high bilateral coordination. By contrast, in the elbow flexion-extension, the differences between the controlling and stimulated arms were slightly more evident. In some exercises, a mismatch was noted between normalized height and minimum angles measurements (Figures 5.27 and 5.35), likely attributable to calibration inaccuracies rather than system limitations. Regarding the stimulation parameters, in the flexion-extension exercise, they were generally higher in four electrodes, indicating that the recruitment of a larger number of muscle fibers was required to complete the movements (Figure 5.13). In contrast, in all other exercises, the two-electrode setup required higher- or at least equal- PW values, yet still allowed for more efficient task execution (Figures 5.21, 5.29, 5.36). Altogether, these findings show that both configurations enable successful task performance, but the two-electrode setup provides overall superior outcomes in terms of speed, precision and number of repetitions- confirming that it offers greater ease and sustainability of movement compared to the four-electrode condition.

Chapter 6

Future Work: Development of the Clinical Trial

As outlined in the previous chapter 5, following the verification of the actual feasibility of a clinical protocol using both electrode configurations- combining task-oriented exercises with the Lazarus device and the RehabCam program- on healthy subjects, and given the consistency of the obtained results with the findings reported in the literature, it was decided to proceed with the development of a clinical trial. This trial will be conducted at Cona Hospital (Ferrara) over a six-month period. The study has been developed in collaboration with the team from the Department of Neuroscience and Rehabilitation at the University of Ferrara and has received ethical approval from the Ethics Committee of the Emilia Center Wide Area (CE-AVEC).

The aim of the study is twofold: first, to assess the usability and clinical feasibility of a protocol combining task-oriented exercises with the Lazarus device and the RehabCam program, and second, to collect feedback from clinicians regarding the integration of the Lazarus device with the Rehabcam program, as well as from patients concerning their experience with the delivered therapy sessions.

6.1 Target population: Patients with Chronic Stroke

As already discussed in the first chapter, stroke represents one of the leading causes of death worldwide and has been described as a true global epidemic [22, 28]. According to the Wold Health Organization (WHO), approximately 15 million people suffer a stroke each year [4]. Notably, only about 10% of post-stroke patients achieve full recovery, while 30% die and nearly 60% experience chronic dysfunctions [50]. Among those with chronic impairments, $60 - 80\%$ develop upper limb motor dysfunctions as a consequence of stroke [26,82]. These patients tend to perform daily activities primarily with the unaffected limb, avoiding the use of paretic one [2,75], which can eventually lead to complete disuse of the affected arm [75]. Since most daily activities require the coordinated use of both hands and upper limbs, the inability to effectively use one arm results in a significant loss of function and a consequent reduction in the ability to perform essential movements. This loss of autonomy often contributes to emotional and physiological challenges such as depression, anxiety, sleep disturbances, and feelings of helplessness, as well as a growing dependence on others, reduced self-esteem, and even physiological pain [13], all of which negatively impact the overall quality of life [102].

In this context, the Lazarus FES device and the RehabCam program may play a crucial role for this category of patients, as they have the potential to make rehabilitation therapy more objective and, consequently, improve the quality of care during task-oriented treatment sessions such as those presented in this thesis. However, before assessing the actual clinical efficacy of proposed system, it is necessary to conduct a usability and feasibility study to determine whether the system, previously developed and tested on healthy subjects, can be effectively applied in

clinical setting.

6.2 Study Design

The study will involve a group of 20 patients with chronic stroke who will be recruited according to the following inclusion and exclusion criteria:

Inclusion Criteria

- Male and female patients aged between 18 and 80 years old;
- Diagnosis of ischemic or hemorrhagic stroke confirmed by brain imaging;
- Severe or moderate upper limb impairment (Fugl-Meyer score < 44);
- Signed informed consent obtained;
- Chronic phase of stroke (>6 months post-onset);
- Ability to understand and follow instructions related to the rehabilitation protocol (Mini-Mental State Examination (MMSE)> 24)

Exclusion Criteria

- Medical conditions that may interfere with safe completion of study protocol;
- Cognitive impairment precluding informed consent;
- Severe visual impairments;
- Upper limb pain (Visual Analogue Scale (VAS)>7);
- Severe cardiopulmonary, renal, or hepatic diseases
- Pregnancy;
- Failure to obtain informed consent;
- Presence of pacemakers or active implanted devices incompatible with FES;
- Neurological or neuromuscular disorders that interfere with response to electrical stimulation.

The MMSE is a brief, standardized tool designed to evaluate global cognitive function, including orientation, attention, memory, language, visuospatial abilities. Scores ranges from 0 to 30, with higher values indicating better cognitive performance; a score above 24 is generally considered within the normal range. The VAS is a simple and reliable instrument for measuring pain intensity. It consists of a 10-centimeter horizontal line, where 0 represents "no pain" and 10 represents "the worst pain imaginable". Participants are asked to indicate their perceived level of pain on the scale, providing a quantitative measure of subjective pain experience.

Upon obtaining informed consent, each participant who meets the inclusion criteria will be evaluated by trained clinical personnel in accordance with the study protocol. Subsequently, each participant will undergo a series of standardized clinical and functional assessments aimed at quantifying upper limb impairment and functional ability using the following clinical scales: FMA-UE, ARAT, Modified Ashworth Scale (MAS), and Stroke Impact Scale (SIS). The MAS will be used to quantify alterations in muscle tone secondary to central nervous system lesions by rating resistance to passive movement of upper-limb segments on an ordinal scale from 0 to 4, with higher scores indicating greater spasticity. The SIS is a patient-reported outcome

measure capturing the perceived impact of stroke across multiple domains- such as strength, memory, communication, mobility, activities of daily living, emotions, and social participation- with domain scores reflecting the individual's self-rated functional status and recovery. In the case of a positive eligibility outcome, anonymized data will be entered into the RehabCam software database. The database will store:

- a unique patient ID;
- date of birth;
- sex;
- social security number;
- upper-limb movement data;
- system generated stimulation parameters (fs and PW);
- event dates;
- score of National Institutes of Health Stroke Scale (NIHSS);
- comorbidities;
- stroke type;
- lesion site;
- number of repetitions per exercises;
- scores from all administrated scales (FMA-UE, MAS, ARAT, SIS).

The NIHSS is a standardized clinical assessment tool used to quantify the severity of neurological impairment following a stroke. It evaluates multiple domains, including level of consciousness, visual fields, facial palsy, limb strength, sensation, language, and coordination. The total score ranges from 0 to 42, with higher scores indicating more severe neurological deficits.

Each participant will receive a therapy session lasting 40 minutes, consisting of 5 minutes for each exercise with 3-minute rest period between exercises. The intervention will include the same exercises presented in this thesis in the fourth chapter 4, with the addition of a more complex task compared to those previously described, which are all based on simple elbow flexion-extension movements. In this trial, in fact, an additional exercise has been introduced in which the patient will wear an Oculus Quest 2 head-mounted display (Facebook Reality Labs, USA) and perform a bimanual motor task (rolling a rolling pin). This integration of the Lazarus FES device with virtual reality was introduced because this approach allows the simulation of practical and functional movements within a more engaging and motivating environment for the patient, thereby enhancing motor learning and adherence to therapy [20, 27, 44]. This scenario has been previously tested by the research team from the Department of Neuroscience and Rehabilitation, University of Ferrara, in the same population [25]. During each of these sessions, the RehabCam software will record the movements of both arms and compare their performance suggesting the optimal parameters, as described in Chapter 4 . The only exception is the rolling pin exercise, for which the software is slightly modified to update the stimulation parameters due to the higher complexity of the movement. In this case, adjustments are also made to the electrode placement and configuration of the Lazarus FES device to better accommodate this specific task. These modifications will be explained in detail later.

At the end of the experimental session, both the participant and the physiotherapist will complete specific questionnaires.

The patient will be asked to fill out a satisfaction questionnaire aimed at evaluating adherence, acceptance, and feasibility of the rehabilitation modality. This questionnaire consists of 13 questions:

- for 7 item, responses are rated using 7 point Likert scale;
- for 5 item, participants must select one response among several options (e.g, among the performed tasks or the number of breaks taken);
- for 1 item, the response is based on a numeric scale ranging from 0 to 5.

In the 7 point Likert scale, values range from -3 to $+3$, with the following meaning:

$+3$: strongly agree;

$+2$: agree;

$+1$: slightly agree;

0: neither agree nor disagree;

-1: slightly disagree;

-2: disagree;

-3: strongly disagree.

The 0-5 scale is interpreted as follows:

0: absent;

1: very mild;

3: moderate;

4: severe;

5: extreme

The patient questionnaire consists of the following questions:

1. Did you enjoy the type of training?
2. Was the training time adequate?
3. Were the exercise goals easy to achieve?
4. How many breaks did you take during the rehabilitation session?
5. In which task did you obtain the best results?
6. In which task did you the worst results?
7. Which task did you find enjoyable?
8. Which task did you find boring?
9. Are you physically tired?
10. Are you mentally tired?
11. How much did you enjoy the session?

12. How satisfied are you with your performance?
13. How much discomfort did you experience?

The physiotherapist will also complete a short questionnaire consisting of 2 questions, both rated using the same 7 point Likert scale described above. This questionnaire consists of the following questions:

1. Was the delivery of the therapy easy to perform?
2. Are you satisfied with the functional outcome achieved during the rehabilitation session?

The data collected from this study will be used to describe the sample through descriptive statistics (mean ± SD). In addition, the questionnaire responses will be analyzed to identify potential improvements to the experimental protocol or to the device itself, depending on the feedback provided by the participants. These data can also be compared with the results obtained in this study to assess whether there are differences between the movement data of healthy and hemiparetic subjects during the execution of the flexion-extension, glasses, cup, and box exercises. The dataset acquired in this work may also be extended to include the rolling pin exercise, allowing the comparison to be completed for this task as well.

6.3 Modifications to the Use of Lazarus and the RehabCam Program for the Rolling Pin Exercise

For the rolling pin exercise, the Lazarus device cannot be used in self stimulation mode by the patient. Instead, it must be operated in therapist-patient mode. This choice was necessary because the proximity between the stimulation electrodes and the Apollux unit would otherwise cause it to detect the stimulation current. This interference would lead to incorrect detection of muscle contractions and cause the ATC signal to saturate, reaching the maximum value recorded during the registration of the movement, as explained in Chapter 3, and consequently causing the current to be locked at its peak level. Since the Lazarus device is used in therapist-patient mode, the use of RehabCam software has also been adapted to this configuration. In this version, the two webcams already included in the setup are now used with different roles: one captures the therapist's arm, while the other captures the patient's hemiparetic arm. Previously, the cameras were used to capture both arms of the same patient- the healthy and the hemiparetic ones. In this case, the Apollux units are placed on the therapist's body, on the side opposite to the patient's hemiparetic side, specifically over the anterior deltoid, biceps brachii, and latissimus dorsi muscles. On the patient, the stimulation electrodes are positioned on the hemiparetic side, on the same muscles where the Apollux units are placed on the therapist. To monitor the parameters, the RehabCam software, used in combination with the Lazarus device, was also modified. The rolling pin exercise can be divided into two distinct movements performed by the patient: pushing the rolling pin forward and bringing it back to the starting position. For this reason, the stimulation channels were divided into two separate parameter update groups. The channel controlling the anterior deltoid and biceps brachii muscles is associated with the parameter set responsible for the forward movement, while the latissimus dorsi channel is linked to the parameters governing the returning movement. Accordingly, the software was updated to extract both the maximum and minimum joint angles. The normalized maximum angle, which corresponds to the forward movement, and the normalized minimum angle, which corresponds to the return movement, are calculated based on the maximum and minimum angles obtained during the RehabCam calibration phase, as described in Chapter 4. The only difference from the other exercises is that, for this phase, the therapist performs the target movement, completing one full rolling pin repetition forward and backward. If the patient's normalized or minimum angle falls outside the defined tolerance threshold- or if one of the two movements

is not performed- the system will update only the parameters related to the movement that failed to meet the required threshold. To accommodate this new exercise, the algorithm was revised to modify the triggering conditions, now extracting the maximum and minimum angles instead of the minimum angle used previously. Furthermore, the wrist coordinates relative to the elbow are now computed using the difference in the x coordinates, rather than the vertical displacement (y-axis) described in Chapter 4. The computation of angles between the forearm and the arm and the wrist velocities, however, remains unchanged from the method described in Chapter 4.

Chapter 7

Conclusion

This study demonstrated the usefulness of a dedicated program "RehabCam" for monitoring stimulation parameters and analyzed the feasibility of its application within a clinically oriented task-based rehabilitation protocol, through the collection of movement data obtained from healthy subjects. These exercises also served to test the Lazarus FES device under new functional conditions, verifying its actual performance on task-oriented movements for which it had not previously been evaluated.

The study therefore presents several advantages. First, it introduces a system capable of making the rehabilitation process more objective, both through real-time parameter control and through the generation of structured rehabilitation report.

However, some limitations must be acknowledged. The current work involved only healthy participants, included a limited set of functional exercises - all primarily focused on elbow flexion-extension- and relied on an algorithm that still requires further refinement.

Nevertheless, the encouraging results of this exploratory study led to the initiation of a clinical trial at the Cona Hospital (Ferrara, Italy), expanding this research to a population of chronic post-stroke patients and including more complex exercises, as explained in Chapter 6. This study will provide all the necessary data to improve the update algorithm based on the movements of pathological subjects, who represent the final users of this system. Moreover, it will allow the identification of potential critical issues related to the Lazarus device, the RehabCam software, or the protocol used, also taking into account the feedback obtained from questionnaires administered to patients and physiotherapists.

Finally, the data obtained from this thesis work, in addition to being used later for comparison with those collected during the clinical trial, will also be employed to address the current limitations related to the parameter-updating algorithm. Specifically, the movement data gathered from healthy participants in this study will be used to optimize and refine the update logic, ensuring that stimulation parameters are adjusted at the most appropriate moment during the exercise, prior to the clinical trial.

Bibliography

[1] Saad Abdullah, Muhammad A Khan, Mauro Serpelloni, and Emilio Sardini. Hybrid eeg-emg based brain computer interface (bci) system for real-time robotic arm control. *Advanced Materials Letters*, 10(1):35–40, 2019.

[2] J. Y. Ahn, H. Kim, and C. B. Park. Effects of whole-body vibration on upper extremity function and grip strength in patients with subacute stroke: A randomised single-blind controlled trial. *Occupational Therapy International*, 2019:5820952, 2019.

[3] Airgovie.com. Box and block test image. `https://www.airgovie.com/boutique/materiel-devaluation/bilans-mesures/box-and-block-test/`. Accessed: 2025-10-10.

[4] Abdulrahman M Alsubiheen, Wonho Choi, Wonjong Yu, and Haneul Lee. The effect of task-oriented activities training on upper-limb function, daily activities, and quality of life in chronic stroke patients: a randomized controlled trial. *International journal of environmental research and public health*, 19(21):14125, 2022.

[5] Pelin Atalan, Guna Bērziņa, and Katharina S Sunnerhagen. Influence of mobility restrictions on post-stroke pain. *Brain and behavior*, 11(5):e02092, 2021.

[6] Mélanie Barbay, Hervé Taillia, Claudine Nédélec-Ciceri, Flavie Bompaire, Camille Bonnin, Jérôme Varvat, Françoise Grangette, Momar Diouf, Emmanuel Wiener, Jean-Louis Mas, et al. Prevalence of poststroke neurocognitive disorders using national institute of neurological disorders and stroke-canadian stroke network, vascog criteria (vascular behavioral and cognitive disorders), and optimized criteria of cognitive deficit. *Stroke*, 49(5):1141–1147, 2018.

[7] Rim Barioul, Sameh Fakhfakh, Houda Derbel, and Olfa Kanoun. Evaluation of emg signal time domain features for hand gesture distinction. In *2019 16th International Multi-Conference on Systems, Signals & Devices (SSD)*, pages 489–493. IEEE, 2019.

[8] Susy Braun, Melanie Kleynen, Tessa van Heel, Nena Kruithof, Derick Wade, and Anna Beurskens. The effects of mental practice in neurological rehabilitation; a systematic review and meta-analysis. *Frontiers in human neuroscience*, 7:390, 2013.

[9] Qing Cao, Chen-Chen Tan, Wei Xu, Hao Hu, Xi-Peng Cao, Qiang Dong, Lan Tan, and Jin-Tai Yu. The prevalence of dementia: a systematic review and meta-analysis. *Journal of Alzheimer's Disease*, 73(3):1157–1166, 2020.

[10] Christopher Chen, Didier Leys, and Alberto Esquenazi. The interaction between neuropsychological and motor deficits in patients after stroke. *Neurology*, 80(3_supplement_2):S27–S34, 2013.

[11] Long Chen, Bin Gu, Zhongpeng Wang, Lei Zhang, Minpeng Xu, Shuang Liu, Feng He, and Dong Ming. Eeg-controlled functional electrical stimulation rehabilitation for chronic stroke: system design and clinical application. *Frontiers of medicine*, 15(5):740–749, 2021.

[12] Woosang Cho, A Heilinger, R Xu, M Zehetner, S Schobesberger, N Murovec, R Ortner, and C Guger. Hemiparetic stroke rehabilitation using avatar and electrical stimulation based on non-invasive brain computer interface. *Int J Phys Med Rehabil*, 5(04), 2017.

[13] Wonho Choi. The effect of task-oriented training on upper-limb function, visual perception, and activities of daily living in acute stroke patients: A pilot study. *International Journal of Environmental Research and Public Health*, 19(6):3186, 2022.

[14] Chih-Hong Chou, Tong Wang, Xiaopei Sun, Chuanxin M Niu, Manzhao Hao, Qing Xie, and Ning Lan. Automated functional electrical stimulation training system for upper-limb function recovery in poststroke patients. *Medical Engineering & Physics*, 84:174–183, 2020.

[15] Veronica Cimolin and Manuela Galli. Summary measures for clinical gait analysis: a literature review. *Gait & Posture*, 39(4):1005–1010, 2014. Epub 2014 Feb 7. PMID: 24613461.

[16] Febo Cincotti, Floriana Pichiorri, Pietro Aricò, Fabio Aloise, Francesco Leotta, Fabrizio de Vico Fallani, J del R Millán, Marco Molinari, and Donatella Mattia. Eeg-based brain-computer interface to support post-stroke motor rehabilitation of the upper limb. In *2012 Annual International Conference of the IEEE Engineering in Medicine and Biology Society*, pages 4112–4115. IEEE, 2012.

[17] Marco Crepaldi, Rune Thorsen, Johanna Jonsdottir, Silvia Scarpetta, Lorenzo De Michieli, Mirco Di Salvo, Giorgio Zini, Matteo Laffranchi, and Maurizio Ferrarin. Fitfes: A wearable myoelectrically controlled functional electrical stimulator designed using a user-centered approach. *IEEE Transactions on Neural Systems and Rehabilitation Engineering*, 29:2142–2152, 2021.

[18] Janis J Daly, Roger Cheng, Jean Rogers, Krisanne Litinas, Kenneth Hrovat, and Mark Dohring. Feasibility of a new application of noninvasive brain computer interface (bci): a case study of training for recovery of volitional motor control after stroke. *Journal of neurologic physical therapy*, 33(4):203–211, 2009.

[19] Rig Das, Paula S Lopez, Muhammad Ahmed Khan, Helle K Iversen, and Sadasivan Puthusserypady. Fbcsp and adaptive boosting for multiclass motor imagery bci data classification: a machine learning approach. In *2020 IEEE International Conference on Systems, Man, and Cybernetics (SMC)*, pages 1275–1279. IEEE, 2020.

[20] Sara Demain, Jane Burridge, Caroline Ellis-Hill, Ann-Marie Hughes, Lucy Yardley, Lisa Tedesco-Triccas, and Ian Swain. Assistive technologies after stroke: self-management or fending for yourself? a focus group study. *BMC health services research*, 13(1):334, 2013.

[21] Liming Dong, Linda S Williams, Devin L Brown, Erin Case, Lewis B Morgenstern, and Lynda D Lisabeth. Prevalence and course of depression during the first year after mild to moderate stroke. *Journal of the American Heart Association*, 10(13):e020494, 2021.

[22] V. L. Feigin, M. H. Forouzanfar, R. Krishnamurthi, G. A. Mensah, M. Connor, D. A. Bennett, et al. Global and regional burden of stroke during 1990–2010: findings from the global burden of disease study 2010. *The Lancet*, 383:245–255, 2014.

[23] Valery L. Feigin, Benjamin A. Stark, Catherine O. Johnson, and et al. Global, regional, and national burden of stroke and its risk factors, 1990–2019: a systematic analysis for the global burden of disease study 2019. *The Lancet Neurology*, 2021. Online ahead of print.

[24] Heather L Flowers, Stacey A Skoretz, Frank L Silver, Elizabeth Rochon, Jiming Fang, Constance Flamand-Roze, and Rosemary Martino. Poststroke aphasia frequency, recovery, and outcomes: a systematic review and meta-analysis. *Archives of physical medicine and rehabilitation*, 97(12):2188–2201, 2016.

[25] Giulia Fregna, Nicola Schincaglia, Andrea Baroni, Sofia Straudi, and Antonino Casile. A novel immersive virtual reality environment for the motor rehabilitation of stroke patients: a feasibility study. *Frontiers in Robotics and AI*, 9:906424, 2022.

[26] Jianming Fu, Ming Zeng, Fang Shen, Yao Cui, Meihong Zhu, Xudong Gu, and Ya Sun. Effects of action observation therapy on upper extremity function, daily activities and motion evoked potential in cerebral infarction patients. *Medicine*, 96(42):e8080, 2017.

[27] Vera Fung, Aileen Ho, Jennifer Shaffer, Esther Chung, and Manuel Gomez. Use of nintendo wii fit™ in the rehabilitation of outpatients following total knee replacement: a preliminary randomised controlled trial. *Physiotherapy*, 98(3):183–188, 2012.

[28] Alan S Go, Dariush Mozaffarian, Véronique L Roger, Emelia J Benjamin, Jarett D Berry, Michael J Blaha, Shifan Dai, Earl S Ford, Caroline S Fox, Sheila Franco, et al. Heart

disease and stroke statistics—2014 update: a report from the american heart association. *circulation*, 129(3):e28–e292, 2014.

[29] Pierre A Grandjean and J Thomas Mortimer. Recruitment properties of monopolar and bipolar epimysial electrodes. *Annals of biomedical engineering*, 14(1):53–66, 1986.

[30] David Alejandro Fernandez Guzman, Stefano Sapienza, Bianca Sereni, and Paolo Motto Ros. Very low power event-based surface emg acquisition system with off-the-shelf components. In *2017 IEEE Biomedical Circuits and Systems Conference (BioCAS)*, pages 1–4. IEEE, 2017.

[31] Maree L Hackett and Kristen Pickles. Part i: frequency of depression after stroke: an updated systematic review and meta-analysis of observational studies. *International Journal of Stroke*, 9(8):1017–1025, 2014.

[32] Graeme J Hankey, Maree L Hackett, Osvaldo P Almeida, Leon Flicker, Gillian E Mead, Martin S Dennis, Christopher Etherton-Beer, Andrew H Ford, Laurent Billot, Stephen Jan, et al. Safety and efficacy of fluoxetine on functional outcome after acute stroke (affinity): a randomised, double-blind, placebo-controlled trial. *The Lancet Neurology*, 19(8):651–660, 2020.

[33] Happybai.ru. Action research arm test (arat) image. `https://www.happybai.ru/2020/12/Action-Research-Arm-Test.html`. Accessed: 2025-10-10.

[34] Yukihiro Hara et al. Rehabilitation with functional electrical stimulation in stroke patients. *Int J Phys Med Rehabil*, 1(6):147, 2013.

[35] Yukihiro Hara, Shigeru Obayashi, Kazuhito Tsujiuchi, and Yoshihiro Muraoka. The effects of electromyography-controlled functional electrical stimulation on upper extremity function and cortical perfusion in stroke patients. *Clinical Neurophysiology*, 124(10):2008–2015, 2013.

[36] Danut Irimia, Nikolaus Sabathiel, Rupert Ortner, Marian Poboroniuc, William Coon, Brendan Z Allison, and Christoph Guger. recoverix: a new bci-based technology for persons with stroke. In *2016 38th Annual International Conference of the IEEE Engineering in Medicine and Biology Society (EMBC)*, pages 1504–1507. IEEE, 2016.

[37] Danut-Constantin Irimia, Marian Poboroniuc, Rupert Ortner, Brendan Z Allison, and Christoph Guger. Preliminary results of testing a bci-controlled fes system for post-stroke rehabilitation. In *GBCIC*, 2017.

[38] MOE JH and POST HW. Functional electrical stimulation for ambulation in hemiplegia. *The Journal-lancet*, 82:285–288, 1962.

[39] Johanna Jonsdottir, Rune Thorsen, Irene Aprile, Silvia Galeri, Giovanna Spannocchi, Ettore Beghi, Elisa Bianchi, Angelo Montesano, and Maurizio Ferrarin. Arm rehabilitation in post stroke subjects: A randomized controlled trial on the efficacy of myoelectrically driven fes applied in a task-oriented approach. *PLoS One*, 12(12):e0188642, 2017.

[40] Zoher Z Karu, William K Durfee, and Aaron M Barzilai. Reducing muscle fatigue in fes applications by stimulating with n-let pulse trains. *IEEE Transactions on Biomedical Engineering*, 42(8):809–817, 2002.

[41] Muhammad Ahmed Khan, Hoda Fares, Hemant Ghayvat, Iris Charlotte Brunner, Sadasivan Puthusserypady, Babak Razavi, Maarten Lansberg, Ada Poon, and Kimford Jay Meador. A systematic review on functional electrical stimulation based rehabilitation systems for upper limb post-stroke recovery. *Frontiers in neurology*, 14:1272992, 2023.

[42] TaeHoon Kim, SeongSik Kim, and ByoungHee Lee. Effects of action observational training plus brain–computer interface-based functional electrical stimulation on paretic arm motor recovery in patient with stroke: a randomized controlled trial. *Occupational therapy international*, 23(1):39–47, 2016.

[43] Alojz Kralj, Tadej Bajd, and Rajko Turk. Enhancement of gait restoration in spinal injured patients by functional electrical stimulation. *Clinical Orthopaedics and Related Research (1976-2007)*, 233:34–43, 1988.

[44] Gert Kwakkel, Roland van Peppen, Robert C Wagenaar, Sharon Wood Dauphinee, Carol Richards, Ann Ashburn, Kimberly Miller, Nadina Lincoln, Cecily Partridge, Ian Wellwood, et al. Effects of augmented exercise therapy time after stroke: a meta-analysis. *stroke*, 35(11):2529–2539, 2004.

[45] Nicolò Landra, Andrea Prestia, Andrea Mongardi, Fabio Rossi, Danilo Demarchi, and Paolo Motto Ros. A biomimetic multichannel synergistic calibration for event-driven functional electrical stimulation. In *2022 IEEE Biomedical Circuits and Systems Conference (BioCAS)*, pages 85–89. IEEE, 2022.

[46] Peter Langhorne, Fiona Coupar, and Alex Pollock. Motor recovery after stroke: a systematic review. *The Lancet Neurology*, 8(8):741–754, 2009.

[47] Ronald M Lazar and Amelia K Boehme. Aphasia as a predictor of stroke outcome. *Current neurology and neuroscience reports*, 17(11):83, 2017.

[48] D.-H. Lee and J.-H. Lee. A study on the physical therapy approach for improving the upper extremity function of spastic ischemic stroke patients. *International Journal of Advanced Nursing Education and Research*, 4:7–12, 2019.

[49] Mingfen Li, Ye Liu, Yi Wu, Sirao Liu, Jie Jia, and Liqing Zhang. Neurophysiological substrates of stroke patients with motor imagery-based brain-computer interface training. *International Journal of Neuroscience*, 124(6):403–415, 2014.

[50] Ning Li, Tie Yang, Peng Yu, Junling Chang, Liang Zhao, Xingang Zhao, Imad H Elhajj, Ning Xi, and Lianqing Liu. Bio-inspired upper limb soft exoskeleton to reduce stroke-induced complications. *Bioinspiration & biomimetics*, 13(6):066001, 2018.

[51] Erik Lundström, Eva Isaksson, Per Näsman, Per Wester, Björn Mårtensson, Bo Norrving, Håkan Wallén, Jörgen Borg, Martin Dennis, Gillian Mead, et al. Safety and efficacy of fluoxetine on functional recovery after acute stroke (effects): a randomised, double-blind, placebo-controlled trial. *The Lancet Neurology*, 19(8):661–669, 2020.

[52] Tácia Cotinguiba Machado, Adriani Andrade Carregosa, Matheus S Santos, Nildo Manoel da Silva Ribeiro, and Ailton Melo. Efficacy of motor imagery additional to motor-based therapy in the recovery of motor function of the upper limb in post-stroke individuals: a systematic review. *Topics in stroke rehabilitation*, 26(7):548–553, 2019.

[53] Maria Julia Machline-Carrion, Eduardo V. Santucci, Luciana P. Damiani, and et al. Effect of a quality improvement intervention on adherence to therapies for patients with acute ischemic stroke and transient ischemic attack: a cluster randomized clinical trial. *JAMA Neurology*, 76:932–941, 2019.

[54] Debapriya Maji, Soyeb Nagori, Manu Mathew, and Deepak Poddar. Yolo-pose: Enhancing yolo for multi person pose estimation using object keypoint similarity loss. In *Proceedings of the IEEE/CVF conference on computer vision and pattern recognition*, pages 2637–2646, 2022.

[55] Nathaniel S Makowski, Jayme S Knutson, John Chae, and Patrick E Crago. Functional electrical stimulation to augment poststroke reach and hand opening in the presence of voluntary effort: a pilot study. *Neurorehabilitation and neural repair*, 28(3):241–249, 2014.

[56] Nebojša M Malešević, Lana Z Popović, Laszlo Schwirtlich, and Dejan B Popović. Distributed low-frequency functional electrical stimulation delays muscle fatigue compared to conventional stimulation. *Muscle & nerve*, 42(4):556–562, 2010.

[57] Aitor Martín-Odriozola, Cristina Rodríguez-de Pablo, and Haritz Zabaleta-Rekondo. Hand dexterity rehabilitation using selective functional electrical stimulation in a person with stroke. *BMJ Case Reports CP*, 14(8):e242807, 2021.

[58] Katie L Meadmore, Timothy A Exell, Emma Hallewell, Ann-Marie Hughes, Chris T Freeman, Mustafa Kutlu, Valerie Benson, Eric Rogers, and Jane H Burridge. The application of precisely controlled functional electrical stimulation to the shoulder, elbow and wrist for upper limb stroke rehabilitation: a feasibility study. *Journal of neuroengineering and rehabilitation*, 11(1):105, 2014.

[59] Scott J. Mendelson and Shyam Prabhakaran. Diagnosis and management of transient ischemic attack and acute ischemic stroke: a review. *JAMA*, 325:1088–1098, 2021.

[60] Yangyang Miao, Shugeng Chen, Xinru Zhang, Jing Jin, Ren Xu, Ian Daly, Jie Jia, Xingyu Wang, Andrzej Cichocki, and Tzyy-Ping Jung. Bci-based rehabilitation on the stroke in sequela stage. *Neural plasticity*, 2020(1):8882764, 2020.

[61] Ministero della Sanità. Linee-guida per le attività di riabilitazione. `https://www.salute.gov.it/`, 1998. Gazzetta Ufficiale n. 124 del 30 maggio 1998.

[62] Mohammad S. Mirshoja, Ahmad A. Pahlevanian, and Mohammad Amoozadeh Khalili. Comparison of fine motor skills in patients with chronic stroke in final stages of brunnstrom and healthy adults. *Middle East Journal of Rehabilitation and Health Studies*, 2(4):e33274, 2015.

[63] Natalie Mrachacz-Kersting, Signe Rom Kristensen, Imran Khan Niazi, and Dario Farina. Precise temporal association between cortical potentials evoked by motor imagination and afference induces cortical plasticity. *The Journal of physiology*, 590(7):1669–1682, 2012.

[64] Masahiko Mukaino, Takashi Ono, Keiichiro Shindo, Toshiyuki Fujiwara, Tetsuo Ota, Akio Kimura, Meigen Liu, and Junichi Ushiba. Efficacy of brain-computer interface-driven neuromuscular electrical stimulation for chronic paresis after stroke. *Journal of rehabilitation medicine*, 46(4):378–382, 2014.

[65] Yoshihiro Muraoka. Development of an emg recording device from stimulation electrodes for functional electrical stimulation. *Frontiers of medical and biological engineering: the international journal of the Japan Society of Medical Electronics and Biological Engineering*, 11(4):323–333, 2002.

[66] Margit Alt Murphy, Katharina S Sunnerhagen, Bo Johnels, and Carin Willén. Three-dimensional kinematic motion analysis of a daily activity drinking from a glass: a pilot study. *Journal of neuroengineering and rehabilitation*, 3(1):18, 2006.

[67] Chuanxin M Niu, Yong Bao, Cheng Zhuang, Si Li, Tong Wang, Lijun Cui, Qing Xie, and Ning Lan. Synergy-based fes for post-stroke rehabilitation of upper-limb motor functions. *IEEE Transactions on Neural Systems and Rehabilitation Engineering*, 27(2):256–264, 2019.

[68] Chuanxin M Niu, Chih-Hong Chou, Yong Bao, Tong Wang, Lin Gu, Xiao Zhang, Lijun Cui, Zhi Xuan, Cheng Zhuang, Si Li, et al. A pilot study of synergy-based fes for upper-extremity poststroke rehabilitation. *Neuroscience letters*, 780:136621, 2022.

[69] P. Hunter Peckham and Jayme S. Knutson. Functional electrical stimulation for neuromuscular applications. *Annual Review of Biomedical Engineering*, 7:327–360, 2005. First published online as a Review in Advance on March 23, 2005. Copyright © 2005 by Annual Reviews. All rights reserved.

[70] Sarah T Pendlebury and Peter M Rothwell. Incidence and prevalence of dementia associated with transient ischaemic attack and stroke: analysis of the population-based oxford vascular study. *The Lancet Neurology*, 18(3):248–258, 2019.

[71] Performance Health. Jamar 9-hole peg test kit image. `https://www.performancehealth.com/jamar-9-hole-peg-test-kit`. Accessed: 2025-10-10.

[72] Lynn Perkes. Handgrip dynamometer strength test image. `https://sixtyandme.com/handgrip-dynamometer-strength-test/`. Accessed: 2025-10-10.

[73] Ceethal K Piyus, V Anjaly Cherian, and Sharmila Nageswaran. Emg based fes for post-stroke rehabilitation. In *IOP Conference Series: Materials Science and Engineering*, volume 263, page 052025. IOP Publishing, 2017.

[74] Zhaoyang Qiu, Shugeng Chen, Ian Daly, Jie Jia, Xingyu Wang, and Jing Jin. Bci-based strategies on stroke rehabilitation with avatar and fes feedback. *arXiv preprint arXiv:1805.04986*, 2018.

[75] P. Raghavan. Upper limb motor impairment after stroke. *Physical Medicine and Rehabilitation Clinics of North America*, 26:599–610, 2015.

[76] Chiara Rigoldi, Emanuela Molteni, Catalina Rozbaczylo, Maria Morante, Giorgio Albertini, Anna M. Bianchi, and Manuela Galli. Movement analysis and eeg recordings in children with hemiplegic cerebral palsy. *Experimental Brain Research*, 223(4):517–524, 2012. Epub 2012 Sep 29. PMID: 23111429.

[77] David Leander Rimmele and Götz Thomalla. Langzeitfolgen von schlaganfällen. *Bundesgesundheitsblatt-Gesundheitsforschung-Gesundheitsschutz*, 65(4):498–502, 2022.

[78] Paolo Motto Ros, Marco Paleari, Nicoló Celadon, Alessandro Sanginario, Alberto Bonanno, Marco Crepaldi, Paolo Ariano, and Danilo Demarchi. A wireless address-event representation system for atc-based multi-channel force wireless transmission. In *5th IEEE International Workshop on Advances in Sensors and Interfaces IWASI*, pages 51–56. IEEE, 2013.

[79] Fabio Rossi, Andrea Mongardi, Paolo Motto Ros, Massimo Ruo Roch, Maurizio Martina, and Danilo Demarchi. Tutorial: A versatile bio-inspired system for processing and transmission of muscular information. *IEEE Sensors Journal*, 21(20):22285–22303, 2021.

[80] Fabio Rossi, Paolo Motto Ros, Ricardo Maximiliano Rosales, and Danilo Demarchi. Embedded bio-mimetic system for functional electrical stimulation controlled by event-driven semg. *Sensors*, 20(5):1535, 2020.

[81] Nikolaus Sabathiel, Danut C Irimia, Brendan Z Allison, Christoph Guger, and Günter Edlinger. Paired associative stimulation with brain-computer interfaces: a new paradigm for stroke rehabilitation. In *International Conference on Augmented Cognition*, pages 261–272. Springer, 2016.

[82] Leire Santisteban, Maxime Térémetz, Jean-Pierre Bleton, Jean-Claude Baron, Marc A Maier, and Påvel G Lindberg. Upper limb outcome measures used in stroke rehabilitation studies: a systematic literature review. *PloS one*, 11(5):e0154792, 2016.

[83] Stefano Sapienza, Marco Crepaldi, Paolo Motto Ros, Alberto Bonanno, and Danilo Demarchi. On integration and validation of a very low complexity atc uwb system for muscle force transmission. *IEEE transactions on biomedical circuits and systems*, 10(2):497–506, 2015.

[84] Marc Sebastián-Romagosa, Woosang Cho, Rupert Ortner, Nensi Murovec, Tim Von Oertzen, Kyousuke Kamada, Brendan Z Allison, and Christoph Guger. Brain computer interface treatment for motor rehabilitation of upper extremity of stroke patients—a feasibility study. *Frontiers in Neuroscience*, 14:591435, 2020.

[85] Anoop S. V. Shah, Kenneth K. Lee, Juan A. R. Pérez, and et al. Clinical burden, risk factor impact and outcomes following myocardial infarction and stroke: a 25-year individual patient level linkage study. *The Lancet*, 7:11–13, 2021.

[86] Keiichiro Shindo, Toshiyuki Fujiwara, Joji Hara, Hideki Oba, Fujiko Hotta, Tetsuya Tsuji, Kimitaka Hase, and Meigen Liu. Effectiveness of hybrid assistive neuromuscular dynamic stimulation therapy in patients with subacute stroke: a randomized controlled pilot trial. *Neurorehabilitation and neural repair*, 25(9):830–837, 2011.

[87] Elisabetta Spinazzola, Andrea Mongardi, Fabio Rossi, Andrea Prestia, Sara Becchi, Rosanna Cavazzana, Federica Savi, Jacopo Secco, Danilo Demarchi, Fabio Pareschi, et al. Motion tracking for automatically controlled functional electrical stimulation system in mirror therapy configuration: the enhanced lazarus solution. *IEEE Access*, 2025.

[88] Mingxu Sun, Christine Smith, David Howard, Laurence Kenney, Helen Luckie, Karen Waring, Paul Taylor, Earl Merson, and Stacey Finn. Fes-upp: a flexible functional electrical stimulation system to support upper limb functional activity practice. *Frontiers in Neuroscience*, 12:449, 2018.

[89] Rune Thorsen. An artefact suppressing fast-recovery myoelectric amplifier. *IEEE Transactions on biomedical engineering*, 46(6):764–766, 1999.

[90] Rune Thorsen, M Cortesi, J Jonsdottir, I Carpinella, D Morelli, A Casiraghi, M Puglia, M Diverio, and M Ferrarin. Myoelectrically driven functional electrical stimulation may

increase motor recovery of upper limb in poststroke subjects: a randomized controlled pilot study. *Journal of Rehabilitation Research & Development*, 50(6), 2013.

[91] Rune Thorsen and Maurizio Ferrarin. Battery powered neuromuscular stimulator circuit for use during simultaneous recording of myoelectric signals. *Medical engineering & physics*, 31(8):1032–1037, 2009.

[92] Diana C Toledo-Pérez, Juvenal Rodriguez-Resendiz, and Roberto A Gomez-Loenzo. A study of computing zero crossing methods and an improved proposal for emg signals. *IEEE Access*, 8:8783–8790, 2020.

[93] Amytis Towfighi, Bruce Ovbiagele, Nada El Husseini, Maree L Hackett, Ricardo E Jorge, Brett M Kissela, Pamela H Mitchell, Lesli E Skolarus, Mary A Whooley, and Linda S Williams. Poststroke depression: a scientific statement for healthcare professionals from the american heart association/american stroke association. *Stroke*, 48(2):e30–e43, 2017.

[94] Connie W. Tsao, Aaron W. Aday, Zainab I. Almarzooq, Alvaro Alonso, Arianne Z. Beaton, Marcio S. Bittencourt, Amelia K. Boehme, Alfred E. Buxton, April P. Carson, Yvonne Commodore-Mensah, Mitchell S. V. Elkind, Kelly R. Evenson, Chikezie Eze-Nliam, James F. Ferguson, Grace Generoso, Jennifer E. Ho, Ruchi Kalani, Sadiya S. Khan, Brett M. Kissela, Kristen L. Knutson, Deborah A. Levine, Tené T. Lewis, Jianwen Liu, Matthew S. Loop, Jun Ma, Maria E. Mussolino, Sankar D. Navaneethan, Amanda M. Perak, Rajendra Poudel, Mona Rezk-Hanna, Gregory A. Roth, Elizabeth B. Schroeder, Sanjay H. Shah, Erin L. Thacker, Lisa B. VanWagner, Salim S. Virani, Jennifer H. Voecks, Nancy Y. Wang, Kristine Yaffe, and Seth S. Martin. Heart disease and stroke statistics–2022 update: A report from the american heart association. *Circulation*, 145(8):e153–e639, Feb 2022. Erratum in Circulation. 2022 Sep 6;146(10):e141. PMID: 35078371.

[95] Ultralytics. Pose-ultralytics yolo. `https://docs.ultralytics.com/it/tasks/pose/#model`, 2024. [Online; accessed 11-October-2025].

[96] Tamaya Van Criekinge, Steven Truijen, Jonas Schröder, Zoë Maebe, Kyra Blanckaert, Charlotte van der Waal, Marijke Vink, and Wim Saeys. The effectiveness of trunk training on trunk control, sitting and standing balance and mobility post-stroke: a systematic review and meta-analysis. *Clinical rehabilitation*, 33(6):992–1002, 2019.

[97] Arthur P Vasen, Stephen H Lacey, Michael W Keith, and John W Shaffer. Functional range of motion of the elbow. *The Journal of hand surgery*, 20(2):288–292, 1995.

[98] Eduardo Villar Ortega, Karin A Buetler, Efe Anil Aksöz, and Laura Marchal-Crespo. Enhancing touch sensibility with sensory electrical stimulation and sensory retraining. *Journal of NeuroEngineering and Rehabilitation*, 21(1):79, 2024.

[99] Alex Efstathios Voinas, Rig Das, Muhammad Ahmed Khan, Iris Brunner, and Sadasivan Puthusserypady. Motor imagery eeg signal classification for stroke survivors rehabilitation. In *2022 10th International Winter Conference on Brain-Computer Interface (BCI)*, pages 1–5. IEEE, 2022.

[100] F. Wang, G. Wang, and B. Lu. YOLOv8-PoseBoost: Advancements in Multimodal Robot Pose Keypoint Detection. *Electronics*, 13(6):1046, 2024.

[101] D. A. Winter. *Frontmatter*. Wiley, Hoboken, NJ, USA, 2009.

[102] Jinlong Wu, Aihua Zeng, Ziyan Chen, Ye Wei, Kunlun Huang, Jiafeng Chen, and Zhanbing Ren. Effects of virtual reality training on upper limb function and balance in stroke patients: Systematic review and meta-meta-analysis. *Journal of Medical Internet Research*, 23(10):e31051, 2021.

[103] Güldal Funda Nakipoğlu Yuzer, Burcu Köse Dönmez, and Neşe Özgirgin. A randomized controlled study: effectiveness of functional electrical stimulation on wrist and finger flexor spasticity in hemiplegia. *Journal of Stroke and Cerebrovascular Diseases*, 26(7):1467–1471, 2017.

[104] Elisa L Zwerus, Nienke W Willigenburg, Vanessa A Scholtes, Matthijs P Somford, Denise Eygendaal, and Michel PJ van den Bekerom. Normative values and affecting factors for

the elbow range of motion. *Shoulder & elbow*, 11(3):215–224, 2019.